UNIVERSIDADE DO ALGARVE
FACULDADE DE CIÊNCIAS E TECNOLOGIA

Development of an operational tool for oil spill forecast: Application to oil exposed regions

João Miguel Leitão Janeiro

Dissertação

Doutoramento em Ciências do Mar, da Terra e do Ambiente, Ramo das Ciências do Mar, especialidade em Modelação

Trabalho efectuado sob a orientação de: Prof. Doutor Flávio Martins

Prof. Doutor Paulo Relvas

2014

UNIVERSIDADE DO ALGARVE
FACULDADE DE CIÊNCIAS E TECNOLOGIA

Development of an operational tool for oil spill forecast: Application to oil exposed regions

João Miguel Leitão Janeiro

Dissertação

Doutoramento em Ciências do Mar, da Terra e do Ambiente, Ramo das Ciências do Mar, especialidade em Modelação

Trabalho efectuado sob a orientação de: Prof. Doutor Flávio Martins
Prof. Doutor Paulo Relvas

2014

Development of an operational tool for oil spill forecast: Application to oil exposed regions

Declaração de autoria de trabalho

Declaro ser o autor deste trabalho, que é original e inédito. Autores e trabalhos consultados estão devidamente citados no texto e constam da listagem de referências incluída.

João Miguel Leitão Janeiro

Acknowledgments

This thesis is the final result of several years of research, travelling, planning, adjusting, smiles, almost tears, excitement and frustrations all packed up in the form of a document, some research papers and many memories.

I would like to thank to my supervisors, Prof. Dr. Flavio Martins and Prof. Dr. Paulo Relvas, for helping me and for the support given throughout this research work. I hope we can continue to collaborate in the future. It was quite a ride!

To Paulo Chambel Leitão, Rodrigo Fernandes, Guillaume Riflet, João Ribeiro, and the rest of Hidromod and Martec Group I would like to thank for the prompt help, good discussions and above all for the great work they are doing in the modelling field here in Portugal.

To Fundação para a Ciência e Tecnologia who supported this research by granting me a PhD scholarship. Thank you for allowing me to embrace this challenge. I'll try paying back the "investment" from now on!

A special acknowledgment to FLAD/IMAR for the financial support provided in the scope of a research grant from the 2011 Luiz Saldanha/Ken Tenore Marine Policy and Strategies Programme, and to U.S. National Oceanic and Atmospheric Administration Office Coastal Services Centre. This was a very important milestone in my PhD. The time I've spent in the US allowed me to understand one of the most important things in my professional career: "This is all about the people" quoting my dear friend and Professor Dr. Mike Orbach.

Part of this research work was carried out within the framework of the project ARGOMARINE. This research project had a key role in this work, not only by adding a new study area, but also by providing me the opportunity to work with a multidisciplinary team of remarkable people. My sincere thanks to all of you!

To my friends and partners in crime Ana Rita Carrasco, Joel Guiomar and Augusto Neves I thank your help, patience, support and dedication throughout these past years. Our adventures will continue after this chapter and the future never looked so brighter!

To the rest of my friends, the ones from old times and the new ones that recently came into my life and already have such a positive effect on me, I hereby thank your support and for caring! You all have part on this too! A special thanks to Joana Santos how listen to my complains, endure the moods and helped me reach this final line…I hope to see your smile by my side for a long time! I thank your patience, dedication and love.

To my family, which has grown bigger since I've started this adventure both in Urra and Faro, I thank your patience, help and above all your love. A special thanks to my niblings: Alice, Joana and Gaspar. Their love, joy and laughs always help me charge batteries and, in the "darkest hours", to put my problems and concerns into perspective!

Finally my last thank you goes to someone who has been daily by my side, both in mind and heart, throughout this journey. Grandmother, I thank all your teachings - some of them I recently understood - and I dedicate this work to you!

Institutional and Financial Support

This work was funded by:

- Fundação para a Ciência e Tecnologia, PhD grant SFRH / BD / 44850 / 2008
- Universidade do Algarve, Research Fellowship FP7-SST-2008-RTD-1-234096 "ARGOMARINE"

Data collection was funded by the following projects:

- CEC FP7-SST-2008-RTD-1 "Automatic Oil-Spill Recognition and Geopositioning integrated in a Marine Monitoring Network (ARGOMARINE)" 2009-2012 (www.argomarine.eu)
- Project IMPACT - 'Long-term effects of continued trawling on deep-water muddy grounds' - EU programme Eurofleets (www.eurofleets.eu)

Other support:

- Hydrodynamic boundary conditions data to force the Algarve coast models is being kindly supplied by Hidromod.
- Hydrodynamic boundary conditions to force the Tuscany Archipelago models were supplied by MyOcean2 project.
- Wind data to force both the Algarve coast and Tuscany Archipelago models is being supplied by the Helenic National Meteorological Service and by the Grupo da Previsão Numérica do Tempo Instituto Superior Técnico.
- Most of the data use to validate the models presented in this work were collected and made freely available by the Coriolis project and programmes that contribute to it (http://www.coriolis.eu.org).
- Other data used in this work was provided by MyOcean2, Ifremer, NASA, EUMETSAT, Instituto Hidrográfico, Direção Geral de Combate à Poluição do Mar e CCMAR.

Para quem tanto me ensinou na vida e não pode compartilhar este momento comigo…

To the person who taught me so much in life and cannot share this moment with me…

Nome: João Miguel Leitão Janeiro

Faculdade: Faculdade de Ciências e Tecnologia

Universidade: Universidade do Algarve

Orientadores: Prof. Doutor Flávio Martins e Prof. Doutor Paulo Relvas

Título da Tese: Development of an operational tool for oil spill forecast: Application on oil exposed regions.

Resumo

O objectivo da presente tese é apresentar uma metodologia de modelação, com base no sistema MOHID, que permite criar de forma robusta e expedita modelos operacionais costeiros tirando partido de modelos operacionais regionais já existentes numa abordagem de malhas encaixadas. Isto permite aumentar a resolução à escala costeira, conseguindo um estudo mais aprofundado da influência dos vários tipos de processos costeiros na dinâmica de derrames, ao mesmo tempo melhorando as previsões fornecidas. Esta metodologia foi usada para a previsão da evolução de manchas de hidrocarbonetos em duas zonas consideradas propensas a este tipo de poluição: Costa Sudoeste Portuguesa e o Arquipélago Toscano (Itália). Em ambos os casos de estudo os modelos operacionais implementados foram validados a um bom nível, utilizando vários tipos de dados oceanográficos disponíveis em bases de dados europeias e globais. A robustez do método foi testada durante as operações de retirada de combustível do navio Costa Concordia, para as quais o sistema forneceu previsões às autoridades Italianas. São ainda considerados na presente tese a interação entre ondas/correntes/vento na dinâmica das manchas de hidrocarbonetos no mar, a detecção de padrões de circulação de mesoescala e sua influência no risco a acidentes, bem como a integração destes métodos numéricos com sistemas de detecção e monitorização.

Palavras-Chave: oceanografia operacional; malhas encaixadas; previsão hidrodinâmica; previsão da deriva de hidrocarbonetos; combate à poluição.

Name: João Miguel Leitão Janeiro
Faculty: Faculdade de Ciências e Tecnologia
University: Universidade do Algarve
Supervisors: Prof. Doutor Flávio Martins e Prof. Doutor Paulo Relvas
Thesis title: Development of an operational tool for oil spill forecast: Application to oil exposed regions.

Abstract

The objective of the following thesis is to present a modelling methodology, based on the MOHID system, which allows the development of coastal operational models by taking advantage of already implemented regional operational models using a downscaling approach. This increase in resolution allows studying the influence of coastal scale processes in the dynamics of oil spills, while contributing to more accurate forecasts. The methodology was used to forecast the evolution of oil spills in two distinct areas both prone to oil pollution events: Southwest Portuguese Coast and the Tuscany Archipelago (Italy). In both regions an operational model was developed and validated to a good level, using several types of oceanographic data available in European and global databases. The method was tested during the Costa Concordia accident, where operational forecasts aided the Italian authorities during the fuel removal operations. Also considered in this work are the interaction between waves/currents/wind in the dynamics of oil spills at sea, the identification of mesoscale circulation patterns and their influence on the risk to accidents as well as the integration of these numeric methods with early detection and monitoring systems.

Keywords: operational oceanography; downscalling; hydrodynamic forecast; oil-drift forecast; pollution response.

Resumo Alargado

Enquanto o transporte marítimo é, e continuará a ser, uma parte central da cadeia logística de transporte mundial, esta atividade marítima coloca nas zonas costeiras e seus ecossistemas uma grande pressão ambiental devido ao risco de poluição. Este risco aumenta consideravelmente quando falamos de acidentes com petroleiros, mas no entanto descargas ilícitas devidas às atividades de rotina dos navios de transporte, são igualmente importantes de considerar.

Olhando para a distribuição das rotas do petróleo que passam por território europeu, o Arquipélago Toscano (Itália) e o corredor marítimo que passa junto á costa sul Portuguesa são dois locais tidos como fortemente vulneráveis a este tipo de acidentes. A convergência de rotas, aliada ao facto de estas intersectarem zonas marinhas protegidas (com ecossistemas de elevado valor ecológico), e sendo estas ao mesmo tempo duas zonas de elevada importância turística e económica para os países em questão, transforma qualquer potencial acidente num emergência nacional. Isto foi verificado ao longo do ano de 2012 e 2013 no Arquipélago Toscano quando o acidente do navio Costa Concordia.

Neste trabalho é apresentada uma metodologia de modelação operacional com potencial para gerir e responder a eventos de poluição por hidrocarbonetos em zonas protegidas e de elevada vulnerabilidade. Tirando partido de modelos operacionais regionais em funcionamento em ambas as áreas de estudo, um conjunto de malhas encaixadas foram implementadas numa filosofia de modelos encaixados, para permitir aumentar a resolução passando da escala regional para a costeira. Este facto trás vantagens não só ao nível da resolução alcançada, mas também pela capacidade de acrescentar e estudar novos processos que afectam quer a hidrodinâmica das áreas de estudo quer a trajetória de manchas, processos esses que não são relevantes a uma escala regional. O sistema de modelação usado neste trabalho é o sistema MOHID. Este foi escolhido por permitir que o calculo de todos os componentes hidrodinâmicos, turbulentos, de transporte e envelhecimento do petróleo se encontre unificado no mesmo sistema, partilhando o mesmo código e trocando informação em tempo real. Este facto é considerado um passo importante na modelação operacional deste tipo de eventos de poluição.

Esta metodologia foi aplicada em duas áreas de risco no que diz respeito a derrames de petróleo, o arquipélago Toscano (Itália) e a costa sudoeste da Península Ibérica (Portugal), através do desenvolvimento de um modelo operacional para cada uma das áreas. Após uma cuidada validação de ambos os modelos, usando diferentes fontes e tipos de dados oceanográficos disponíveis, os resultados obtidos demonstram a boa capacidade do método para reproduzir as condições hidrodinâmicas de ambas as zonas de estudo, bem como a trajetória de derivadores oceânicos. Em ambos os locais, esta ferramenta foi integrada em diversas atividades quer na área da resposta e gestão de acidentes quer na áreas da investigação dos processos associados a evolução das trajetórias de derrames no mar.

No âmbito do projeto FP7 ARGOMARINE (Automatic Oil-Spill Recognition and Geopositioning integrated in a Marine Monitoring Network) o modelo operacional desenvolvido foi integrado num sistema de detecção, monitorização e resposta a derrames de petróleo aplicado ao arquipélago Toscano. Aqui, para além da sua integração com várias tecnologias, o modelo operacional foi usado também para investigar a influência da interação das ondas/correntes/vento na dinâmica das trajetórias de derrames. Importantes conclusões foram retiradas acerca da importância da inclusão da deriva de Stokes nas trajetórias das manchas para esta área de estudo. O trabalho desenvolvido permitiu também testar a robustez do método apresentado neste trabalho, durante a situação de emergência vivida com o acidente do navio Costa Concordia na ilha de Giglio. Para o local do acidente, encontrando-se este dentro da área de estudo, foi criada rapidamente uma malha de alta resolução (250 m) recebendo condições de fronteira do nível de mais alta resolução implementado no sistema operacional (1 km). Esta nova malha foi adicionada ao sistema operacional, e as previsões dadas foram integradas nas ações de resposta por parte das autoridades da Guarda Civil Italiana. Os resultados alcançados permitiram ter confiança na metodologia não só pelos resultados obtidos, mas principalmente pelo tempo de resposta alcançado e a facilidade de integração de mais uma malha no sistema operacional.

Paralelamente ao trabalho desenvolvido no Arquipélago Toscano, a mesma metodologia deu os primeiros passos na costa do Algarve. Tendo como base, numa primeira fase, apenas o estudo da circulação costeira na zona adjacente ao Cabo de São Vicente e a sua influencia no transporte de derrames de petróleo, a análise dos mecanismos de gestão do espaço marítimo nacional bem como as dificuldades aliadas à sua implementação, aliada a um conhecimento mais profundo dos princípios de gestão do risco, alteraram este objectivo inicial. Mantendo-se o objectivo inicial de desenvolver um sistema de resposta e gestão a acidentes de petróleo, o sistema cresceu em dimensão geográfica de forma a tornar-se uma ferramenta regional de apoio a politicas de desenvolvimento e proteção ambiental, ao tecido empresarial ligado ao mar bem com à investigação científica. O novo sistema operacional foi então implementado e validado, utilizando dados oceanográficos disponíveis em várias bases de dados europeias e mundiais. Estes dados foram selecionados não só tendo em conta a sua distribuição geográfica, de forma a cobrir ambas as malhas implementadas, como também um distribuição temporal alargada, incluindo assim a variabilidade natural da região. Os resultados mostraram também aqui as vantagens da aplicação desta metodologia. Da análise dos resultados da validação, foram ainda levantadas questões, transversais às retiradas anteriormente para o Arquipélago Toscano, acerca da importância da qualidade dos forçamentos nos resultados obtidos, principalmente no que diz respeito às trajetórias do petróleo. A não inclusão de descargas de água doce associadas aos principais rios também foi apontada como uma explicação para algumas diferenças encontradas sobretudo nas comparações entre a salinidade observada e simulada. Tirando partido de tecnologias remotas de detecção implementadas pela European Maritime Safety Agency (EMSA), que monitorizam e alertam para potenciais manchas de petróleo dentro das Zonas Económicas Exclusivas dos vários Estados Membros da União Europeia, o sistema operacional desenvolvido para a costa Sudoeste Ibérica foi testado numa aplicação real, em cujo objectivo foi a simulação inversa (backtracking) de uma detecção do sistema CleanSeaNet. Para este fim foi apresentada uma metodologia que, aliando a trajetória obtida por simulação inversa às posições de navios que passavam na zona, obtidas por AIS, indicou aqueles cujo potencial de responsabilidade pela mancha seria maior. Esta metodologia diferencia-se ainda pela inclusão dos erros obtidos durante o processo de validação para as comparações com derivadores seguidos por satélite, tornando-a mais robusta. Ainda na região Sudoeste Ibérica, as características oceanográficas, que, ligadas a circulação atmosférica de larga escala, apresentam padrões sazonais foram investigadas. Com o objectivo de relacionar esses padrões, facilmente detectados por satélite através de imagens de temperatura da superfície do mar, com a trajetória de derrames na região, o objectivo deste trabalho consistiu numa primeira fase na avaliação da capacidade do modelo reproduzir este tipo de padrões regionais, e numa segunda fase de retirar conclusões acerca da possibilidade de usar estes padrões como indicadores para incluir nos planos de resposta e planeamento regionais a derrames de petróleo. Imagens de satélite da temperatura da superfície do mar são atualmente um produto disponível de forma operacional e cuja cobertura espacial e resolução à escala costeira (1 km) têm o potencial para fornecer informações adicionais acerca da hidrodinâmica da região em estudo. Especialmente numa região em que fenómenos de mesoescala associados a grandes gradientes térmicos são uma das características hidrodinâmicas bem conhecida e estudada, a sua relação com as trajetórias de derrames tem-se como uma mais valia. Os resultados mostram que, apesar das diferenças existentes entre temperaturas observadas e simuladas, que o modelo consegue reproduzir em boa medida os padrões de mesoescala conhecidos na região. Mostra-se também, que estes padrões tem um papel fundamental na dinâmica das manchas simuladas, sendo facilmente relacionadas as trajetórias das manchas com a dinâmica observada através das temperatura da superfície do oceano. Assim, factores com a sazonalidade associada a estes eventos, bem como a sua inércia, poderão ser usados como informação complementar à existente, para melhor planear e responder a este tipo de poluição no contexto regional.

Para terminar, são ainda apontadas as principais lacunas identificadas ao longo deste trabalho, e apontadas soluções como trabalho futuro. Estas soluções passam em grande medida pela inclusão de mais fontes de forçamento operacionais, como forma de potencialmente aumentar a qualidade das previsões, mas também por contribuir para a redundância destas fontes de dados necessárias para o funcionamento do sistema operacional. Incluir as descargas de água doce em ambos os sistemas, bem como a introdução de metodologias de assimilação de dados para a temperatura da superfície do oceano, altimetria, e para as observações operacionais disponíveis são também apontadas como solução para melhorar a performance dos sistemas operacionais apresentados.

Contents

Acknowledgments....................4
Resumo....................8
Abstract....................9
Resumo Alargado....................10
List of Figures....................18
Chapter I – Introductory Notes....................21
Chapter II - ARGOMARINE: A new oil early warning system integrating modelling, in-situ and remote sensing....................26

1. Introduction....................27

2. The ARGOMARINE suite of systems....................28

2.1. Information and Communication Systems....................28
2.2. Remote Sensing....................30
2.3. In Situ Data....................31
2.4. Mathematical modelling....................31

3. Conclusions....................36

Chapter III – Enhancing the management response to oil spills in the Tuscany Archipelago through Operational modelling....................37

Abstract....................38

1. Introduction....................38

2. The Operational System....................42

2.1. Hydrodynamic model description and implementation....................42
2.2. Wave Model description and implementation....................44
2.3. Lagrangian and oil spill weathering models....................45

3. Model validation....................50

3.1. Hydrodynamic validation....................50
3.2. Wave model validation....................57
3.3. Lagrangian model validation....................59

4. Discussion....................63

5. Conclusions....................68

Chapter IV - Towards the development of an operational tool for oil spills management in the Algarve coast....................69

Abstract....................70

1. Introduction **70**

2. Regional background **71**

3. State of the art **75**

4. A new approach **81**

Chapter V – The European Marine Strategy: Contributions and Challenges from a Portuguese perspective ***87***

Abstract **88**

1. Introduction **89**

2. Brief overview on the EU Marine Strategy Directive **90**

3. The MSFD and Portugal **92**

3.1. Contributing to the MSFD 92

3.2. MSFD and the Portuguese Institutional Framework 93

3.3. Long-term adequacy: links to marine spatial planning, climate change and the financial crisis 96

4. Conclusions **102**

Chapter VI - Marine spatial planning and oil spill risk analysis: Finding common grounds ***103***

Abstract **104**

1. Introduction **104**

2. Methods: analysing MSP and OSRA frameworks **106**

2.1. Marine spatial planning: data on existing conditions 106

2.2. Oil spill risk analysis: features and phases 108

2.2.1. Hazard potential specificities 111

2.2.2. Vulnerability specificities 112

2.2.3. ESI mapping system 115

3. Results and discussion: linking MSP and OSRA **116**

3.1. MSP and OSRA commonalities: a flow of key information 116

3.2. ESI mapping system: an operational tool to implement the MSP– OSRA link? 120

4. Final remarks **123**

Chapter VII – Integrating technologies for oil spill monitoring in the South Iberian Coast ***125***

Abstract **126**

1. Introduction **126**

2. Methods **128**

3. Results **131**

4. Backtracking **143**

5. Discussion **145**

6. Final Remarks **149**

Chapter VIII – Mesoscale patterns and their role on oil spill trajectories in the Southwest Iberian coast ***151***

Abstract **152**

1. Introduction **153**

2. Methods **155**

2.1. Mesoscale Patterns 155

2.2. Model Simulations 158

2.3. Oil trajectories 163

3. Discussion **167**

4. Conclusions **170**

Chapter IX – Conclusion and future work ***171***

References ***174***

List of Figures

Figure 1 *- The ARGOMARINE global structure: Remote Sensing, In-situ Sensors and Mathematical Models connected through the ICS to MIS centers.* 29

Figure 2 *- Wind fields (gray), velocity fields at the surface (white) and oil particles of a punctual discharge for the dates a) 12/11/2007-1:00; b) 14/11/2007-9:00; c) 15/11/2007-22:00; and d) 16/11/2007-15:00.* 35

Figure 3 *- SAR monitoring of the Mediterranean Sea from 1999 to 2004, with a zoom at the Tuscany Archipelago study area. A) Oil spill density estimation (extracted from Ferraro et al., 2009. B) Distribution of MPAs in the Mediterranean Sea (extracted from Abdulla et al., 2008).* 40

Figure 4 *- Model implementation region and bathymetry for: A) hydrodynamic level 1; B) hydrodynamic level 2; C) hydrodynamic level 3; D) SWAN wave model.* 43

Figure 5 *- A cloud of particles being advected across three horizontally aligned grids. The grids order of priority is the following: blue, red and grey.* 46

Figure 6 *- A: Geographical location of the stations used to validate the hydrodynamic and wave models; B: Drifter's trajectories used to validate the lagrangian model.* 51

Figure 7 *- Comparison between observed and modelled tide elevation in four tide gauge stations along the Italian coast.* 52

Figure 8 *- Temperature and salinity vertical profiles in glider station P103 (A) and glider station P502 (B). MOHID results (red) are plotted against the observed glider profile (blue), both compared with MFS forcing conditions (black).* 53

Figure 9 *- Temperature, salinity and density vertical distribution for CTD profile 1 (A) and CTD profile 2 (B). Model Level3 results (red) and CTD observations (blue).* 54

Figure 10 *– Comparison between MODIS 4km daily SST images (top) and MOHID Level 2 (bottom) SST results for three seasonal periods in 2012. From left to right, Winter, Spring and Summer situations.* 56

Figure 11 *- Accessing SWAN H_s and T_m performance against Giglio and Gorgona wave buoys during: A) December 2009 and B) February 2010.* 57

Figure 12 *- Directional distribution of Hs obtained from the wave buoys (left) and output from SWAN (right) for December 2009 (top) and February 2010 (bottom).* 59

Figure 13 *- Lagrangian model validation accessed by comparing the trajectories of drifting buoys (orange) with model tracers centre of mass. A) Validation with tracers trajectories at 50 m depth (green); B) Validation with tracers at the surface considering the Stokes drift effect (red) and not considering it (blue).* 63

Figure 14 *- Distance model to buoy computed for the drifting buoys considered in this study. The depths considered were: 50 m and surface (with and without Stokes drift effect).* 66

Figure 15 *- Operational oil spill scenario simulated during the fuel diesel removal operations from the Costa Concordia ship.* 67

Figure 16 *- Geographical location of the study area: a—The Iberia Peninsula b—Algarve coast; C - Cape São Vicente. Adapted from Google Earth, Google™.* 72

Figure 17 *- Cumulated ship route map in European waters between 2002 to 2009 a and ship maps data acquired before b and after c the amendment on the existing separation scheme for Cape da Roca and Cape São Vicente implemented on 1 July 2005 by the Maritime Safety Committee. Data derived from the Advanced Synthetic Aperture Radar (ASAR) instrument on European Space Agency (ESA) Envisat satellite. Courtesy of ESA.* 73

Figure 18 *- Oil movements in the Iberian Peninsula during 2005. Source: The International Tanker Owners Pollution Federation Limited.* 74
Figure 19 *- Top 100 world Tanker incidents. A zoom into the Iberian Peninsula. Source: The International Tanker Owners Pollution Federation Limited.* 75
Figure 20 *- Output of the POSEIDON OSM and its web based GUI. Adapted from http://www.poseidon.hcmr.gr.* 77
Figure 21 *- CYCOFOS model architecture. MFS as the higher domain supplies the boundary conditions to the ALERMO sub regional model that in turns forces the high resolution CYCOM. A zoom showing the five regions users can select for more detailed information. Adapted from http://www. oceanography.ucy.ac.cy/cycofos.* 78
Figure 22 *- The MEDSLIK software graphical user interface.* 80
Figure 23 *- The proposed nesting scheme for the operational model. Adapted from Google Earth, Google™.* 82
Figure 24 *- Bathymetries of the nested domains.* ***a*** *Algarve coast: 148×424 cells, 550 m resolution.* ***b*** *São Vicente Cape: 170×380 cells, 150 m resolution.* 83
Figure 25 *- Lagrangean tracers simulations in the Algarve coast using a southeast wind event.* ***a*** *- evolution of the tracers 3 h after being released;* ***b*** *—tracers position 1 day after scenario a.* 85
Figure 26 *- Lagrangean tracers simulations in the Algarve coast using a southwest wind event.* ***a*** *— evolution of the tracers 6 h after being released;* ***b*** *— tracers position 1 day after scenario a.* 86
Figure 27 *- Steps for the preparation of marine strategies according to the Marine Strategy Framework Directive. The arrows represent the existing links between all steps. Steps 2, 3 and 4 are directly connected to step 1 as all of them take the initial assessment into consideration. As well, step 4 furthermore considers the environmental targets (from step 3) in its development. MW: marine waters. GES: good environmental status.* 91
Figure 28 *- Portuguese public entities that must provide relevant information and data to the Portuguese Water Institute (INAG) in the scope of the Marine Strategy Framework Directive implementation, according to the Portuguese Decree-Law No. 108, from 2010. In particular, the Portuguese Environment Agency has to provide additional information pertaining to the OSPAR Convention.* 96
Figure 29 *- Current Portuguese Exclusive Economic Zone (Continental, Azores and Madeira fractions) and submitted Extended Continental Shelf. Adapted from Task Group for the Extension of the Continental Shelf (2009).* 98
Figure 30 *- Main steps in a full marine spatial planning process. Highlight is given to the expected outcomes from step 2 – 'defining existing conditions'.* 106
Figure 31 *- Oil spill risk analysis (OSRA) framework.* 109
Figure 32 *- Schematic representation of the connection between marine spatial planning (MSP) and oil spill risk analysis (OSRA). OSRA provides information on oil spill risk (both vulnerability and oil spill potential dimensions) to MSP, while MSP provides data on coastal/marine resources (both biophysical and human-use resources) to OSRA. Environmental Sensitivity Index (ESI) mapping emerges as an operational model to implement such connection.* 117
Figure 33 *- Degree of commonality between variables from marine spatial planning (MSP) and from Environmental Sensitivity Index (ESI) mapping, according to data type (human dimension versus biophysical dimension). Percentage values are based on the total number of variables from Table VI that are: (1) exclusive to ESI mapping, (2) exclusive to MSP or, (3) common to both.* 121
Figure 34 *– The spatial coverage and grid limits for the two levels that composed SOMA. The ship traffic separation corridors are presented in blue while in green are the Protected areas encompassed in the model domain.* 130
Figure 35 *– Distribution of the sensors providing time series observations used in the validation of SOMA. The grid levels implemented in the system are enclosed in black.* 133

Figure 36 *– Assessment of Level 1 (bottom) seasonal SST model performance by using available images (top) from both METOP-A and MODIS-AQUA satellites. From left to right: winter, spring and summer situations.* ____ *135*
Figure 37 *– Distribution of the vertical profiles used in the validation process in the model domain. Argo buoys profiles (blue), XBT profiles (white) and CTD profiles (red). The white filled rectangle represent the area were the ADCP transects were made while the grid levels implemented in the system are enclosed in black.* ____ *136*
Figure 38 *– Model validation against ADCP transects. The U and V components of the model are compared with the ones measured using the ADCP. The direction of the boat during each transect is represented by a black arrow.* ____ *138*
Figure 39 *- Validation of model results, for both Level 1 (L1) and Level 2 (L2), against HFR observations in the eastern coast of Algarve.* ____ *140*
Figure 40 *– Validation of the lagrangian model. Trajectories for satellite-tracked drifters (green) are compared with the centre of mass of the lagrangian cloud of particles for: Sim 1 corresponds to the release of 200 particles at 15 m depth (black), Sim 2 corresponds to the release of 200 particles at the surface (yellow), Sim 3 corresponds to the release of 200 particles at the surface but considering 3% of the wind velocity affecting the lagrangian particles (red). The limits of the two grid levels are also presented.* ____ *142*
Figure 41 *– Absolute distances between model and satellite-tracked drifter for each of the drifters considered in the study and for scenario Sim 3.* ____ *144*
Figure 42 *– Backtracking results for a CleaSeaNet detection in the southern Portuguese coast. The backtracked trajectory was combined with AIS positions for the ships in the region during the simulated period contributing to identify the potential source of this pollution event. The type of ship was color classified: tankers (red), cargo (green) and unknown type (grey).* ____ *146*
Figure 43 *- Map of the study area displaying the location of the operational buoys used during the validation of the model and grid level comprising the operational system.* ____ *154*
Figure 44 *- Distribution of the SST satellite images considered in this study to define regional mesoscale patterns: (A) MODIS-Aqua; (B) METOP-A; (C) Distribution of the representative mesoscale events during the study period.* ____ *156*
Figure 45 *- Mesoscale events considered the most representative of South Iberian coast and classified from the available MODIA-Aqua e METOP-A SST images.* ____ *157*
Figure 46 *– Mesoscale events considered in the study derived from both MODIS and METOP-A SST dataset. For each particular event model results are presented in the right while SST images in the left.* ____ *161*
Figure 47 *- Oil spill scenarios simulated for each classified upwelling event (left). The orange dots correspond to the initial position of the spill while the red line shows the trajectory associated with each spill and in black the final position of the spill. The grey rectangle marks the Northern and Eastern limits of level 1, the outer model grid. Green areas represent protected areas. To the right the correspondent simulated SST distribution in the study area is presented* ____ *164*

Chapter I – Introductory Notes

Among the most important environments on Earth, coastal areas not only support a diverse richness in habitats but also an increasingly production of anthropogenic goods and services, with an estimated value of 12.5 trillion USD per year (Costanza et al., 1997). This figure underpins the increase in occupation of these regions worldwide. In fact, data from 1990 suggests that 23% of the world population already lived within 100km of the coastline (Small and Nicholls, 2003). The acceleration in human occupation brings threats to coastal regions that directly affect, not only the availability and quality of the available coastal resources, but also the safety of human activities. Emerges the need to better understand and manage activities and impacts in coastal regions, towards a sustainable use of coastal and marine resources.

Particularly in Europe, the Marine Strategy Framework Directive establishes a framework within which member states must take the necessary measures to achieve, or maintain, good environmental status throughout their marine environments (water column, seabed and subsoil) from coastal waters to the entire exclusive economic zones (EEZ) by 2020. Member states have to develop and implement marine strategies for its marine regions accounting for the transboundary effects on the quality of the marine environment within each of those regions. These strategies are intended to: protect and preserve marine ecosystems (preventing its deterioration or improving its restoration) and to prevent or reduce the anthropogenic inputs in the marine environment, by consistent application of an ecosystem-based approach to the management of human activities.

Due to the multiplicity of scales and factors controlling coastal ecosystems, sustainable policies involve multidisciplinary insights as well as the need to monitor and forecast processes and changes that affect human activities, either from natural or anthropogenic causes. This is the field of Operational Oceanography. Defined by the European Global Ocean Observing System (EuroGOOS) as *the activity of systematic and long-term routine measurements of the seas, oceans and atmosphere, and their rapid interpretation and dissemination*, its integration with advanced numerical models allow its use as an effective decision support system and as a management tool for coastal activities (Santoro and Stel, 2005). With the growing use of the sea as resource, particularly in the coastal areas (e.g. Aquaculture, Energy, Tourism), the continuous improvements in operational oceanography systems and the advances of computational power, new pressing societal issues to which operational oceanography can make substantial contributions have evolved. They are now diverse, in both nature and purpose, and further focused on smaller scales. To provide answers in an adequate manner, high-resolution observation and forecasting systems need to be in place.

While maritime transport is, and will continue to be, a central part of the world transport logistic chain, this human activity increases the environmental pressure in coastal regions and their ecosystems due to the risk of pollution by hydrocarbon sources. This risk increases considerably when we look at accidents caused by oil tankers, although smaller illicit discharges due to ships' maintenance activities are also important to consider. Looking at the distribution of Europe's maritime routes, the Tuscany Archipelago (Italy) and the maritime route parallel to Southwest Iberian coast (Portugal) are two European areas most vulnerable to oil pollution. In both regions, the convergence of shipping routes intersecting marine protected areas with unique ecosystems and coastal regions of high touristic and economic importance, highlights the need to properly manage and respond to potential accidents. The use of operational oceanography to respond and manage oil spill emergencies at sea has been growing during the last decade, with several operational systems already in place. With the advances in computational power, operational systems are now converging to the coastal scale, where high resolution models, forecasting both sea and weather conditions, and advanced oil spill models encompassing new physical processes that affect the behaviour of oil at a coastal scale, need to be implemented to improve the decision making process during these pollution events.

All the above mentioned is what motivated this work. In the next chapters an approach that allows in a robust way the downscaling of regional ocean forecasts products to a coastal scale, and its integration with a state of the art numerical model that includes major advances in both processes and methods to simulate more accurately the evolution of oil spills at sea, will be presented. This methodology was implemented in both the Tuscany Archipelago and the Algarve Coast where two operational systems were developed and fully validated.

Under the scope of the EU funded project *Automatic Oil-Spill Recognition and Geopositioning integrated in a Marine Monitoring Network* (ARGOMARINE), during the following two chapters the operational system implemented for the Tuscany Archipelago is presented. In Chapter 2 an introduction is given to the main goals of the project, as well as a brief description of the technologies developed and how they are integrated in a decision support tool. Chapter 3 gives a detailed approach on the numerical methods behind the forecasting system, the results from the validation procedure and a brief description on how the operational system was successfully used during the Costa Concordia emergency in Giglio Island.

Parallel to the work developed in Italy, the same modelling methodology started to be applied in the Algarve Coast with a special focus on Cape São Vicente. Chapter 4 introduces the initial ideas behind the operational system, with a special focus on the importance of implementing this technology in the region and reviewing the state of the art in the field of operational oil spill forecasting modelling presenting some examples.

During 2012, after begin awarded with the IMAR Luiz Saldanha/Ken Tenore prize, I had the opportunity to attend a course in Ocean Conservation and Policy at Duke University (USA) followed by one-month trainee scholarship in the NOAA Coastal Services Centre. The program was devoted to the principles of conservation and preservation of the coastal and oceanic environment, but focused on interdisciplinary problem solving using natural and social science theory to tackle real-world environmental problems by linking people, information, and technology. Although a more comprehensive field, this experience changed the initial view defined for the work started in the Southwest Iberia coast. The recent implementation of the Marine Strategy Framework (at the time being transposed for the Portuguese law), the emphasis on potentiate the sea economy at the European and nationally level, and the growing role that operational oceanography was playing in the European context thorough several projects (eg. MyOcean) were also key factors in this shift. In Chapter 5, a review on the European Marine

Strategy and the challenges of its implementation in Portugal is presented. From this work several core issues and challenges facing decisions makers in Portugal were identified regarding the implementation of the Marine Strategy, providing important clues on the new framework for the operational system. Understanding the crucial importance instruments such as hazard potential, vulnerability, and risk profiles/maps have in supporting contingency planning, as well as decision-making and risk management (Abascal et al. 2010; Castanedo et al., 2009), in Chapter 6 the link between Marine Spatial Planning and Oil Spill risk analysis is analysed, highlighting the benefits of linking both processes. The role of operational systems with the ability of forecasting the evolution of oil spills and its integration with information systems managing different sources of geographical information was identified as of paramount importance to access oil spill risk.

Incorporating these new ideas and concepts while keeping the main goal of developing a forecasting tool to aid in the response and management of oil spill accidents, the system grew in geographical coverage in order to become also a broader tool with the objective to contribute to the regional management, economic development and scientific study. In Chapter 7 the "new" operational system for the Southwest Iberian coast (SOMA) is presented. The main focus of this Chapter is to integrated detection technologies and operational modelling tools to provide answers in the case of pollution events. After an extensive validation procedure, SOMA has successfully backtracked an oil spill detection, provided by EMSA's CleanSeaNet system, to its possible origin. A methodology to integrate trajectory errors into backtrack simulations is also presented. Chapter 8 reinforces the discussion regarding the importance of regional mesoscale features in the scale of human activities. Here, SOMA is used to better understand the effect of regional circulation features in the dynamics of oil spills while finding potential ways for a possible integration of this knowledge in future regional planning and response operations for oil spills.

Finally in Chapter 9, the major findings in this work are presented. Some hints are given to further improve SOMA in future work, contributing to enhance its response to oil pollution events and to the growing society issues related to the sustainable management of the sea.

Chapter II - *ARGOMARINE: A new oil early warning system integrating modelling, in-situ and remote sensing*[1]

[1] This chapter is published in the Proceedings of the 9th International Conference on Hydroinformatics as: **Martins, F., Janeiro, J., Babwah, S., Verelest, N., Cocco, M., 2009.** ***ARGOMARINE: A new oil spill early warning system integrating modelling, in-situ and remote sensing.*** **Proceedings of the 9th International Conference on Hydroinformatics. Tianjin, China.**

1. Introduction

Short Sea Shipping is a central part of the logistics chain for transport in Europe, delivering nearly 40% of the total tonne-kilometres per year, only superseded by road transport with 44%, Ferraro et al., (2006). Between 1995 and 2004 the transport in this sector increased by 32% in EU-25 countries, and while increase in sea transport can be desirable from an economic point of view, it places a growing burden on the marine and coastal zone environment due to the risk of pollution. The Mediterranean Sea is particularly exposed due to its intense oil transport. It gives maritime way to Europe, for the oil produced in the Middle East, in Northern Africa and in the Caucasus. According to the Regional Marine Pollution Emergency Response Centre for the Mediterranean Sea (2002), 360-370 million tons of oil and refined products is transported annually through Mediterranean Sea, representing 20-25% of the world total. Due to this the Mediterranean Sea is often quoted as one of the places in the world with the highest risk of oil pollution.

Decision-makers need efficient pollution monitoring and forecasting systems providing continuous and reliable real time access to all available observations as well as forecasts of sea variables and oil spill fate for the area of interest. These systems must seamlessly integrate all data and must have software for analysis, decision-support and intervention planning. The ARGOMARINE system is a pilot study implementation of this concept, currently under construction for the Tuscany archipelago (Italy). A Marine Information System (MIS) consisting of a network for data storage, data mining and analysis, decision-support, data warehouse and a web-GIS portal carries out the top control. The communication relies on an Integrated Communication System (ICS), developed to ensure reliable and efficient data transmission from different sensors and models to the MIS. When fully operational the system will be receiving data from the modelling system and also from Synthetic Aperture Radar (SAR) images, airborne Hyperspectral/Thermal Imaging, AUV/Glider mounted sensors and Electronic Noses. For this project a consortium was created consisting of nine top research institutions in Europe: National Technical University of Athens, Greece; National

Research Council – Institute of Information Science and Technologies, Italy; Nansen Environmental and Remote Sensing Centre, Norway; Environmental and Marine Research Centre – University of Algarve, Portugal; Sciensive Technologies Limited, UK; National Maritime Park of Zakinthos, Greece; Joint Research Centre – Institute for the Protection and Security of the Citizen; NATO Undersea Research Centre and National Park of the Tuscany Archipelago, Italy, the coordinator.

In this article a global perspective of the ARGOMARINE system is given, followed by a detailed description of the mathematical models being developed for sea and oil spill forecasts.

2. The ARGOMARINE suite of systems

2.1. Information and Communication Systems

The core of ARGOMARINE is the Marine Information System (MIS), it collects, converts, store and process data from a large set of different data sources, including remote sensing data, in situ data and mathematical model results. The communication network is managed by the Integrated Communication System (ICS) as represented in **Figure 1.** The MIS possesses tools for data storage and retrieval, data manipulation and analysis, as well as for graphical presentation. The interface is divided in two parts: The HI (Human Interface) used by the operator and the DEI (Data External Interface), for interfacing the MIS with other networks/structures such as GMES services and systems. The DEI is developed using a web-based GIS portal. The main functions of the MIS are: analysis of signals coming from external data sources, data storage in data warehouse, GIS connection, data mining algorithms, management of a control console with interactive panels and implementation of decision Support System routines. MIS is being designed looking to a robust fault tolerance: some entry-level servers, distributed on the territory will enable a decentralization of the data storage and the calculation. The MIS decisional and storage architecture will be structured into levels: a first level allow the handling of global information, a second pre-computation level sorts which information has to be written in the data warehouse and finally a third "data warehouse" level extracts information by data mining techniques. This architecture will integrate robustness and reliable calculation and, in order to support catastrophic events, it will be parallel and redundant as well as able to reallocate computational tasks from one computer to other as a consequence of the workload, or drawbacks.

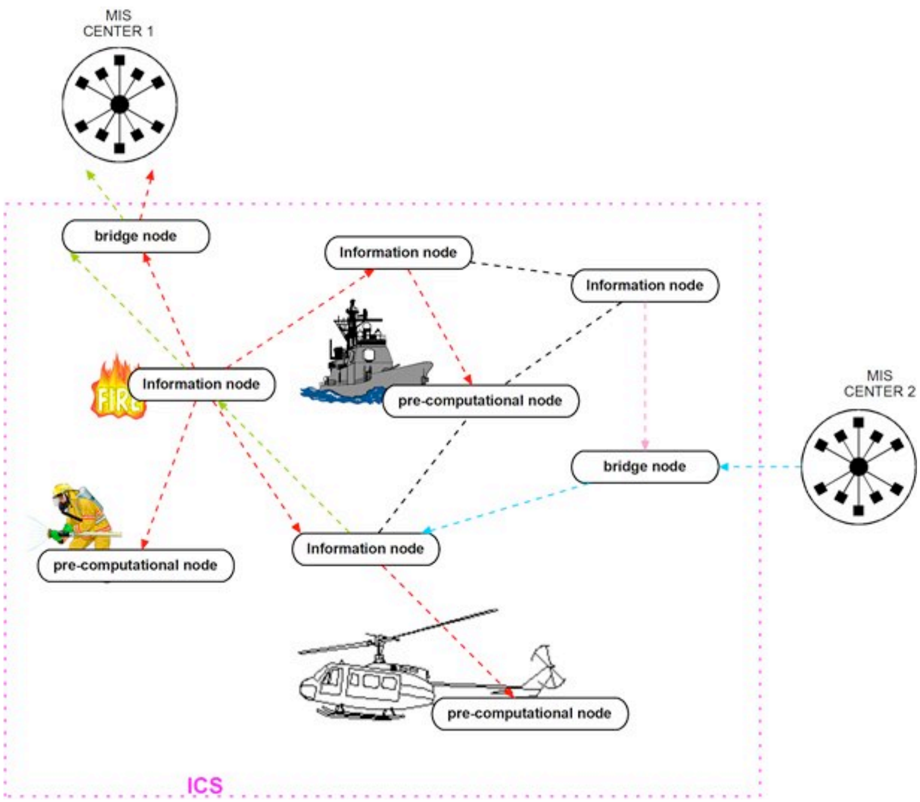

Figure 1 - The ARGOMARINE global structure: Remote Sensing, In-situ Sensors and Mathematical Models connected through the ICS to MIS centres.

The ICS is a communication structure with the objective of transfer data between passive and active actors presents in the geographic area to be monitored. It will be structured as a network where the nodes that can be associated to the functions: informative Intranet flow, informative flow towards other nets and capability of simple elaborations of the collected data. This last function permits to use the net of the integrated informative system at its best as a nervous digital system able to adapt quickly to new situations and to send alarms in case of anomalies.

From a logical point of view, the pre-computational nodes are placed between the informative nodes and the bridge nodes. Pre-computational nodes will get raw-data flow from the informative nodes. They can be located in fixed or mobile positions, the last by a suitable data routing. The mobile nodes can be set up by portable devices like mobile phones, palm tops etc. or computers installed on jeeps, boats etc.

2.2. Remote Sensing

Synthetic Aperture Radar (SAR) images from many of the available satellites will be used (ERS-1, ERS-2, ENVISAT-ASAR, Cosmo-SkyMed, TerraSAR-X). Satellite SAR images can be obtained day and night and independently from the cloud coverage and weather conditions, furthermore they are capable of showing not only oil spills, but also ships. This capability will be exploited in combination with shore-based AIS to obtain a complete picture of shipping density and infer oil spill risks. Oil spills are obtained indirectly from SAR images by changes in sea roughness. However dark areas in the pictures may also be caused by other phenomena, like locally low winds, currents or natural sea slicks called "look-alikes". The DopRIM model, Johannessen et al., (2008), and the CDop model, Collard et al., (2008), will be implemented and results incorporated in the oil spill detection algorithm. Hyperspectral Compact Airborne Spectrographic Imager (CASI) and Thermal Airborne Broadband Imager (TABI) will be mounted on helicopters and tested in the scope of ARGOMARINE. These RS systems cannot replace satellite platforms because they cannot be operated continuously but offer a highly detailed view over a specific area, complementing satellite imagery during surveillance and are crucial during accidents. The CASI Hyperspectral sensor acquires digital spectral data in the visible and near infrared wavelengths. The method is based on the simultaneous use of spatial and spectral information by extended mathematical morphology operations. It also uses signal-processing tools to correct aircraft position and movement errors. With this method CASI has proved to be capable of defining the shape of slicks with high contrast and spatial resolution, moreover it is also able to penetrate to depths of 20-30 m in clean water to see the submerged oil Salem and Kafatos (2001). The TABI sensors will acquire infrared images with refractive optics, uncooled and with a thermally stabilized micro bolometer, showing a resolution of 0.1ºC. Thermal imagery will be pre-processed, i.e. georeferenced, filtered, enhanced and transformed to equivalent temperatures. The resulting temperature differences will lead to potential oil spill formations and will permit to infer the thickness of the oil slick, Maya et al., (2008).

2.3. In Situ Data

Chemical (electronic nose) sensors are rather selective for hydrocarbons and oils Sobanski et al., (2006). In ARGOMARINE a new type of sensor will be developed to rapidly detect volatile chemicals (VOCs) associated with oil and fuels in the seawater. A new version of the Scensive (Bloodhound® ST214) will be developed, it is a 14 sensor instrument (13 outputs and 1 internal sensor) with an integral flow system to allow sampling to be done in transient sniffing mode. The sensors are all pure semi conductive polymers deposited electrochemically on interdigitated gold on silicon transducers and the system is run by proprietary electronics. The electronic nose sensors will be mounted experimentally in a fixed buoy for testing after which will be installed in an autonomous underwater glider. The glider will be of the Folaga type, which combines gliding capabilities with active propulsion Alvarez et al., (2009). The system will be useful in two different types of missions: surveillance (patrolling) and accident assessment.

2.4. Mathematical modelling

The modelling suite is composed by a 3D nested system of hydrodynamic models, a wave model and an oil transport and weathering model based on a

Lagrangian transport model. The system is linked upstream assimilating data and receiving boundary conditions from external operational data products currently running for the global Mediterranean Sea: The system is linked downstream via the ICS to populate the MIS databases.

2.4.1. Hydrodynamic Model

The hydrodynamic model used is the "Hydrodynamic Module" of the MOHID modelling system Martins et al., (2001). It is a 3D baroclinic model that solves the shallow water equations with the Boussinesq approximation:

$$\frac{\partial u_i}{\partial x_i} = 0$$

Equation 1

$$\frac{\partial u_i}{\partial t} + \frac{\partial (u_i u_j)}{\partial x_i} = -\frac{1}{\rho_0}\frac{\partial p_{atm}}{\partial x_i} - g\frac{\rho(\eta)}{\rho_0}\frac{\partial \eta}{\partial x_i} - \frac{g}{\rho_0}\int_{x_3}^{\eta}\frac{\partial \rho'}{\partial x_i}dx_3 + \frac{\partial}{\partial x_j}\left(\nu\frac{\partial u_i}{\partial x_j}\right) - 2\varepsilon_{ijk}\Omega_j u_k$$

Equation 2

Where u_i are the velocity vector components in the Cartesian x_i directions, η is the free surface elevation, ν the turbulent viscosity, and p_{atm} is the atmospheric pressure. ρ is the density and ρ' its anomaly. The last term in Equation 2 represents the Coriolis apparent force: Ω_j is the Earth rotation and ε_{ijk} the Kroneker operator. Density is computed by the UNESCO EOS-80 equation of state from the salinity (S) and temperature (T) values computed by the model. S and T are transported using the same methods used for momentum. The equations are discretized using the finite volume method on a structured grid and solved by the ADI semi-implicit technique. The vertical coordinate in MOHID is of a generic type, meaning that several types of coordinates can be used, such as sigma, Cartesian, Isopycnic or Lagrangian. This is accomplished directly by the use of the finite volume method instead of using coordinate transformations, as explained by Neves et al., (2000). Initial and boundary conditions will be obtained from currently running global Mediterranean operational models: initial and boundary values of S, T, u_i and u_j from the MFS model (http://gnoo.bo.ingv.it/mfs/) while meteorological will be imported from the SKIRON system (http://forecast.uoa.gr/). The initial free surface elevation η will be obtained from MFS and the boundary values from FES2004 (http://poc.obs-mip.fr/pages/research_topics/gravity_waves/waves.htm#fes2004). The boundary conditions will follow the general method proposed by Leitão et al., 2005, i.e. a Flow Relaxation Scheme is applied to S, T, u_i and u_j combined with a radiation scheme for η. The baroclinic mode use also a radiation condition with a constant celerity typical of the internal waves (obtained from the first baroclinic Kelvin mode).

2.4.2. Lagrangian and Oil Spill Models

The Lagrangean transport model computes the evolution of discrete water (or oil) masses (referred hereafter as particles), along lagrangean coordinates using the velocity fields produced by the hydrodynamic model, complemented by the wind and wave fields. Besides this direct influence of winds and waves in the particles movements they are also influencing indirectly the movement through the hydrodynamic fields. The turbulence contributes both to the displacement and to the spreading of the particles: the vortices larger than the particle (the Nyquist wavelength) will induce velocities while those smaller than the particle will contribute to its spreading. The implementation of the movement follows the method of Allen (1982). The Lagrangian model uses a multi-mesh approach, meaning that the lagrangian particles can move over all the computational meshes being computed at the moment. The nested meshes have a priority rank associated, to allow the particle to "choose" the best velocity field available in each position. The Oil Weathering Module uses variables from the hydrodynamics and the Lagrangian transport modules and computes oil density, viscosity, and the weathering processes. Weathering processes include oil spreading, evaporation, dispersion, sedimentation, dissolution, emulsification, degradation (biodegradation and photo- oxidation), oil beaching and removal techniques. The detailed formulation of these processes can be found in Janeiro et al., 2008.

2.4.3. Preliminary Results

The modeling suite is applied to a computational domain centered at Pianosa Island in the Tuscany Archipelago (Italy), as shown in Figure 2. The bathymetric data was obtained from GEBCO (http://www.gebco.net/), a global 30 arc-second grid generated by combining quality-controlled ship depth soundings with interpolation between sounding points guided by satellite-derived gravity data. GEBCO data is then interpolated using a triangulation method to a 0.015º (aprox. 1500 m) 160x60 cells grid. A vertical discretization of the Cartesian type was chosen for the two domains. In this situation this is preferred for the other type of possibilities due to the sharp depth gradient close to the islands. A sigma coordinate for example would lead to excessive spurious errors in the baroclinic term (the so called "sigma error"). Twenty Cartesian layers are used, starting from 6 meters thickness at the surface and increasing using a double exponential law to a maximum of 128 meters at a maximum depth of 1287 meters. In these first preliminary results the model is only simulating the external barotropic mode, being forced by free surface height at the open boundaries and wind stress at the surface. This configuration will not produce accurate results from the point of view of the water column velocity field but from the point of view of superficial oil spill movement it accounts for the most important mechanisms. The boundary values of the free surface elevation are obtained from FES2004 and the velocity field is obtained from Italy's Institute for Environmental Protection and Research (ISPRA) Civitavecchia operational buoy (http://www.mareografico.it). An instantaneous oil spill accident is simulated by discharging instantaneously 1000 particles with a total initial volume of 100 m3 in a position 15 Km west off the Elba Island, which corresponds to a zone of intense traffic. The evolution is simulated for 5 days.

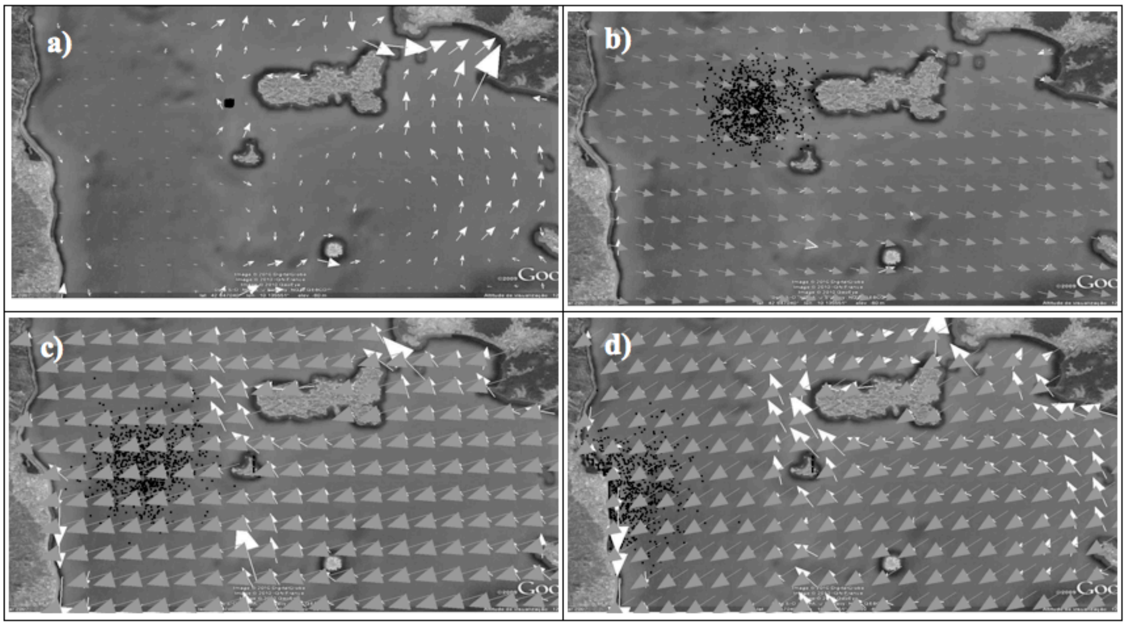

Figure 2 - Wind fields (gray), velocity fields at the surface (white) and oil particles of a punctual discharge for the dates a) 12/11/2007-1:00; b) 14/11/2007-9:00; c) 15/11/2007-22:00; and d) 16/11/2007-15:00.

In Figure 2 the velocity fields and the particles positions are represented in 4 time instants subsequent to the discharge. It can be seen that the barotropic velocity field is much more intense in the shallow region between the islands and the Italian coast (East part of the domain) than in the deep region between the Elba Island and Corsica. This scenario is expected to change dramatically with the introduction of the baroclinic mode. Nonetheless the particles are much more influenced by the wind field than by the hydrodynamic field. The later only play arole during very low wind periods. The relative importance of the hydrodynamic field is expected to increase for sub-superficial oil spills, justifying the introduction of baroclinic forcing in future simulations. These are preliminary results and a full calibration procedure will be performed during the project's lifetime both for the hydrodynamic and for the oil spill model.

3. Conclusions

The ARGOMARINE concept for oil spill surveillance, early warning and management is presented briefly, in all its components, with a special focus on the mathematical modeling techniques. Preliminary results of oil spill simulations are presented to demonstrate the potentialities of the system.

Chapter III – *Enhancing the management response to oil spills in the Tuscany Archipelago through Operational modelling*[2]

[2] This Chapter was published in the Marine Pollution Bulletin as: **Janeiro. J., Zacharioudaki, A., Sarhardi, E., Neves, A., Martins, F., 2014.** ***Enhancing the management response to oil spills in the Tuscany Archipelago through operational modelling*****. Marine Pollution Bulletin, 85, 574 – 589.**

Abstract

A new approach towards the management of oil pollution accidents in marine sensitive areas is presented in this work. A set of nested models in a downscaling philosophy was implemented, externally forced by existing regional operational products. The 3D hydrodynamics, turbulence and the oil transport/weathering models are all linked in the same system, sharing the same code, exchanging information in real time and improving its ability to correctly reproduce the spill. A wind-generated wave model is also implemented using the same downscaling philosophy. Observations from several sources validated the numerical components of the system. The results obtained highlight the good performance of the system and its ability to be applied for oil spill forecasts in the region. The success of the methodology described in this paper was underline during the Costa Concordia accident, where a high-resolution domain was rapidly created and deployed inside the system covering the accident site.

1. Introduction

While short sea shipping is, and will continue to be, a central part of Europe's logistics chain for transport, this growing sea activity places an also growing burden on marine and coastal zone environments due to the risk of pollution. This risk arises not only from pollution caused by accidents with tankers, but also from illicit sources due to ship routine operations. In fact, degassing, deballasting and other ship operations that involve the voluntary discharge of oil residues (including sludge and bilges) in violation of MARPOL 73/78 Annex I, have been estimated to cause as much as eight times the amount of oil pollution each year as accidental and negligent spills such as the Exxon Valdez (OECD 2003). According to PriceWaterhouseCoopers (2006) this means, that in 2005, approximately 50100 tonnes of illegal oil entering EU seas produced an estimate of

€7.5 billion leaving EU safes in economic costs (including environmental degradation and all other economic and societal costs), estimated following the methodology of Etkin et al (2004). Acknowledging the paramount socio-economic and environmental impact of illegal oil spills, under the establishment of the European Union Ship Source Pollution Directive (EU/2005/35) and the operational mandate for the European Maritime Safety Agency (EMSA) in the field of oil pollution monitoring with the CleanSeaNet system, there is now the requirement for each Member State and EMSA to prevent illegal discharges through routine surveillance.

With the status of Special Area according to MARPOL 73/78 Annex I since October 1983, the Mediterranean Sea is particularly sensitive to this type of operational pollution. Here, according to the Regional Marine Pollution Emergency Response Centre for the Mediterranean Sea (REMPEC), 360 to 370 million tons of oil and refined products are transported annually, representing between 20 and 25% of the world total, and being one of Europe's main oil routes (REMPEC, 2002). Although, due to the lack of confirmed oil spills, exact figures for illegal oil spills are difficult to estimate, the work of Ferraro et al., (2009) based on the analysis of 18947 SAR images between 1999 and 2004, produced an oil density distribution for the Mediterranean Sea (Figure 3A). When comparing the high oil density areas with the distribution of Marine Protected Areas (MPAs) in the Mediterranean Sea (Figure 3B), it becomes imperative to ensure measures that address the protection and preservation of these areas against oil pollution. The study site considered was the Tuscan Archipelago in Italy (Figure 3), which is one of the areas with the highest oil spill density according with the work of Ferraro et al. (2009). Located in the Mediterranean Sea, between the Ligurian Sea and the Tyrrhenian Sea, the Archipelago is a Natura 2000 network that comprises the largest protected area of the European seas, and in which lays the Pelagos Sanctuary (Figure 3B), an area of the International Sanctuary for the protection of sea mammals in the Mediterranean.

Although detection (e.g. SAR imagery, electronic nose, mooring buoys) is the first step to prevent and act in the event of an oil spill, forecasting its trajectory is a key factor to response and clean-up operations. In fact, the integration of satellite detection systems with operational regional sea models applying state of the art algorithms to model the drift, weathering and impact of oil spill in the coastal zones is an outlook onto the future of EU operational services for Member States in this field (Trieschmann, 2008).

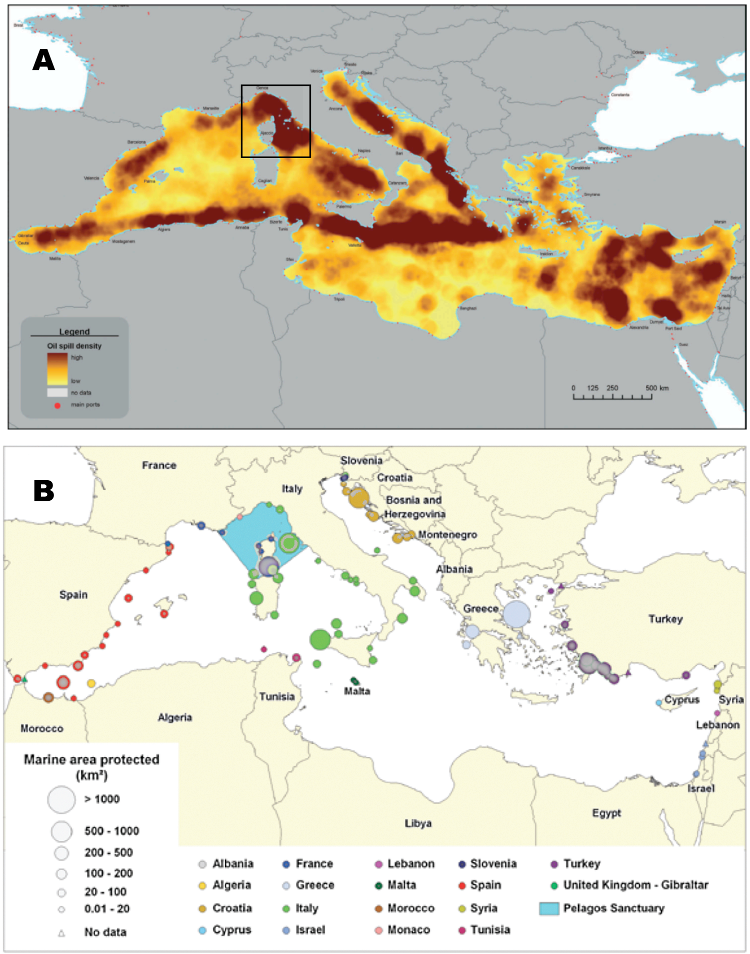

Figure 3 - SAR monitoring of the Mediterranean Sea from 1999 to 2004, with a zoom at the Tuscany Archipelago study area. A) Oil spill density estimation (extracted from Ferraro et al., 2009. B) Distribution of MPAs in the Mediterranean Sea (extracted from Abdulla et al., 2008).

Several operational hydrodynamic and wave models are implemented in the Mediterranean, providing regional (e.g. the Mediterranean Forecasting System), sub-regional (e.g. Adriatic Forecasting System) and shelf (e.g. Malta Shelf Hydrodynamic Model) coverage for almost the entire Sea. Regional models (horizontal resolutions between 10km and 5km), have data assimilation methods implemented using available observations (SST, SSH, ARGO, XBT and mooring buoys) and supply 5 to 7 days of ocean forecasts that typically are use to drive sub-regional and shelf models (horizontal resolutions between 5km and 1km). Increasing model horizontal resolution brings the potential to improve model results. This is true for trajectory modelling, particularly near the coast, where adequate bathymetry data and coastline resolution can impact the quality of results. Oil pollution response is then one of the operational applications that can benefit from this increase in resolution.

A review of two operational systems (POSEIDON and CYCOFOS-MEDSLIK) in place to support the decision process in the event of oil spills in the Mediterranean Sea can be found in Janeiro, et al. (2012). Typically ocean forecasts from operational models are used to force oil drifting and weathering models, which in general run offline of the operational system. In this study, an already implemented regional operational system for the study area to provide initial and boundary conditions, the focus of this work is to downscale its solution to the local (coastal) scale (1km). At this scale, local effects of wind, waves and currents are important to the trajectory of a spill, and cannot be disregarded. The MOHID water modelling system (Martins et al., 2001; Balseiro et al., 2003; Leitão et al., 2005) was applied in this study. It is a modular system including modules for several processes of the marine environment (physical, chemical and biological). This modular system where all the modules are included in the MOHID architecture is the main difference when comparing with other operational modelling systems, as it allows the exchange of information in real time between all the modules.

The principal aim of this research paper is to evaluate the benefit of a high resolution integrated hydrodynamic and oil spill model for oil spill forecasts. Model implementation and validation results will be presented and discussed to evaluate the quality of the system and its suitability to be used as an oil spill forecasting tool. The paper is organized as follows: in chapter 2 the operational system and its several components are described; chapter 3 will focus on the validation of the system; in chapter 4 the results are discussed and chapter 5 summarizes the main conclusions of this study.

2. The Operational System

2.1. Hydrodynamic model description and implementation

To solve the spatial hydrodynamic variability of the region without compromising the computational requirements of an operational system, a three level nesting downscale methodology was implemented. Level1 (Figure 4A) is a two dimensional barotropic model with a constant horizontal resolution of 6.5km. The main purpose of this level is to propagate tide for Level 2 at the same time allowing the solution from Level 2 to freely propagate outward, avoiding reflections and spurious flows at the boundaries. Tide is imposed at the open boundaries of Level 1 using the FES2004 solution (Lyard et al., 2006).

Level 2 (Figure 4B) is a three-dimensional model, with a constant horizontal resolution 6.5km, 71 unevenly spaced Z coordinate levels and a time discretization of 30s. Boundary conditions for temperature, salinity and velocities are extracted every day from the Mediterranean Forecast System (MFS) daily solution, operationally available from the MyOcean 2 server. A complete description of the MFS model can be found in Tonani et al. (2008). At the boundary, a Blumberg and Kantha (1985) condition is applied to the water level and a Flow Relaxation Scheme (FRS) Martinsen and Engedahl (1987) is used for the velocities, salinity and temperature. This allows for a slow forcing of the model and a weighting of internal and external solution to prevent an overshoot of the dynamic equilibrium. In the outer grid cells a sponge layer was applied to attenuate reflected spurious baroclinic flow oscillations. To increase the model resolution in the Tuscan Archipelago, a more refined model grid was created for this region. Level3 (Figure 4C) is a three-dimensional model with a regular 1.5 km spatial resolution grid, which includes the Archipelago islands. The bathymetry was created using the GEBCO Digital Atlas published by the British Oceanographic Data Centre on behalf of IOC and IHO (2003). It has 71 unevenly spaced Z coordinate levels and a time discretization of 15s.

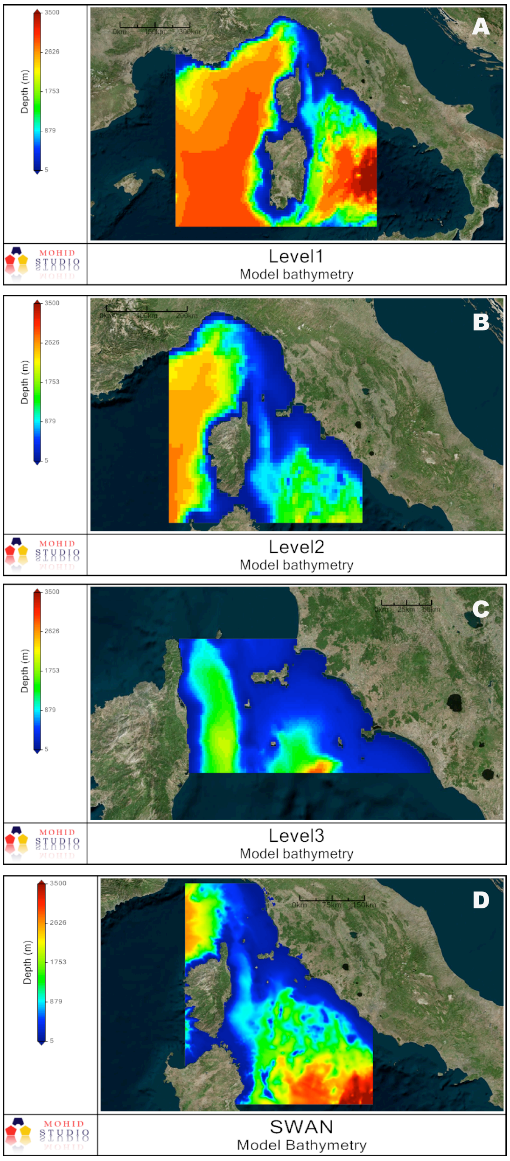

Figure 4 - Model implementation region and bathymetry for: A) hydrodynamic level 1; B) hydrodynamic level 2; C) hydrodynamic level 3; D) SWAN wave model.

The communication between Levels 2 and 3 is made by relaxation of the zonal and meridional horizontal velocity components, through an eight cells band adjacent to the lateral boundary. The FRS is also used to pass the information from Level 2 to Level 3. The use of these boundary conditions is consistent with the conclusions of Blayo and Debreu (2005) that considered relaxation methods to be suitable boundary conditions, giving reliable results in practical applications. To calculate the turbulent diffusion coefficient, MOHID embeds the General Ocean

Turbulence Model (GOTM, Umlauf and Burchard, 2005). The mixing-length scale parameterization proposed by Canuto et al. (2001) is used.

Atmospheric forcing conditions are supplied by the regional weather forecasting system SKIRON, developed for operational use at the Helenic National Meteorological Service (Kallos, 1997; Papadopoulos et al, 2001). The SKIRON model is a non-hydrostatic NWP model (Janjic et al., 2001), which includes a 3D data assimilation package to produce high-resolution analysis fields (Albers, 1995). It provides hourly data of wind U and V components, air temperature, specific humidity, total cloud cover, sea level pressure, total precipitation, upward and downward long wave flux, evaporation, latent heat flux and sensible heat flux at a resolution of 5km. SKIRON results are used in the operational system as forcing fields for the hydrodynamic, wave and lagrangian models.

2.2. Wave Model description and implementation

Wave forcing is coupled in the operational system by means of a local SWAN implementation for the study area. Figure 4D shows the computational domain of SWAN and the model bathymetry. A complete description of the SWAN model can be found in Booij et al. (1999) and SWAN Team (2009a). For this study, the SWAN wave model was favored over other wave models due to the complex bathymetry of the Tuscan Archipelago. The latter dictated the need for a resolution higher than that typically used in deep water applications, capable of resolving important regional features, and for a model of high numerical stability. The computational domain extends (from 8.6º E to 12.5º E and from 40.2º N to 44º N) and grid resolution (2km) has been determined considering a balance between accuracy and computational efficiency (Figure 4D). Temporal discretization has been defined at 60s. The bathymetry used as input to SWAN is the GEBCO bathymetry (IOC and IHO, 2003). The wave forcing at the lateral boundaries of SWAN consists of wave spectra given at 0.1° spatial intervals and updated every hour. The wave spectra were provided by 3G spectral wave model WAM, operational at the National University of Athens (UoA) (AM&WFG, 2010). The model is forced with hourly wind fields of the same horizontal resolution and operates in deep water mode without refraction. This is particularly important for obtaining accurate results in sub basins characterized by complex topography, like is the Tyrrhenian Sea (Ardhuin et al., 2007; Sotillo et al., 2008). The surface wind fields input to SWAN to force local wind-wave generation are supplied by the SKIRON weather forecasting system.

2.3. Lagrangian and oil spill weathering models

Lagrangian models are very useful to simulate localized processes with sharp gradients like oil spills (Carracedo et al., 2006; Janeiro et al., 2008). MOHID's Lagrangian module uses the concept of particles, being its position (x,y,z) the most important property of a particle . The spatial evolution of the particles is computed integrating the definition of velocity:

$$\frac{dx_i}{dt} = U_i(x_i, t)$$

Equation 3

where

$$U_i = u_{1i} + u_{2i} + u_{3i} + u_{4i} + u_{5i}$$

Equation 4

In traditional Lagrangian models a particle is tied to a specific mesh, so, when a particle leaves the mesh it is eliminated. In the ocean this is not necessarily true, because if the flow inverts the particle could potentially return to the model domain. MOHID Lagrangian module uses a multi-mesh approach. Here, particles are able to change seamlessly between different model meshes (Figure 5). The association between a particle and the mesh is made via the particle position, with the user defining the descending priority of each nested meshes. This is useful when several domains/data sources with different resolutions exist. Depending on its position, a particle gets the hydrodynamic and wave information from the high-resolution mesh available, while being able to move to other lower resolution grids if its position changes in time.

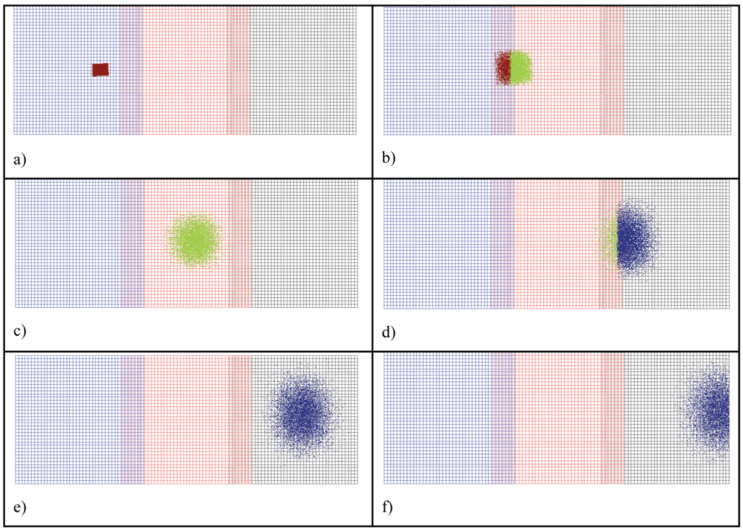

Figure 5 - A cloud of particles being advected across three horizontally aligned grids. The grids order of priority is the following: blue, red and grey.

Looking at Equation 4, u_{1i} is the current velocity calculated in the hydrodynamic module and taken at a user specified depth. In our approach both the hydrodynamic and the Lagrangian modules share the same model architecture, thus the Lagrangian module runs in real time with the hydrodynamic module. The time step used in both modules can be of the same magnitude, which avoids unnecessary interpolations, improving model trajectories by avoiding "sliding effects". These occur when the time step of the Lagrangian module is much larger than the time step of the hydrodynamic module. When that happens, in curvilinear regions of the flow the curvilinear path of the particles cannot be simulated smoothly, being approximated as straight leaps tangential to the streamlines for every time step. The result is a particle trajectory diverging from the theoretical trajectory. Nevertheless no sensitivity analysis was done on this assumption, and the time discretization used in the lagrangian module was 60s. u_{2i} is the drift velocity due to the wind defined as:

$$U_{wind} = C_D \times W_{x_{10}}$$
$$V_{wind} = C_D \times W_{y_{10}}$$

Equation 5

where C_D is a user defined wind drag coefficient and $W_{x_{10}}$ and $W_{y_{10}}$ are respectively the zonal and meridional components of the wind speed at 10 m height. Although several authors (e.g. ASCE, 1996; Reed et al., 1994) mentioned that the wind induced speed of the oil typically varies from 2.5 to 4.4% of the wind speed, with a mean value of 3–3.5%, this approach is usually used to account with the effects of courser numerical grids, which might not solve accurately the Ekman surface currents. In this study the top layer has a 3 m thickness, which is considered small enough to solve the Ekman boundary layer, thus drift velocity due to the wind was not considered ($C_D = 0$). u_{3i} is the velocity due to the spreading of oil (which is calculated in the oil module and updated by the lagrangian module). The algorithm used to compute spreading is based in the thickness differences inside the oil slick assuming that the existence of a thickness gradient generates a "spreading force" opposite to the gradient direction (NOAA, 2000). The tracers will thus move from computational cells with larger thickness to cells with smaller thickness. The velocities in the x and y directions are computed in each cell face as (NOAA, 2000):

$$u_{cell} = k \frac{\Delta h}{\Delta x}$$
$$v_{cell} = k \frac{\Delta h}{\Delta y}$$

Equation 6

where $\frac{\Delta h}{\Delta x}$ and $\frac{\Delta h}{\Delta y}$ are the thickness gradients of the cell, based on the thickness of the particles present inside it. k is the spreading coefficient given by:

$$k = k_1 \sqrt{\left(\frac{\Delta g V^2}{\nu_W^{1/2}}\right)^{1/3}}$$

Equation 7

where V is the volume of the oil, ν_w is the water kinematic viscosity and k_1 is a sensitivity parameter dependent of the grid geometry. u_{4i} is the random velocity due to diffusive transport (Allen, 1982):

$$u_{4i} = K_x \times \nu_w \left(x, y, d\right) + K$$

Equation 8

where $v_W(x, y, d)$ is the water velocity at the specified depth, and K_x and K are the turbulent diffusion coefficients used to define the variance of the random movement velocity. Random displacement is computed using the mixing length and the standard deviation of the turbulence velocity component, as given by the turbulence closure of the hydrodynamic model. This velocity is maintained by the particles during the time needed to perform the random movement, which is dependent of the local turbulent mixing length (Miranda et al., 1999). This represents another advantage of the shared architecture, as turbulent quantities are made available to the Lagrangian module in real time throughout the run.

Wind-waves may contribute to the advection of the oil particles through three different mechanisms: 1) through a wave-induced net transport in the direction of wave propagation, broadly known as Stokes drift (Stokes, 1847); 2) through the induction and/or modification of nearshore currents as a result of wave-induced stresses, known as wave radiation stresses (Longuet-Higgins and Stewart, 1960); 3) through turbulence by injecting turbulent kinetic energy (TKE) at the surface to simulate the effect of breaking waves (Craig and Banner, 1994). Although all the above mechanisms are accounted in MOHID code, only Stokes drift was considered in this work. Wave-induced stresses are particular important to simulate processes in the nearshore and breaking zone, which, although important to model more accurately the dynamics of oil spills near land, is out of the scope of this study. Nearshore processes encompass even higher grid resolutions requirements to the ones considered in this approach, making them infeasible to be used in this operational modelling system. The effect of breaking waves in the turbulence, as proposed by Craig and Banner (1994), can be simulated with the injection of TKE at the surface that leads to a thin surface boundary layer, in which the vertical transport of TKE and its dissipation approximately balance. This layer is sometimes called the transport layer. As shown by Craig and Banner (1994), an analytical solution for the one-equation model can be derived, but only inside the transport layer, according to which the TKE (and all other turbulence quantities) follows a power-law. In this study this effect was not considered, as the model vertical resolution at the surface (3m in the first layer) is not high enough to effectively simulate this transport layer.

The stokes drift (u_{5i}), is defined as Fernandes et al., 2013:

$$u_{5i} = a^2 \cdot \omega \cdot k \frac{cosh\left[2 \cdot k\left(z-h\right)\right]}{2 \cdot sinh^2\left(k \cdot h\right)} + C$$

Equation 9

where h (m) is the water depth, z (m) is the depth of the particle, a (m) is the wave amplitude ($a=H/2$), ω (rad/s) is the wave circular frequency ($\omega=2\pi/T$) and k (m^-1^) is the wave number. C is a depth dependent term:

$$C = -\frac{a^2 \cdot \omega \cdot sinh(2 \cdot k \cdot h)}{4 \cdot h \cdot sinh^2(k \cdot h)}$$

Equation 10

The wave parameters from SWAN are interpolated to force the Lagrangian module. To simulate the weathering processes that affect a spill in the ocean, the lagrangian module interacts with the oil-weathering module (Janeiro et al., 2008). This module calculates the physical processes of the oil (density and viscosity) and the weathering processes (e.g. evaporation, dispersion, emulsification, dissolution) that affect them. A detailed description of the MOHID oil module and the oil weathering processes implemented can be found in Janeiro et al. (2008).

3. Model validation

3.1. Hydrodynamic validation

Data collection effort to validate a system of models such as the one presented is a demanding task, thus it was decided to use available data provided freely by the scientific community (e.g Coriolis and MyOcean portals). The stations used for validation of both hydrodynamic and wave models are presented in Figure 6A. To estimate the quality of the comparisons, quantification of the differences between measured and modelled elevations were performed using the Pearson correlation coefficient (R) defined as:

$$R = \sum_{i=1}^{i=N} \frac{\left(\hat{\partial}_i - \bar{\partial}\right)\left(\partial_i - \bar{\partial}\right)}{(N-1)S\hat{\partial}S\partial}$$

Equation 11

where $\hat{\partial}$ represents model predictions, ∂ represents the observed values, N is the sample size, and $S\hat{\partial}$, $S\partial$ are the sample standard deviations of the model predictions and observed values respectively. When measuring the linear relationship between two interval level variables, the stronger the association of the two variables, the closer R will be to either +1 or -1 depending on whether the relationship is positive or negative, respectively.

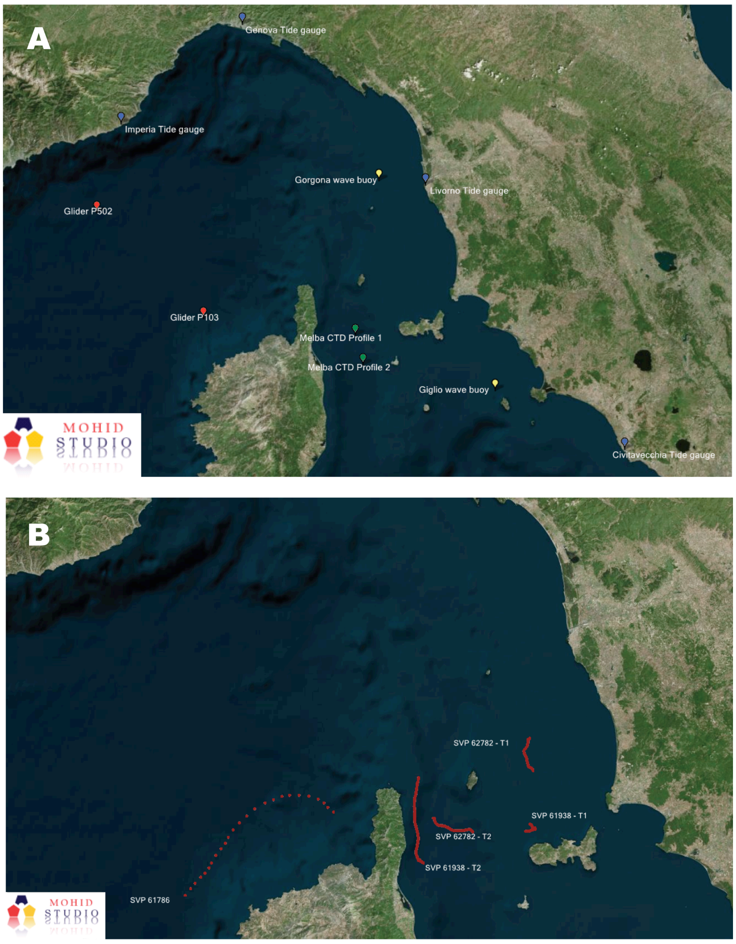

Figure 6 - A: Geographical location of the stations used to validate the hydrodynamic and wave models; B: Drifter's trajectories used to validate the lagrangian model.

The water height results given by the model were assessed using tidal gauge data from Istituto Superiore per la Protezione e la Ricerca Ambientale (ISPRA) network of coastal monitoring stations from 14-07-2012 to 31-07-2012. In order to avoid high frequency signals present in the tidal record, a Fourier analysis was performed in both modelled and observed data, using the methodology proposed by Pawlowicz et al., (2002). This filter is needed as the forcing solution from FES does not include subinertial (meteorological) components. From this analysis, significant constituents were retrieved and used to synthesize the elevation for each station.

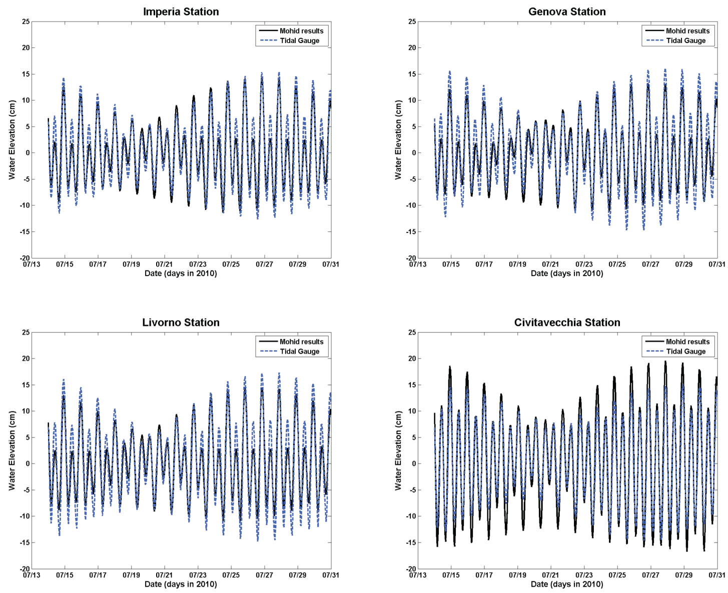

Figure 7 - Comparison between observed and modelled tide elevation in four tide gauge stations along the Italian coast.

Figure 7 shows the comparison between observed and model results, while Table I resumes the *R* values obtained. The modelled elevation results can be considered good reproductions of the observed elevations.

Table I - Estimated errors between observed and modelled water level results for each tide gauge station considered in the study.

Station	***R***
Imperia	**0.9549**
Genova	**0.9469**
Livorno	**0.9565**
Civitavecchia	**0.9832**

Two glider profiles located near the model boundary (Figure 6A) were used to validate the model ability to reproduce vertical variations in temperature, salinity and density.

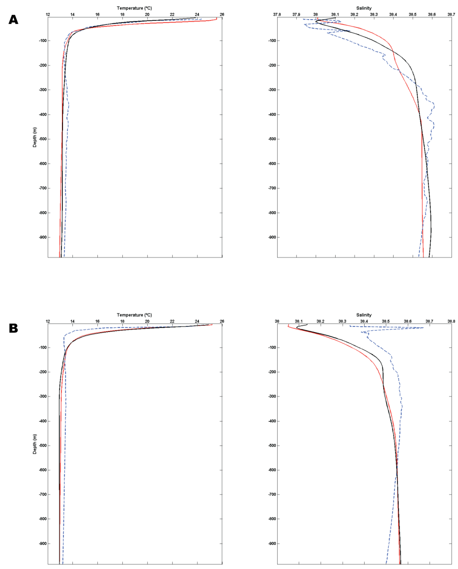

Figure 8 - Temperature and salinity vertical profiles in glider station P103 (A) and glider station P502 (B). MOHID results (red) are plotted against the observed glider profile (blue), both compared with MFS forcing conditions (black).

Figure 8 shows the comparison between the two glider profiles and Level 2 results for temperature and salinity. A profile from the MFS forcing solution was also considered here to assess the behaviour of the boundary conditions implemented. For each of the two glider profiles, both MFS and the Level 2 have R value above 0.9 for temperature, while for salinity R is above 0.6 in profile 502 and above 0.9 in profile 103 (**Table II**). R values between Level 2 and MFS are quite similar, showing a good performance of the boundary conditions chosen. Two CTD profiles collected by the French Oceanographic unit Europe, managed by Ifremer, during the campaign MELBA-2011 were used to validate the high resolution Level 3 (**Figure 9**).

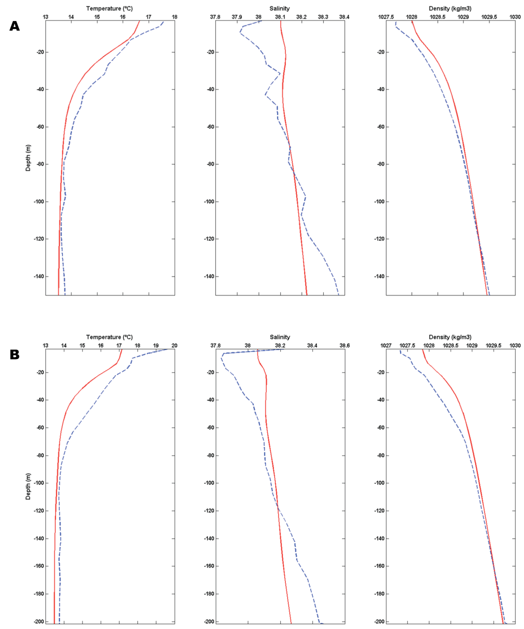

Figure 9 - Temperature, salinity and density vertical distribution for CTD profile 1 (A) and CTD profile 2 (B). Model Level3 results (red) and CTD observations (blue).

A quantitative analysis of these results is presented in Table II. *R* values are above 0.9 for temperature in both CTD profiles, while property salinity is above 0.8 on CTD profile 2, being better represented on CTD profile 1.

Sea surface temperature (SST) from Level 2 was compared with satellite images from MODIS Aqua SST in three different seasonal conditions (Winter, Spring and Summer). Satellite data was retrieved from NASA's Ocean colour webpage (NASA, 2012) and it consisted on a dataset of 10 days in the months of January, April, May, July and August 2012 for MODIS binned 4km (night time 11µm) daily images. From this dataset of images a quality control was applied. Based on the flagging methodology only "excellent data" (FLAG 1) was considered.

Table II - Error estimation between MOHID results, GLIDER observations and MFS forcing (Level2) and between MOHID results and CTD profiles (Level3).

Model	*Profile*	*Property*	*R*
MFS	*GLIDER_P502*	*Temperature*	0.9166
		Salinity	0.6413
	GLIDER_P103	Temperature	0.9782
		Salinity	0.9464
MOHID	*GLIDER_P502*	Temperature	0.9357
		Salinity	0.6778
	GLIDER_P103	Temperature	0.9738
		Salinity	0.9350
MOHID	CTD Profile 1	Temperature	0.9879
		Salinity	0.9386
		Density	0.9981
	CTD Profile 2	Temperature	0.9740
		Salinity	0.8879
		Density	0.9967

Figure 10 shows the comparison between MODIS daily 4km and Level 2 for the periods described above. Qualitatively, the results indicate a good agreement between Level 2 and MODIS. The main features in the images are reproduced to a good extend by the model throughout the three scenarios, with a small bias in the maximum temperatures registered.

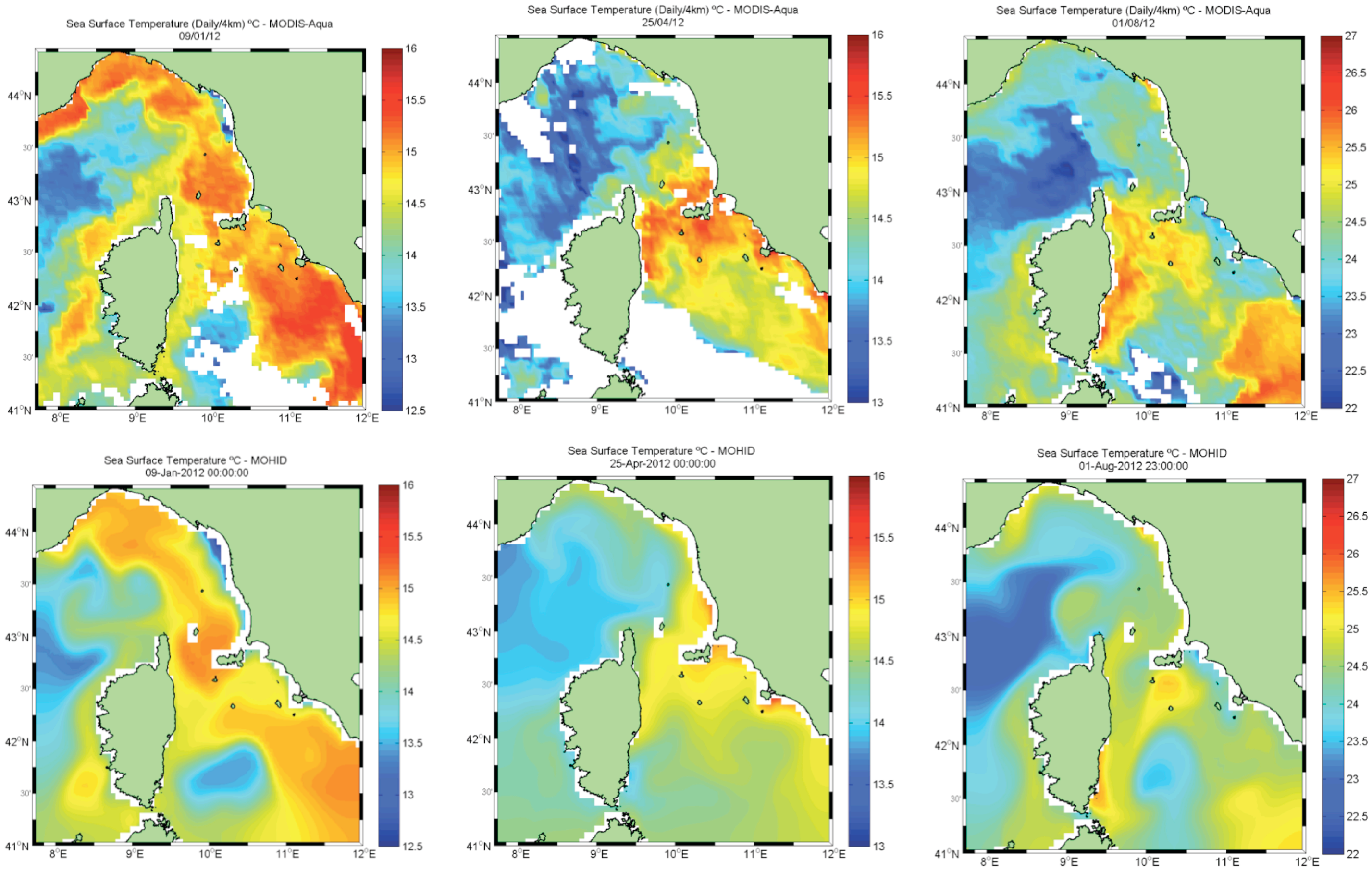

Figure 10 – Comparison between MODIS 4km daily SST images (top) and MOHID Level 2 (bottom) SST results for three seasonal periods in 2012. From left to right, Winter, Spring and Summer situations.

3.2. Wave model validation

The SWAN model implementation was validated using data from two wave buoys available in the study area (Figure 6A). A time-series comparison between H_s, and mean wave period (T_m) parameters obtained from the wave buoys and those computed by SWAN for December 2009 and February 2010 is presented, respectively, in Figure 11A and Figure 11B.

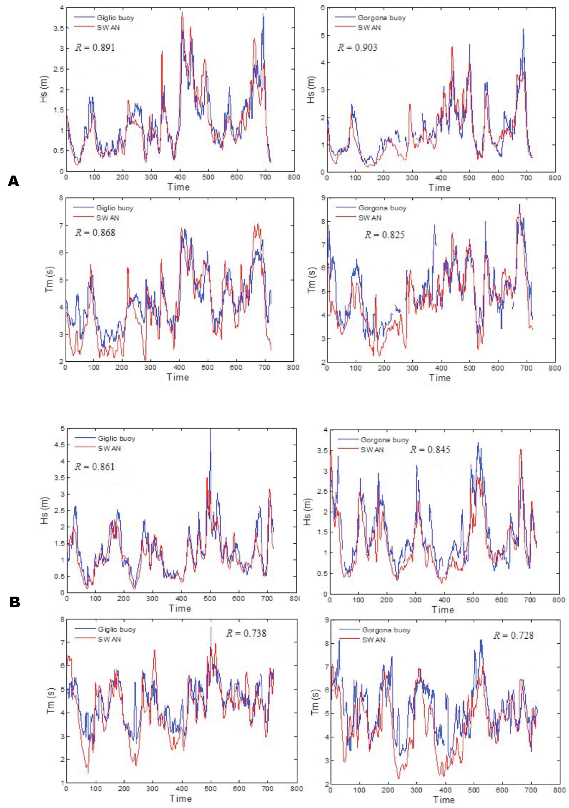

Figure 11 - Accessing SWAN H_s and T_m performance against Giglio and Gorgona wave buoys during: A) December 2009 and B) February 2010.

Statistics for the above comparisons, obtained in accordance to Equation 11, are included in the figures. Generally a good agreement between SWAN H_s and measured H_s exists, whilst a fairly good agreement is found for T_m. SWAN seems to underestimates the wave height at the area, leading always to a negative relative bias. Nonetheless, it is observed herein that SWAN H_s underestimation is common in low to medium values of H_s whilst H_s peaks are occasionally overestimated. An overall underestimation of T_m is observed. More specifically, and in terms of statistics, in December 2009 at Giglio (Figure 11A), H_s underestimation by SWAN around H_s peaks is up to 34% (peak at 573 hr). Overestimation of H_s by SWAN ranges from 5% to ≈ 30% at the 336 hr peak. During the high storm of long duration between 400 and 500 hr, SWAN overestimates H_s by up to 11% with the overall R being 0.891. At the same buoy, in February 2010 (Figure 11B), the picture shows again a H_s underestimation, which varies from 18% to up to 60% around the 500 hr peak. Occasional H_s overestimation does not exceed 10%. The overall statistics are similar to the ones obtained for December 2009. At Gorgona, alike the situation at Giglio, SWAN H_s overestimation occurs mainly in December while in February underestimation is dominant. The former is mostly less than 10% whilst the latter varies mostly within the range 16 – 30%. The overall statistics are generally worse than those obtained at Giglio (except for R in December). With respects to T_m, this is clearly underestimated by SWAN for T_m < 4 s. This may be partly explained by the typical cut-off frequency of a wave buoy that does not exceed 0.3 - 0.5 Hz corresponding to a wave period of 2 to 3 s, below which the cut-off frequency value is assigned. Nevertheless, some of the high peaks in the record are still overestimated by SWAN. The overall statistics are better at Giglio than at Gorgona. Specifically, R at Giglio is 0.868 and 0.738 whilst at Gorgona is 0.825 and 0.728.

Figure 12 compares SWAN output and wave buoy measurements in terms of wave direction. Specifically, the directional distribution of H_s is depicted in the form of wave roses. Results for both December 2009 (top 4 plots) and February 2010 (bottom 4 plots) are presented. In all occasions, it appears that the dominant directions - SW and W at Giglio and SW at Gorgona - are coinciding with the directions of approach of the highest waves in the time series, being well represented by SWAN. Nevertheless, with the focus on Giglio, the model returns more frequent and higher waves from the dominant sectors in December. In February, SWAN waves from these sectors match better the observations in terms of percentages but remain somewhat higher.

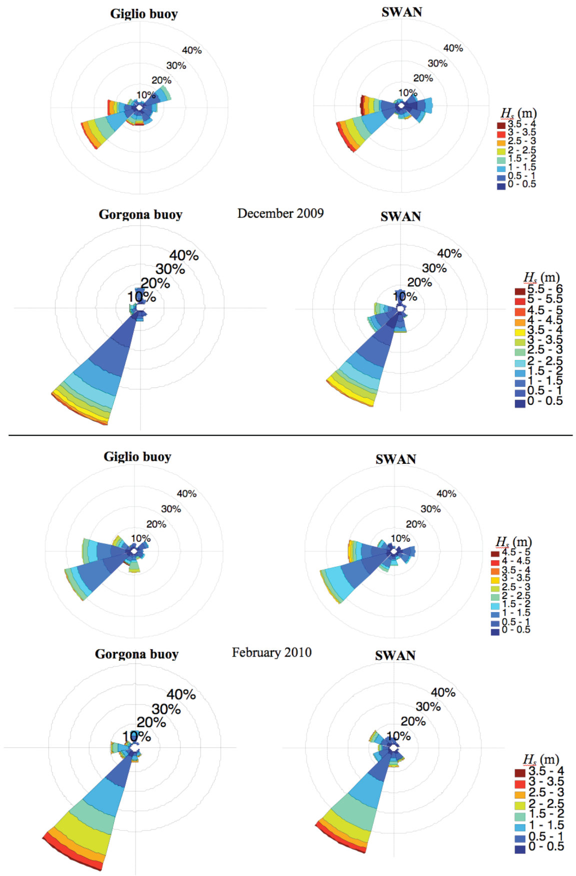

Figure 12 - Directional distribution of Hs obtained from the wave buoys (left) and output from SWAN (right) for December 2009 (top) and February 2010 (bottom).

3.3. Lagrangian model validation

Several studies (e.g., Thompson et al., 2003; Barron et al., 2007) suggest that model simulated drifter trajectories can be directly compared with independent drifter experiments. Model drifters are released in the location where satellite-tracked drifters are observed, and their separation distance is a direct measurement of the trajectory model skill. This method was carried out using available published data from 5 Surface Drifting Program (SVP) drifting buoys with an anchor depth of 50 m (Figure 6B) and sparse in time. The data was collected and made freely available by the Coriolis project and programmes contributing to it (http://www.coriolis.eu.org). The buoys positions were compared with the simulated trajectory of 200 lagrangian particles during two days. The total release may be envisaged as a particle “cloud” which represents the probability of the buoy position, being thus described as a “probability cloud”. In this approach a particle cannot be subdivided and is unable to interact with other particles.

The multi-mesh approach ensures that the high-resolution hydrodynamics (Level 3) is used whenever the particles move into its geographical boundaries. Turbulent diffusion coefficients were adjusted to better represent the drifters spreading. The cloud of lagrangian tracers will spread based on this turbulent diffusion coefficient (K_x), therefore high current velocities will increase tracers spreading due to high standard deviations for the random velocities. The optimal combination was then considered to be K_x = 0.05 and K = 0.0 for the turbulent diffusion coefficients. To compare the buoy trajectory with the model results, the centre of mass of the lagrangian particles outputted by the model was calculated. The centre of mass in a system of cloud particles is defined as the average of their positions, weighted by their masses (m):

$$\bar{X} = \frac{\sum m_i x_i}{\sum m_i}, \quad \bar{Y} = \frac{\sum m_i y_i}{\sum m_i}$$

Equation 12

To access the performance of the model, a Lagrangian trajectory-based non-dimensional index proposed by Liu and Weisberg (2011) was applied. Defined as:

$$s = \sum_{i=1}^{N} d_i \Big/ \sum_{i=1}^{N} l_{oi}$$

Equation 13

d_i is the separation distance between the modelled and observed endpoints of the Lagrangian trajectories at time step i after start, l_{oi} is the length of the observed trajectory, and N is the total number of time steps (Liu and Weisberg, 2011). In this way a total agreement is reflected by an *s* value equal to zero. As an initial step, a model scenario assuming the release of 200 particles at 50 m depth (anchor depth of the drifters) was simulated. The *s* results for the five drifters considering the 50 m model depth are presented in Table III.

Table III - Results obtained for the validation of the Lagrangian module using the Lagrangian trajectory-based non-dimensional index proposed by Liu and Weisberg (2011).

Drifter Code	*Model Depth*	*Stokes Drift*	*S index*
SVP 61786	*50 m*	*Considered*	0.50
	Surface	*Not Considered*	0.42
		Considered	0.44
SVP 61938 T1	*50 m*	*Considered*	0.29
	Surface	*Not Considered*	0.32
		Considered	0.30
SVP 61938 T2	*50 m*	*Considered*	0.65
	Surface	*Not Considered*	0.89
		Considered	0.84
SVP 62782 T1	*50 m*	*Considered*	0.93
	Surface	*Not Considered*	0.31
		Considered	0.37
SVP 62782 T2	*50 m*	*Considered*	0.94
	Surface	*Not Considered*	0.45
		Considered	0.45

At this depth, discrepancies were found in four of the five comparisons, which presented a high *s* with the exception of drifter 61938 T1 (*s* = 0.29).

While several factors might be directly affecting the drifters' trajectories (e.g. change in anchor depth), in practical terms the current velocity responsible for the drifters trajectories is not just the current velocity at the anchor depth but rather an integration of the current velocities from the surface to the anchor depth, along the connecting cable, considering that velocities in depth will have more weight than the ones at the surface due to the drifter's sock. To further investigate the discrepancies, simulations using the surface as release point for the lagrangian particles were run. Since at the surface the main physical factors affecting the model particles are hydrodynamics and the Stokes drift effect, scenarios with and without Stokes drift were simulated. This allowed accessing the impact of the Stokes drift on the ability of the model to reproduce more accurately the drifters trajectories. A clear improvement was achieved in the three of the drifters when comparing their trajectories with the model trajectories at the surface. Exceptions are drifters 61938 T1 and 61938 T2. While for the first drifter the *s* index is almost unchanged throughout the scenarios, for the second drifter the *s* index value of 0.65 at 50 m depth deteriorates to 0.84 and 0.89 for the surface scenarios with and without Stokes drift respectively. Nevertheless the *s* index values achieved for this drifter are relatively high when compared to the ones found for the rest of the drifters. Graphically, **Figure 13**A and **Figure 13**B present the trajectories for the three drifters, that show significant improvement in *s* values when considering the surface. In **Figure 13**A model results (green) are compared with the trajectories (orange) obtained at 50 m depth, while in **Figure 13**B the results obtained for the surface release can be observed for the two Stokes drift scenarios considered: with Stokes drift (red) and without Stokes drift (blue). Regarding the use of the Stokes drift in the simulations, there is no clear trend in the s index results. While for some drifters (61938 T1) an improvement is achieved when including the Stokes drift, for others (62782 T1 and 61786) the same doesn't happen.

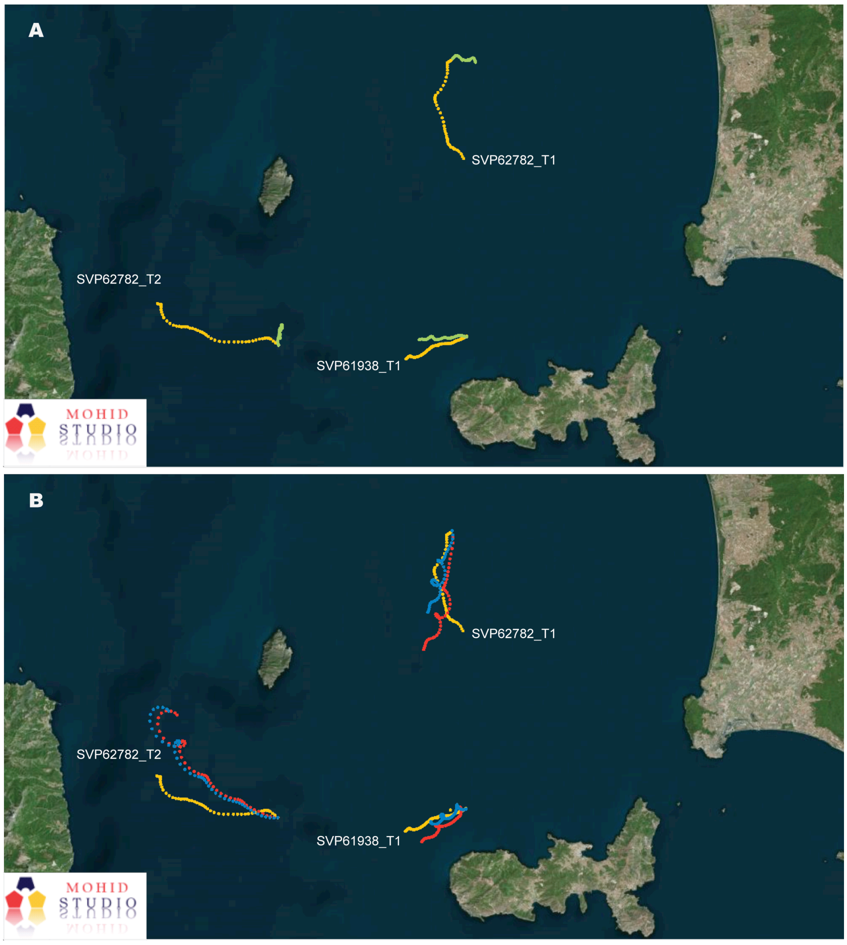

Figure 13 - Lagrangian model validation accessed by comparing the trajectories of drifting buoys (orange) with model tracers centre of mass. A) Validation with tracers trajectories at 50 m depth (green); B) Validation with tracers at the surface considering the Stokes drift effect (red) and not considering it (blue).

4. Discussion

Based on results obtained in the validation procedure, the presented operational system has proved to simulate hydrodynamics, waves and drifter trajectories with good accuracy in the study area. Nevertheless, differences between observations and model results were found and are worthwhile to discuss. As pointed by Price and Bush (2006), the differences between models and observations can be due to many factors: the input fields (winds, waves and currents) are provided by numerical models which have their own errors. Also the satellite-tracked drifters may contain location errors due to their long period at the sea, which directly affects the comparisons. In the hydrodynamics, the bathymetry resolution can explain the differences found between tidal gauge observations and model results. This is more relevant in the proximity of land, where the tidal gauges are located. In these areas bathymetric gradients are sharper, giving a possible explanation to the differences observed. The validation of temperature and salinity in depth, despite the good results achieved, also presented some errors in both glider and CTD profiles. As the major differences between observations and model results occur at the surface (above 100 m), part of the errors can be due to the vertical discretization used in model. The freshwater water balance (Evaporation-Percipitation-Runof) in the region is not being taken into account by the model also explaining part of the errors. This is especially true for salinity, which presents lower R values when compared with temperature. The SST bias verified in the model validation with MODIS images can be explained if we consider that satellite images capture the temperature of the ocean surface skin layer, with a few millimetres thick, while on the other hand, the surface layer in the model has 3 meters due to computation limitations. These different vertical scales can explain the cooling bias observed.

Regarding waves validation, overestimation of the high Hs peaks at Giglio buoy may be associated with waves approaching from W-SW sectors. Besides that, SWAN also produce more waves from the E and SE sectors in the expense of waves from the S and NE. SWAN underestimation of the highest waves directly from the S is noticeable in both months examined. At Gorgona, the highest waves from the dominant SW sector do not seem to be overestimated by SWAN. On the contrary, in December, they appear somewhat underestimated whilst at the same time a lower percentage of waves from this sector are simulated. This overestimation is in agreement with other Mediterranean wave model implementations (e.g. Magne and Ardhuin, 2009) and has been attributed to an underestimation of wind speeds in the Mediterranean Sea, varying from place to place, being more severe over regions of complex orography, especially over the Tyrrhenian Sea (Cavaleri and Sclavo, 2006; Ratsimandresy et al., 2008). In both months, especially in December, modeled waves are more spread around the dominant direction. Furthermore, in

February, SWAN simulates a substantial number of waves from the NW, almost inexistent in the measurements. At the same time, modelled waves from the W and N are less frequent compared to the observations. In terms of statistics, the simulated mean wave direction at Giglio diverges from the measured one by 43° in December and 37° in February. At Gorgona, this deviation is 23° and 26° respectively.

As mentioned above, the lagrangian tracers are forced by the hydrodynamics, the turbulence and the waves, integrating these effects in its movement. This fact makes drifter comparisons a good validation tool for the entire system. In overall terms the lagrangian module is considered validated with results reproducing to a good extend the trajectories of satellite-tracked drifters. While in the initial simulation at 50 m depth (**Figure 13**A) there were discrepancies in the comparisons, they seem to be solved when the surface was considered in the model (**Figure 13**B). This points out for the fact that the hydrodynamics affecting the drifter movement is the entire water column from the surface to the anchor depth of the drifter.

While the model results obtained are considered good reproductions of drifter trajectories, focusing in the ability of the model to solve the Ekman surface layer to a good extend, the fact of considering the surface in the validation, instead of the drifters anchor depth (or for this matter an integrated velocity from the surface to the 50 m depth), may raise the question that the model might be underestimating the surface velocities. As mentioned above, the 50 m anchor depth given for the drifters may not reflect their actual depth, as the sock may have been deteriorated with time since their release. This is a plausible explanation that also encompass the fact the model results at 50 m depth present a better comparison with drifter 61938 T1 than when using the surface. Considering the drifters anchor depth unchanged, in fact, a possible underestimation of the surface velocities may occur. The vertical discretization implemented – that affects the baroclinic component of the hydrodynamics -, together with underestimations in the wind fields calculated by the atmospheric model – affecting the model velocity in the Ekman layer - appear as the most likely explanation for this possibility. With no available current measurements either at surface or at depth to validate the model hydrodynamics, only these hypothetical assumptions can be discussed.

As noted by Price et al. (2006) and later by Abascal et al. (2009), estimating the separation distance between model and satellite-tracked drifter trajectories during short time scales, is useful to assessing applications to oil spill trajectories. Hence, the Lagrangian results were also accessed in terms of absolute distance from model to drifter (**Figure 14**). The improvement when using the surface forcing is clear. In average terms, and except for drifter 61938 T2, the separation distance is approximately 5 km. This value is half the average separation distance when we consider the 50 m depth in the model.

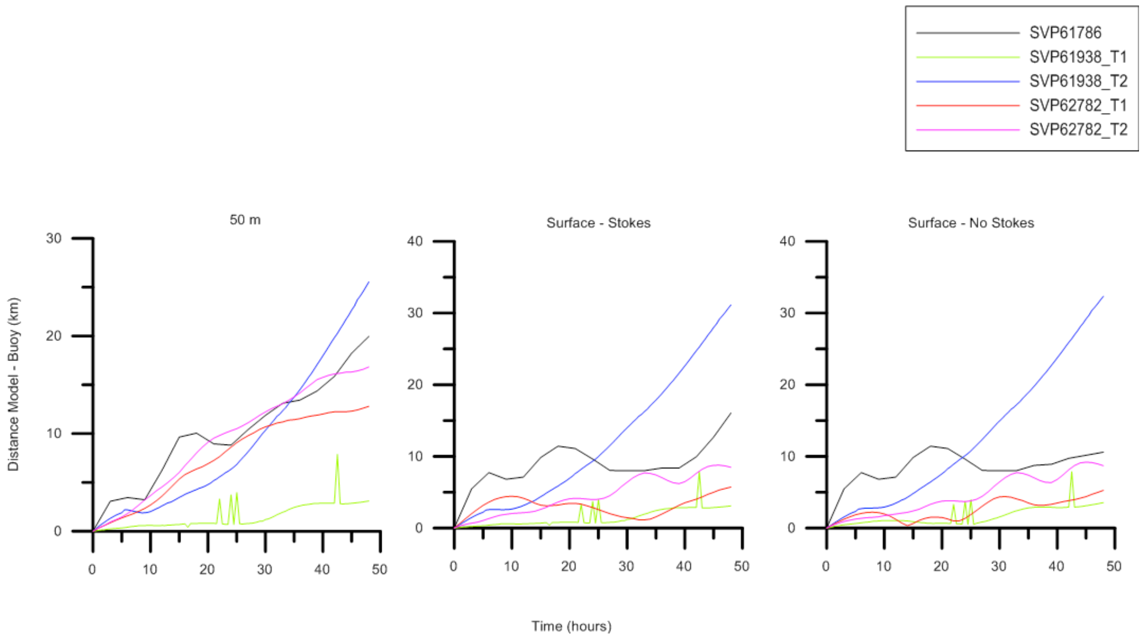

Figure 14 - Distance model to buoy computed for the drifting buoys considered in this study. The depths considered were: 50 m and surface (with and without Stokes drift effect).

Regarding the use of the Stokes drift in the simulations, the differences found are not significant enough to lead to a conclusion. The more likeliness of such differences might be associated with the ability of the wave model to better reproduce the wave fields in some situations than others, as discussed previously. Nevertheless the relative importance of the Stokes drift in the trajectory of oil spills is considered a topic for further research.

The development of fast, easy deployable and semi-automatic mechanisms to create high-resolution emergency oil spill simulations is one of the future applications for this type of methodology. With this approach, coastal areas with complex bathymetries can be easily integrated in regional operational systems and respond quickly to punctual emergency situations. An example was the Costa Concordia accident, which occurred in Giglio Island in January 2012, inside the domain of the operational system. Quickly after the accident this downscaling methodology was applied, and a 250 m grid was created around the accident location as a submodel of Level 3. This configuration of the system was producing operational forecasts during the fuel diesel removal operations from the ship (Figure 15).

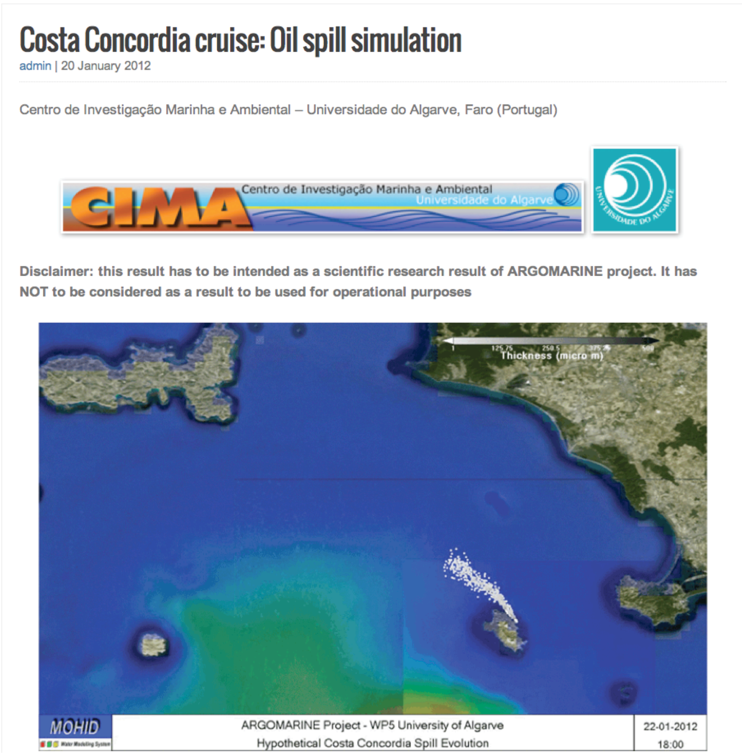

Figure 15 - Operational oil spill scenario simulated during the fuel diesel removal operations from the Costa Concordia ship.

5. Conclusions

An operational model to plan and respond to oil spill accidents was successfully implemented in the Tuscany Archipelago region. The integration of the hydrodynamics, oil trajectories and weathering processes in the same model architecture ensures reduced lagrangian forcing errors, while it allows downscaling the model solutions to very high resolutions. In overall terms the results obtained for the several components of the model were considered very satisfactory and the model considered fit to represent the hydrodynamics of the region. Some discrepancies were identified during the validation of the hydrodynamics and wave models, which were associated with the model resolution, vertical discretization implemented, errors in forcing conditions and errors associated with the numerical limitations of the methods used. Results for the comparison of model trajectories with satellite-tracked drifter trajectories in general were also found precise, with the model presenting a good ability to simulate the drifter's trajectory. This fact, besides adding assurance in the hydrodynamics results, also highlights the advantages of the downscaling methodology used for oil spill simulations, which represents a clear step forward in the operational modelling of oil spill accidents in coastal regions.

Chapter IV - *Towards the development of an operational tool for oil spills management in the Algarve coast*[3]

---

[3] This Chapter was published in the Journal of Coastal Conservation as: **Janeiro, J., Martins, F., Relvas, P., 2012.** ***Towards the development of an operational tool for oil spills management in the Algarve Coast*****. Journal of Coastal Conservation, 16, 449 - 460,**

Abstract

Portugal is strongly vulnerable to sea hazards due to intense vessel traffic and sea conditions. The southwest region off the Iberian Peninsula lies in the main route from the Mediterranean and Southern Hemisphere to the North- ern Europe, causing a ship concentration in a narrow band off Cape São Vicente. Tankers represent a significant part of the vessel traffic and the occurrence of oil spills cannot be disregarded. Cape São Vicente region is part of a Natural Park with 110 Km of coastline, integrated in the European Natura 2000 network and its socio-economic context is closely related with sea resources exploitation, particularly fishing and tourism. Recognizing the importance of accurate information systems for the decision making process in an oil spill situation, this work presents the development of an integrated tool to support the process in the Algarve coast. The system relies in a regional operational mathematical model based on the MOHID modelling system. In the system core, three models (3D hydrodynamics, wave and Lagrangian transport) are all linked in the same system exchanging information in real time. Oil advection and weathering processes are coupled to the Lagrangian transport model. The overall operational system includes external operational data products as inputs, to ensure a successful validation of the results. The system is linked to stakeholders and response authorities using a geographic referenced database based on Mapserver technology that will include relevant information for oil spill management.

1. Introduction

The increase of human occupation in the world coastlines makes oil spill impacts more harmful today than 40 years ago. Nowadays, impacts in industries like tourism, aquaculture and energy must be added to the impacts on the environment and fishing. If we also add the growing environmental awareness among the general public and media coverage, the response decision to oil spills becomes a politically sensitive task.

The processes that govern both the transport and weathering processes of oil in water are complex and depend not only from oil characteristics, but also from the hydrodynamic and atmospheric conditions at the spill site (Mackay and McAuliffe 1988). To deal with this complexity and trans- form it in a predictable solution, operational modelling systems assimilating observed sea state an atmospheric data, coupled with models that can simulate the oil weathering processes are required.

In fact, monitoring and forecasting the fate of marine pollution, including oil spill, is one of the focus applications in operational oceanography with most coastal nations supporting monitoring and response services for oil spill response. Although prediction services can play an important role in decision-making during incidents, their use can be extended for designing the response services (Hacket et al. 2008).

A good link between the operational results and stakeholders is another key element in these types of operational instruments. Due to the vast array of different environmental and socio-economic impacts of a spill, a multitude of stakeholder groups with diverging interests are expected and should be address during the development/planning phase of the system.

The aim of this work is to present a new approach towards an integrated tool for decision making and emergency response for the Algarve coast, that addresses not only authorities directly involved on the pollution accident, but also regional and local stakeholders that might be affected.

2. Regional background

The Algarve coast (**Figure 16**) is one of the most important touristic regions of Portugal and Europe, and a particular good example of an economically and environmentally highly sensitive coast to an oil spill accident. From the natural point of view this region is characterized by high litologic diversity, with two major types of shoreline, rocky- cliffs and sandy beaches as described by Dias, 1988, and for encompassing several important natural parks. Examples are the Ria Formosa Natural Park, a natural reserve with more than 18000 ha and an important hide-away for migrating birds, as well as a nursery ground for many marine species (Bebiano 1995). Near Cape São Vicente, where the western and southern Portuguese coasts intersect subjected to the constraint of abrupt topography, the Natural Park do Sudoeste Algarvio e Costa Vicentina with an area of 74500 ha and 110 Km of coastline (part of the Natura 2000 network) and the protected Biogenetic Natural Reserve are filled with a wide biodiversity of different species and natural habitats, many of which are quite unique in the world.

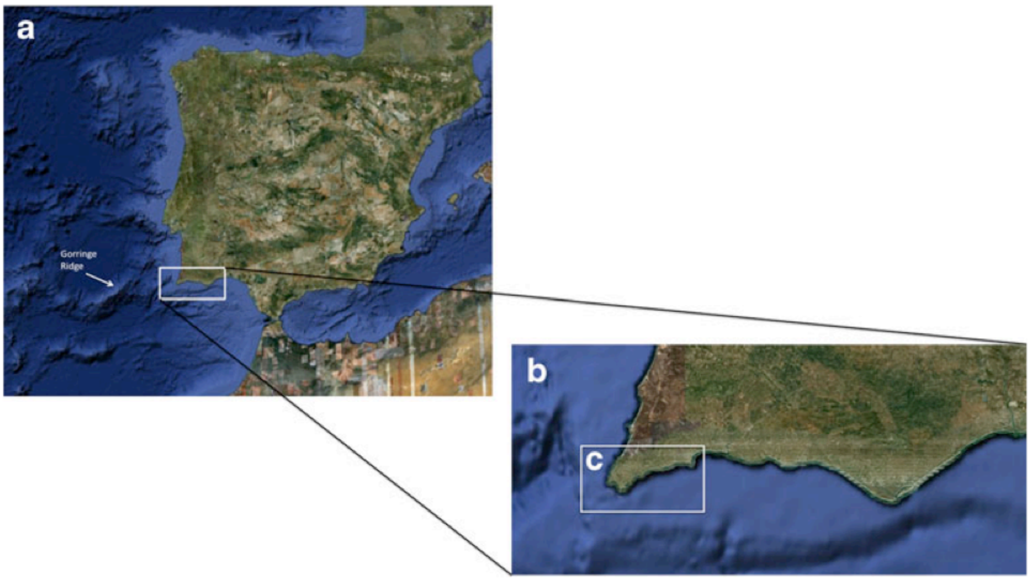

Figure 16 - Geographical location of the study area: a—The Iberia Peninsula b—Algarve coast; C - Cape São Vicente. Adapted from Google Earth, Google™.

Due to a concentration of shipping routes (**Figure 17**) between land and the Gorringe Ridge seamount, the Northwest area offshore of the Cape São Vicente is one of the most problematic areas of this coast when considering a potential oil spill accident.

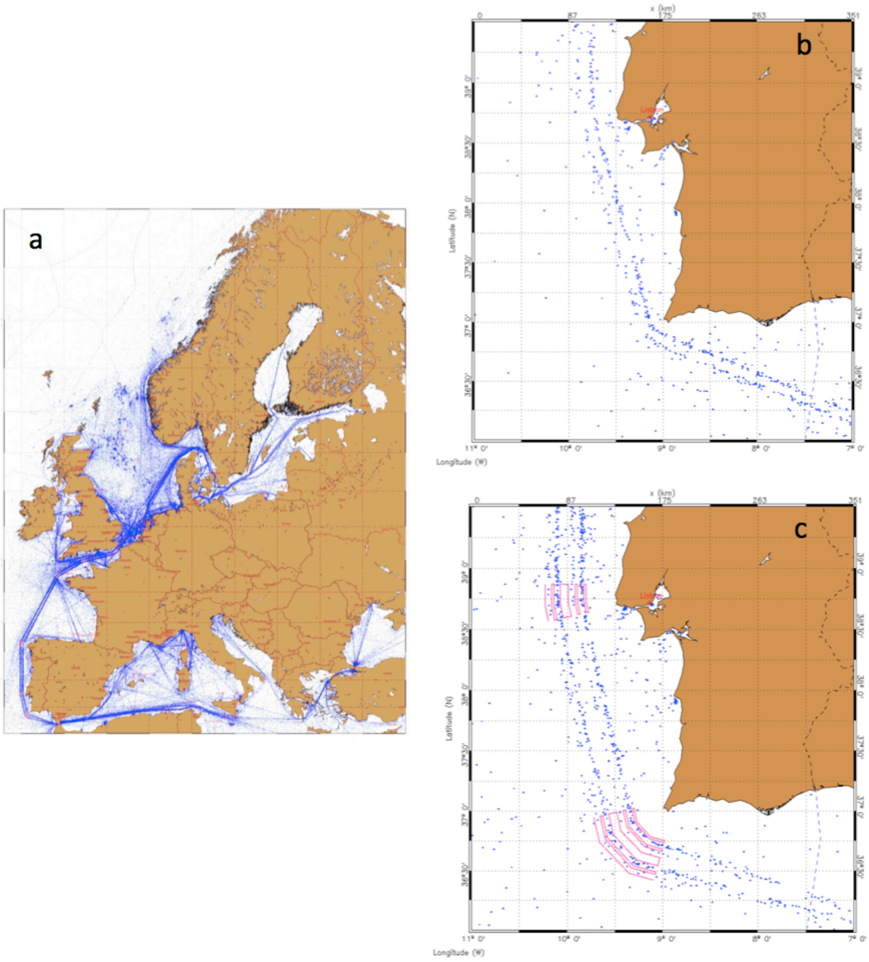

Figure 17 - Cumulated ship route map in European waters between 2002 to 2009 a and ship maps data acquired before b and after c the amendment on the existing separation scheme for Cape da Roca and Cape São Vicente implemented on 1 July 2005 by the Maritime Safety Committee. Data derived from the Advanced Synthetic Aperture Radar (ASAR) instrument on European Space Agency (ESA) Envisat satellite. Courtesy of ESA.

Exact figures are difficult to obtain, but the region lies in the main route from the Mediterranean and Southern Hemi- sphere to the Northern Europe (**Figure 18**). Tankers represent a significant part of the vessel traffic and the occurrence of oil spills cannot be disregarded.

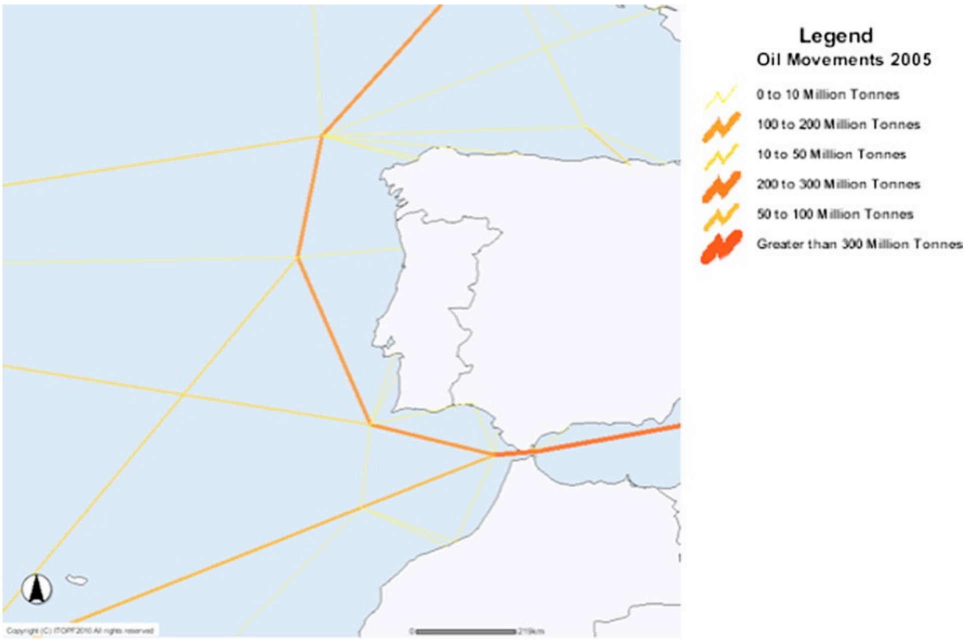

Figure 18 - Oil movements in the Iberian Peninsula during 2005. Source: The International Tanker Owners Pollution Federation Limited.

The regional socio-economic system is closed linked to the sea. The economy of the region relies 46.0 % on the tourism, mainly in the coastal area, that represent directly 44.7 % of the regional Gross Domestic Product (GDP) and 37.1 % of the employment. Fisheries represent 3.7 % of the regional employment against 0.7 % at national level (INE— Instituto Nacional de Estatística 2008).

Recently, the Prestige accident and oil-spill crisis entered the statistics of oil spills occurring in the Iberian Peninsula. The spill entered the top 100 world Tanker incidents as shown in **Figure 19.** This accident highlighted the limitations of the Spanish operational oceanography capability to respond effectively to a crisis of this nature. Particular shortcomings were identified, the lack of operational systems able to forecast currents and transports being the most pressing one Sotillo et al., 2008. The maximum amount available for compensation under the 1992 Civil Liability Convention and the 1992 Fund Convention in respect of the Prestige incident is €171.5 million while the figures given in May 2003 by the Governments of the three States affected by the incident (Spain, France and Portugal) as to the damage caused, indicated that the total amount of the damage could be as high as €1 050 million (IOPCF 2009).

Figure 19 - Top 100 world Tanker incidents. A zoom into the Iberian Peninsula. Source: The International Tanker Owners Pollution Federation Limited.

3. State of the art

In Europe operational oceanography and data assimilation systems have been growing in importance for the last few years. All these systems use different operational capacities, data streams and expertise. They aim to support a wide range of scientific and operational services and applications including oil spill monitoring, marine safety as well as offshore oil industry Daniel and Dandin, 2005. Examples are the POSEIDON System (Nittis et al., 2001), and the CYCOFOS-MEDSLIK system (Zodiatis et al. 2003a, b, c; Lardner et al. 1998).

Funded by the Financial Mechanism of the European Economic Area (EFTA) and the Hellenic Ministry of National Economy, the POSEIDON system has been developed and operated by the Hellenic Center for Marine Research (HCMR). It is based on OCEANOR's Seawatch System, (Hansen and Stel 1997), consisting of separate yet interrelated components. The spine of POSEIDON is an integrated

network of ten oceanographic buoys and ten wave buoys deployed in several locations in Greece, equipped with a variety of sensors for monitoring the sea environment. Properties like wind speed and direction, air pressure and temperature, surface water temperature, sea-surface current speed and direction, wave height and direction, water temperature and salinity, dissolved oxygen, chlorophyll-a and nitrates are measured, quality controlled, stored and pre-processed in a automated way through a computing system and software present in all sensors and are near real-time remotely transmitted to the Operational Centre of HCMR by a two-way telecommunication. The control and surveillance of the POSEIDON system is made through the Operational Centre located at HCMR's installations. POSEIDON forecast ability comes from the Aegean Operational Forecasting System (AOFOS), which consists of a set of separated but interacting numerical simulation/forecast models adapted to the Greek seas environment. They consist of a weather prediction model, an open sea wave forecast model, a 3D hydrodynamic model, a shallow water wave prediction model and a buoyant pollutant transport model. A detailed description of the system and a preliminary evaluation of its forecasting skill are included in Nittis et al. (2001).
The POSEIDON OSM (Oil Spill Model) can be started through a web based user interface and can be used either in forecasting mode for the next 5 days or in hindcasting mode using the archived data. The user is allowed to submit into the system oil spill simulation scenarios by providing all the required parameters. The final output (**Figure 20**) consists of a series of sequential graphs showing the oil spill dispersion for the requested time period (Soukissina and Chronis 2000).

CYCOFOS (Operational Cyprus Coastal Ocean Forecasting and Observing System) has been developed within the framework of several European research projects promoting operational oceanography.

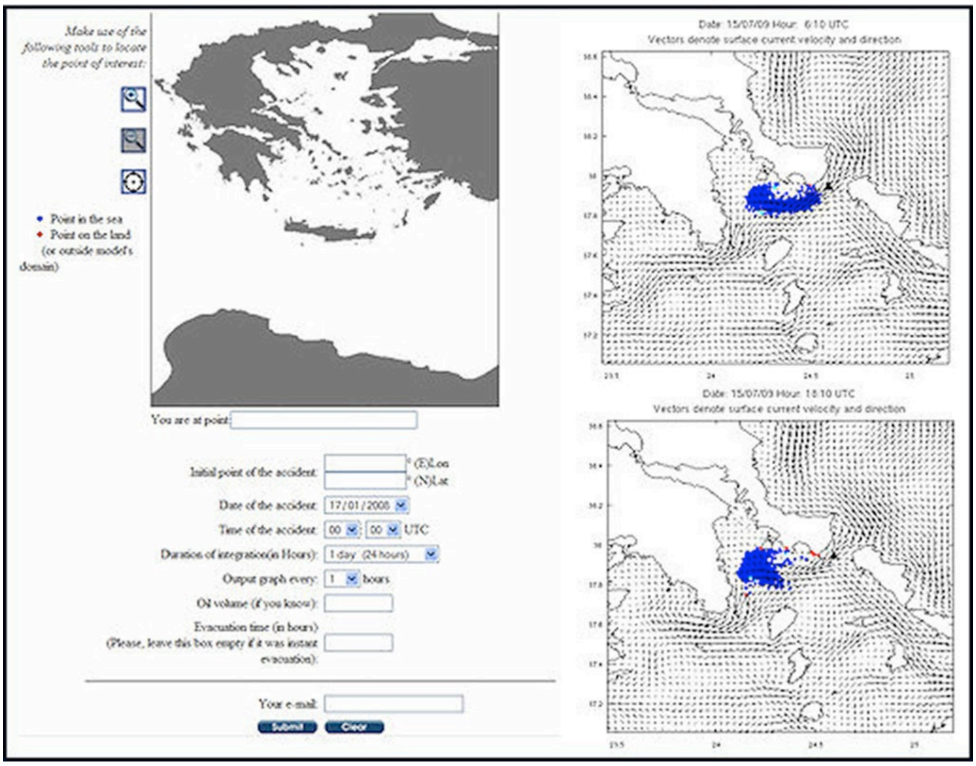

Figure 20 - Output of the POSEIDON OSM and its web based GUI. Adapted from http://www.poseidon.hcmr.gr.

The system provides near real time forecasts of sea currents, water temperature, salinity, sea level, significant wave height and direction and covers the sea areas around Cyprus, the Levantine Basin, and Eastern Mediterranean. CYCOFOS model architecture (**Figure 21**) consists in several modules. The 7 km resolution Mediterranean Forecast System (MFS), detailed in Pinardi et al., (2003), supplies the forcing data to the sub regional, 3 km resolution, Aegean Levantine Eddy Resolving model (ALERMO) through one-way nesting (Korres and Lascaratos 2003). The atmospheric forcing comes from SKIRON weather forecast system (Kallos and the SKIRON group 1998), one-way coupled with ALERMO.

The Cyprus Ocean Model (CYCOM), described in detail in Zodiatis et al. (2003a, b, c) is the high resolution model in CYCOFOS, with a spatial step of 1.5 km. Its boundary conditions are supplied from ALERMO 5 day's forecasts and high frequency (hourly) meteorological forecasts from SKIRON. For offshore wave forecasts, CYCOFOS uses WAM model (WAMDI Group 1988) in a three levels domain. The intermediate level, the Levantine basin, is nested with the

Mediterranean wave forecast model (first level) and forced with wave height and direction, together with SKIRON wind velocity, every 3 h. Waves around Cyprus (third level) are simulated with a high-resolution SWAN model (Holthuijsen et al. 1997), forced by the wave conditions obtained from the second level domain, and by hourly SKIRON winds (Zodiatis et al. 2005).

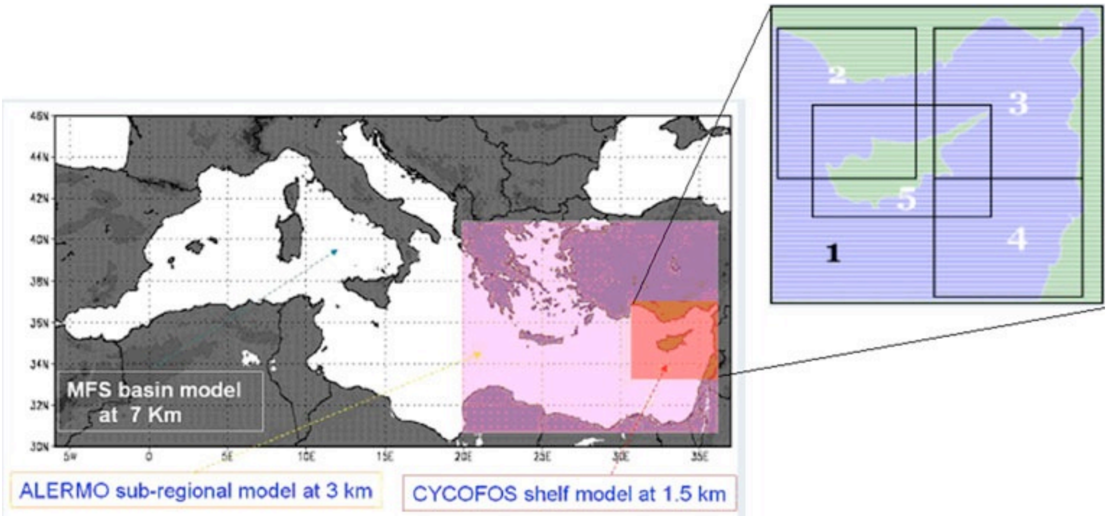

Figure 21 - CYCOFOS model architecture. MFS as the higher domain supplies the boundary conditions to the ALERMO sub regional model that in turns forces the high resolution CYCOM. A zoom showing the five regions users can select for more detailed information. Adapted from http://www. oceanography.ucy.ac.cy/cycofos.

CYCOFOS components are all integrated within a network of near real time data from observations. The MFS assimilates two satellite altimeters along track data, satellite daily sea surface temperature, and vertical hydrological profiles of Temperature (T) and Salinity (S) from XBT and ARGO profilers as described in Dobricic et al. (2005, 2006). Levantine Basin is being monitored through an ocean observation station, MedGOOS-3, that measures conductivity and temperature and pressure and communicates with CYCOFOS by satellite. A coastal station, MedGloss, located in Paphos (Cyprus) supplies the operational system with coastal levels, water temperature and air pressure. A satellite ground receiving station, operational since 2001 collects sea surface temperature images from NOAA

AVHRR satellites, and clorophyll-a images using NASA MODIS AQUA (Zodiatis et al. 2003a, b, c). MEDSLIK is a 3D oil spill model designed to predict the transport, fate and weathering of an oil spill and has been coupled operationally to the MFS, CYCOFOS, ADRICOSM, ROSARIO operational ocean forecasting systems, as well with the SKIRON weather forecasting system, for the Levantine, Adriatic, Central Mediterranean and the entire Mediterranean. The MEDSLIK oil spill model in preoperational mode was first developed in 1997 (Lardner et al. 1998) to assist the objectives of the EU LIFE project "Sub regional contingency Plan for Preparedness and response to Major Pollution Incidents in the Eastern Mediterranean-Levantine". The MEDSLIK algorithms are based on an earlier version of the OILPOL model (Al-Rabeh et al. 1995). It uses REMPEC's list of over 200 oils together with their physical parameters and communicates with the user through a software package (**Figure 22**) that requires as input data the type of oil and its characteristics, wind field, sea surface temperature and three-dimensional sea currents. Within the frame of several EU research projects MEDSLIK has improved substantially.

In Portugal a national contingency plan - "Plano Mar Limpo" (Clean Sea Plan) - was approved in April 1993. This plan gives overall responsibility for spill response to the National Maritime Authority (Autoridade Marítima Nacional) and, in particular, to its coordinating body, the Maritime Authority Directorate General (Direcção-Geral da Autoridade Marítima), all part of the National Navy. This response however is more related to the containment and recovery at sea, and clean-up operations in shore, the operational models to forecast spill trajectories and to assist field operations are being developed and maintained by the Hydrographic Institute (Instituto Hidrográfico), part of the Portuguese Navy, in charge of supporting the Navy actions in the field of marine science and technology.

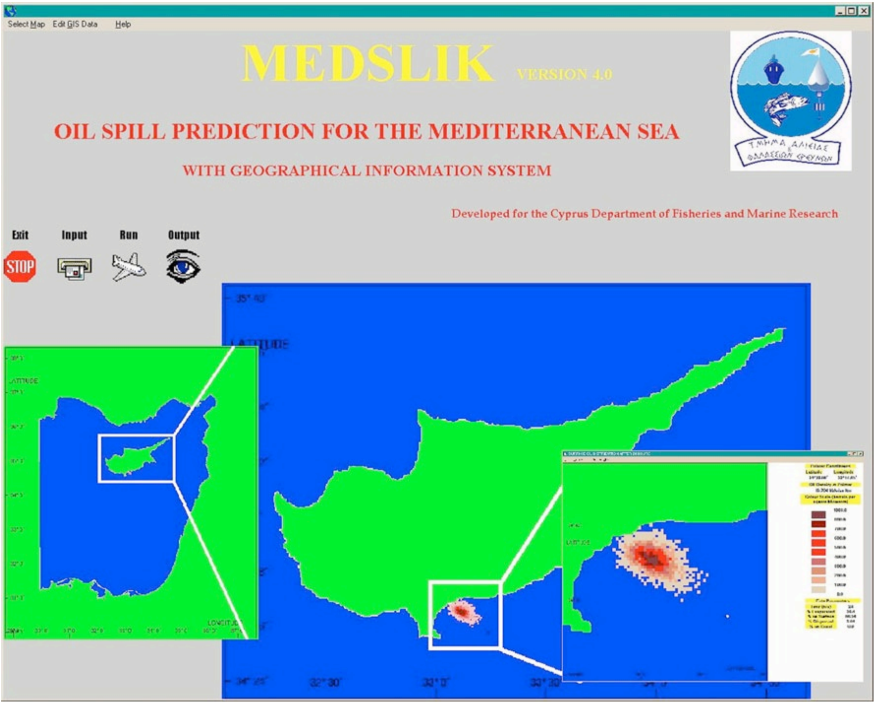

Figure 22 - The MEDSLIK software graphical user interface.

Similar to the operational systems described above the Hydrographic Institute (IH) developed the MOCASSIM system. It uses a broad range of observations provided both from IH observational networks (wave buoys, tidal gauges) and programs (hydrographic surveys, moorings) as well as from external sources. The MOCASSIM system integrates a circulation model based on the Harvard Ocean Prediction System (HOPS) and a wave model based on the Wave-Watch3 (WW3) model, which provides wave conditions in the North Atlantic basin, and on the SWAN model that is used to improve the wave forecasts on coastal or other specific areas of interest. Meteorological forcing is accomplished in the framework of collaboration with the Portuguese Meteorology Institute using ALADIN model predictions for the entire country (Vitorino et al. 2003).

For the prediction of oil spills the system uses a simple trajectory model, that doesn't take into account oil weathering processes, instead it relies on a more accurate characterization of the sea and wind state to forecast spill trajectory. Future IH strategy for operational modelling is divided in the implementations of new numeric models, like ROMS and HYCOM, to improved operational forecasts, the deployment of real time data observation systems to support the modelling forecasts and the development of an oil spill module to include in the operational system (Vitorino, J., personal communication, February 1st, 2010).

The MOCASSIM system has already been used in several operational contexts. These included the operational environmental assessment during both national and NATO navy exercises and the monitoring of the oceanographic conditions in the NW Iberian area affected by the oil spill of MV "Prestige". The system is also being used in the framework of national and European funded projects in the on-going research on the oceanography of the Portuguese continental margin, which is presently being conducted at IH (Vitorino et al. 2003).

4. A new approach

As previously mentioned the main goal of this work is to create an operational model for the Algarve coast, with the ability to predict the behaviour and evolution of an oil spill in the marine environment and linking it to an online risk assessment/contingency response tool available for stakeholders. The system will include a set of mathematical models to predict the hydrodynamic conditions of the sea surface (wind, waves, currents, temperature, salinity) and to simulate the drift and dispersion of oil spills after pollution events. For this purpose the MOHID water modelling system (Martins et al 2001; Balseiro et al 2003; Leitão et al 2005) will be used. It is a modular system including modules for several processes of the marine environment (physical, chemical and biological). For this study the Hydrodynamic, the Lagrangian transport, and the oil spill modules will be used. This modular system where all the modules are included in the MOHID architecture is the main difference when comparing with the operational systems described before, as it allows the exchange of information in real time between all the modules. As an example, running simultaneously the Lagrangian module and the Hydrodynamic model allows the exchange of turbulence information in real time between both modules, with practical results when simulating an oil spill. This type of approach also eliminates the need for data interpolation and increases the uniformity of the data analysis methods used by the model. Local implementations of high-resolution mathematical models including a 3D hydrodynamic model, a wave model and an oil spill model are being developed for the Algarve coast. Due to its geographical location (close to the main routes for oil ships that come from the Mediterranean and Africa towards north), complex current system, biological diversity and irregular shoreline Cape São Vicente will be a particular case study inside the Algarve region. For that, a submodel will be created for this area (son model), and linked to the Algarve model (father model) in a one-way downscaling scheme (**Figure 23**), where the communication between the father and son models is made by relaxation of the zonal and meridional horizontal velocity components, through an 11 cell band adjacent to the lateral boundary.

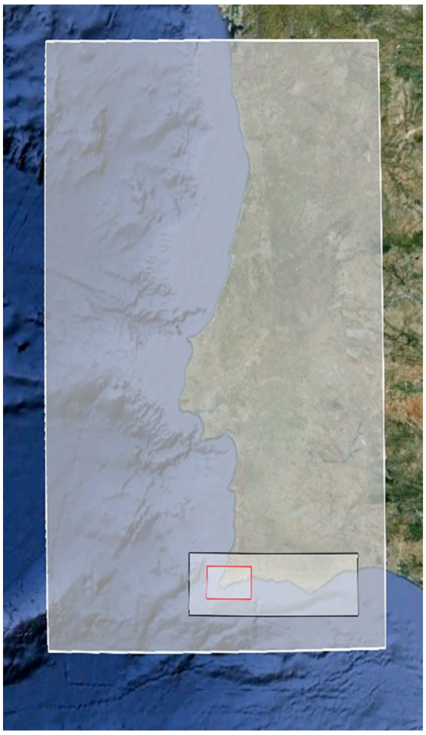

Figure 23 - The proposed nesting scheme for the operational model. Adapted from Google Earth, Google™.

The relaxation scheme of Martinsen and Engedahl (1987) is used to pass the information from the father model to the son model. The use of these boundary conditions is consistent with the conclusions of Blayo and Debreu (2005) that considered relaxation methods to be suitable boundary conditions, giving reliable results in actual applications. Boundary conditions for both models will be downscaled from a regional operational model for the Portuguese coast (PCOM) currently maintained by the MARETEC group at Instituto Superior Técnico and described in Riflet et al. (2008). **Figure 24** shows the bathymetries created for the nested domains.

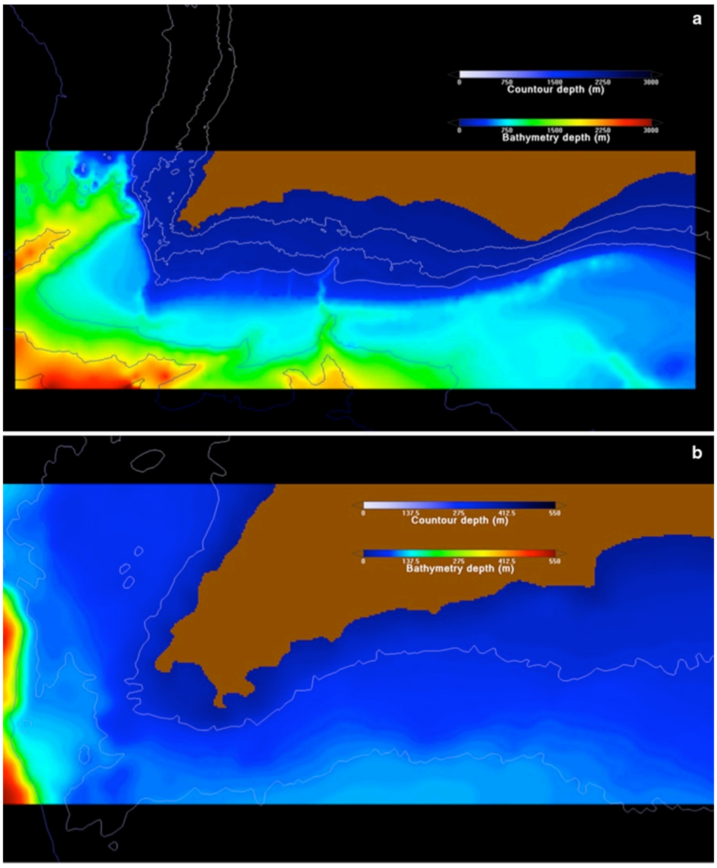

Figure 24 - Bathymetries of the nested domains. **a** Algarve coast: 148×424 cells, 550 m resolution. **b** São Vicente Cape: 170×380 cells, 150 m resolution.

To simulate the diversity of processes affecting oil weathering and advection MOHID Oil Spill module will be used for the oil spill simulations Janeiro et al., 2008. This module is based in a Lagrangian transport model that drives an oil slick evolution model. The Lagrangian transport model was restricted to a single mesh, however modifications have been made to allow several meshes of increasing resolution to be run simultaneously. This has the advantage of having high spatial resolution near the oil spill region without increasing too much the computational need. The current version of the Oil Spill module already include important processes such as oil density, viscosity, oil spreading, evaporation, dispersion, sedimentation, dissolution, emulsification and interaction with the coast. A review and update of these processes will be done, as well as the inclusion of other important processes such as mechanical spreading, dispersion and sedimentation. The implementation of new algorithms that allow, - based on the actual hydrodynamics, spill time and its physical-chemical properties -, an automatically decision from the module about the best response measure to use on a particular spill will also be implemented.

Data coming from different sources (meteorological, remote sensing, buoys, etc) will be used to prepare the best possible estimate of the true state of the system, to be assimilated by the model and to allow calibration. Adaptation is needed in the control structure of the model to run the system in operational mode. An operational framework to run the model will be constructed in .NET platform in order to execute and monitor all the required operational tasks, such as managing data input to the system, running the model, generate model maps and animations.

To make the bridge between the system and the end-users a web based geographic referenced database using Mapserver technology and including relevant information for oil spill management (bathing beach locations, aquaculture sites, natural sensitive areas, civil protection team's headquarters, etc) will be created. Methods will also be developed to automate tasks related to management of oil spills, linking the model predictions with the operations on the field.

In parallel with this study a similar operational modelling system is being developed for the Tuscany archipelago (Italy) under the 7th Framework Programme project ARGOMARINE (Automatic oil-spill recognition and

Geopositioning integrated in a Marine Monitoring network). The overall objective of the ARGOMARINE project is to develop and test a Marine Information System (MIS) capable of providing precise and punctual pollution control in coastal zone areas with vulnerable or protected habitats, and/or are exposed to risk of accidental or intentional contamination due to their vicinity to industrial or highly densely populated settlements, or crossed by a heavy ship traffic. A Marine Information System (MIS) consisting of a network for data storage, data mining and analysis, decision-support, data warehouse and a web-GIS portal carries out the top control of ARGOMARINE. The communication relies on an Integrated Communication System (ICS), developed to ensure reliable and efficient data transmission from different sensors and models to the MIS. A pre-operational high-resolution mathematical modelling system to forecast hydrodynamic conditions and prediction of oil slick spreading during emergency situations, as part of an early warning system, will be created during the project. The modelling system to be used is the MOHID, and the methodologies followed are the same of those described above allowing and two-way improvement and validation of the methods in use. When fully operational the system will be receiving data from the modelling system and also from Synthetic Aperture Radar (SAR) images, air-borne Hyperspectral/Thermal Imaging, AUV/Glider mounted sensors and Electronic Noses. The synergies between the two works will potentiate the results and the validity of the methods proposed.

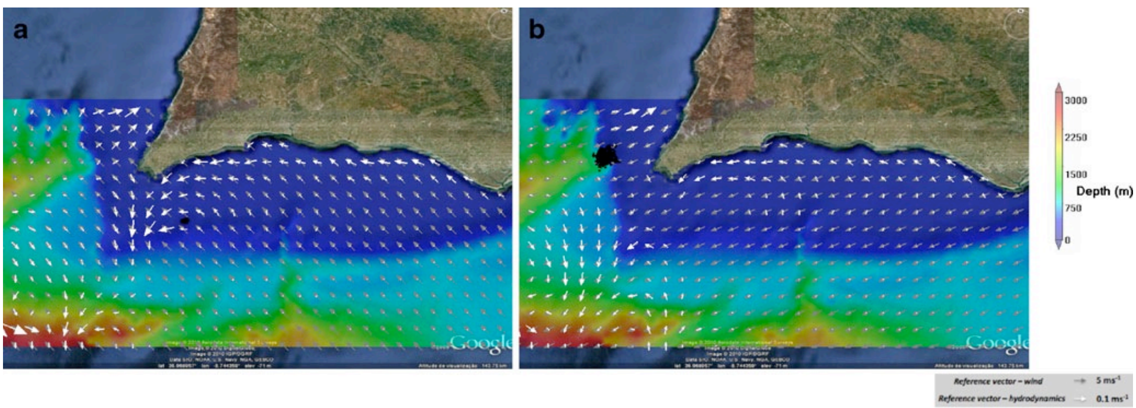

Figure 25 - Lagrangean tracer's simulations in the Algarve coast using a southeast wind event. **a** - evolution of the tracers 3 h after being released; **b** —tracers position 1 day after scenario a.

Preliminary results of Lagrangean tracers launched in the Algarve coast are shown on Figure 25 and Figure 26. The 2D hydrodynamic field was obtained using FES2004 global tide model harmonics and wind data observed in Faro Airport as boundary conditions. The wind data was analysed, and two events were chosen for the simulations. The events represent two of the main wind directions observed in the study area, southwest and southeast. Both grid resolutions presented above are used in these simulations using the described nesting scheme. The Lagrangean module evaluates in each time step the best available hydrodynamics results in order to use them to drive the tracers.

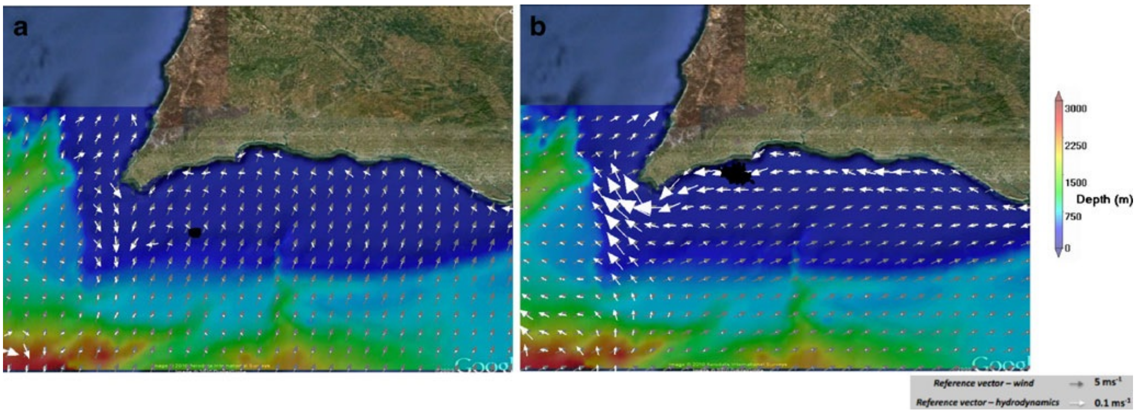

Figure 26 - Lagrangean tracers simulations in the Algarve coast using a southwest wind event. **a** — evolution of the tracers 6 h after being released; **b** — tracers position 1 day after scenario a.

Despite the encouraging preliminary results showing the potential threat that an oil spill event can represent for the study area, still much work needs to be done. Coupling these high-resolution grids with the PCOM results in order to accomplish reliable 3D hydrodynamic fields for the area, and then use these fields to drive the oil spill module and simulate oil advection and weathering processes are the next steps.

Chapter V – *The European Marine Strategy: Contributions and Challenges from a Portuguese perspective*[4]

[4] This chapter is published in the Marine Policy as: **Frazão Santos, C., Teixeira, Z., Janeiro, J., Gonçalves, R., Bjorkland, R., Orbach, M., 2012. The European Marine Strategy: Contributions and Challenges from a Portuguese perspective, Marine Policy, 36, 963-968.**

Abstract

The EU Marine Strategy Framework Directive (MSFD) is considered to be the environmental pillar of the EU Integrated Maritime Policy, establishing a framework within which member states must take the necessary measures to achieve, or maintain, good environmental status in their marine waters. This study presents Portugal contributions to the Directive development, describes the Portuguese institutional framework within the MSFD and, finally, highlights the opportunities and threats to the success of the MSFD implementation in Portugal. The latter entails an analysis of the Directive's long-term adequacy in its link to (1) marine spatial planning, (2) climate change and (3) the economic/financial crisis. With one of Europe's largest Exclusive Economic Zones, Portugal interest on the MSFD is paramount. Efforts towards the approval of the final document were assured during the Portuguese presidency of the European Council of Ministers, in 2007, while chairing a thorough discussion between the Council and the European Parliament. In the Portuguese context, the Directive implementation will rely on the Water Institute as the authoritative entity, which will be responsible for coordinating all necessary efforts at the national level. The success of such process depends on a close cooperation among the institutions involved as well as on how approved measures account for long term issues. In addition, the MSFD implementation must be built on lessons learned within the Water Framework Directive, in order to be successful. Although it poses a methodological challenge to Portugal, the MSFD implementation is expected to contribute significantly to the improvement of coastal/marine conservation and management at the national level.

1. Introduction

In 2007, the European Commission adopted an Integrated Maritime Policy (IMP) that replaces compartmentalized resource management with a holistic and integrated ecosystem-based approach to the management of human activities (EBM) while simultaneously encompassing all elements of maritime activity (Meiner, 2010).

The European Union (EU) Marine Strategy Framework Directive[5] (MSFD), established in 2008 (European Union, 2008), is considered to be the environmental pillar of the IMP because it requires EU member states to achieve and maintain good environmental status (GES) in their marine environments, as well as to apply the EBM concept (European Commission, 2008). In fact, although the MSFD does not directly regulate maritime activities, their impacts have to be accounted for in the determination of GES. Despite the unquestionable relevance of EBM in achieving sustainable development (Crowder, 2008; Douvere, 2008), there is still a gap between theory and practice because governments and stakeholders lack the necessary operational tools to implement it (Douvere and Ehler, 2009; Espinosa et al., 2011).

In an effort to meet one of the IMP's strategic initiatives – the development of new tools to implement EBM – several EU member states expressed their intention to use marine spatial planning (MSP) as a means to implement EBM and, subsequently, MSFD goals (Meiner, 2010, European Commission, 2008, Maes, 2008). In fact, the international efforts to develop MSP during the last decade, as well as its increasing importance in European policy (Douvere, 2008), demonstrate its potential. MSP is a key tool that facilitates the coordinated planning of competing activities and strategic management of maritime space, thus promoting sustainable development and use of resources (European Commission, 2008; Maes, 2008).

[5] The MSFD is also referred to as "the Directive" throughout this article.

In the Portuguese context, both the MSFD and MSP are in their early stages. The MSFD implementation process began late in 2010, and the development of the first Portuguese marine spatial plan started in 2008 (Calado et al., 2010; Rulling No 32277, 2008). The present work highlights the opportunities and challenges to the success of the MSFD implementation in Portugal, as well as the Directive connection to some topics relevant to its long-term adequacy such as MSP, climate change and the present financial crisis.

2. Brief overview on the EU Marine Strategy Directive

The MSFD – Directive 2008/56/EC of the European Parliament and of the Council (European Union, 2008) – establishes a framework within which member states must take the necessary measures to achieve, or maintain, GES throughout their marine environments, including the water column, seabed and subsoil, from coastal waters to the entire exclusive economic zones (EEZ) by 2020. In order to do so, each member state has to develop and implement marine strategies (MS) for its marine regions/sub-regions accounting for the transboundary effects on the quality of the marine environment within each of those regions/sub-regions. These MS are intended to (1) protect and preserve marine ecosystems (preventing its deterioration or improving its restoration) and (2) prevent or reduce the anthropogenic inputs in the marine environment, by consistent application of an EBM approach.

The MSFD outlines a plan of action that begins with the preparation of MS followed by the development of a programme of measures for these strategies. To properly implement the strategies, member states have to build upon relevant international forums and instruments, including the mechanisms and structures of Regional Sea

Conventions[6], and use existing cooperative structures, e.g., from the Water Framework Directive. The preparation of MS includes four steps (**Figure 27**): (1) the initial assessment, (2) the determination of GES, (3) the establishment of environmental targets and (4) the establishment and implementation of monitoring programmes. To adequately fulfil both the first and the last step of the MS preparation, member states have to ensure that methodologies are consistent across marine regions/sub-regions in order to facilitate the comparability of results and thus take into account the transboundary effects.

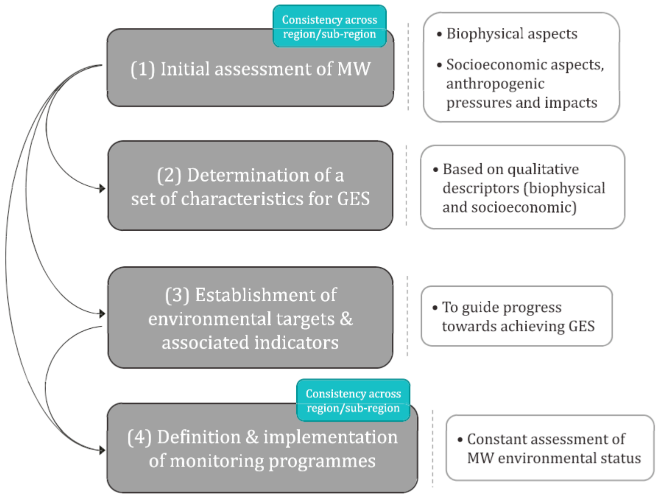

Figure 27 - Steps for the preparation of marine strategies according to the Marine Strategy Framework Directive. The arrows represent the existing links between all steps. Steps 2, 3 and 4 are directly connected to step 1 as all of them take the initial assessment into consideration. As well, step 4 furthermore considers the environmental targets (from step 3) in its development. MW: marine waters. GES: good environmental status.

Based on the initial assessment, and by reference to environmental targets, each member state must then (1) identify the measures needed to attain GES, and (2) subsequently integrate them into a programme, indicating how they are to be implemented and how they will contribute to the achievement of the environmental targets (European Union, 2008). According to Long (2011), the

[6] Such as, the OSPAR Convention, the Helsinki Convention (HELCOM), the Barcelona Convention (UNEP-MAP) or the Bucharest Convention (European Commission, 2011).

programme of measures is the key mechanism of the MSFD for delivering sustainable use of the marine environment, because it is based on the precautionary principle and the principles that preventive action should be taken. Although the Directive does not mention what specific management measures each member state has to adopt in their programmes, some guidelines are provided (see European Union, 2008; Long, 2011). Overall, sustainable development and the socioeconomic impacts of measures must be accounted for when drawing up the programme, and measures need to be cost-effective and technically feasible. Transboundary effects are again a relevant aspect, and the programmes' implications on subjacent waters have to be considered in order to minimize risk and negative impacts.

Regarding more general aspects of the MSFD, it is crucial that MS are kept up to date; thus every six years after the initial establishment they have to be reviewed. Public participation is also a major concern, and member states have to ensure that all interested parties are given real opportunities to participate in the MSFD implementation process. With regards to financial support, the implementation of the MSFD is to be supported by existing European Community financial instruments, and the programmes drawn up by each member state are to be co-financed by the EU in accordance with existing instruments. Finally, the entire Directive will be reviewed and adjusted as necessary by 2023.

3. The MSFD and Portugal

3.1. Contributing to the MSFD

The EU began the MSFD development process in 2002 and negotiations continued for almost six years ahead. Although a political agreement among member states was reached in July 2007, critical points of disagreement between the European Council of Ministers (CM) and the European Parliament (EP) were still to be resolved[7]. Portugal took the lead over this negotiation while assuming the presidency of the CM in the last semester of 2007. During the six-month period of the presidency, Portugal chaired a thorough discussion between the CM and the EP until an agreement was achieved and the MSFD was voted and approved. The outcomes from this discussion are presented in **Table IV** (European Union, 2008a; Silva, 2008).

3.2. MSFD and the Portuguese Institutional Framework

The Portuguese legislation that establishes the legal framework, within which Portugal must achieve the MSFD goals, thus transposing the MSFD into national law, was published in 2010 through the Decree-Law No. 108 (2010). This statute establishes the Portuguese Water Institute (INAG) as the authoritative entity, responsible for coordinating the MSFD implementation at the national level (Decree-Law No. 108, 2010). INAG's overall mission is to monitor the environmental quality of national waters, as well as the implementation of national policies pertaining to water resources, thus ensuring their sustainable management and use (Portuguese Water Institute, 2011).

With the criteria and methodological standards on good environmental status of marine waters defined since September 2010 (European Commission, 2010), member states are now preparing to assess the current status of their marine waters and to determine the GES. In Portugal, INAG must gather relevant information and data from several other public entities, which provide information according to their field of expertise (Figure 28) Decree-Law No. 108 (2010). In particular, the Portuguese Environment Agency has to provide information pertaining to the OSPAR Convention, since information on the North-East Atlantic

[7] Although the EP has the authority to put forward amendments and comment on intended legislation, the CM is the central and ultimate decision-making body in the union, and no legislation can be issued, or amended, unless it agrees with it (European Union, 2011).

Environment Strategy is vital to ensure coordination and cooperation between the two legal instruments (European Commission, 2010; OSPAR Commission, 2010).

Table IV - Points of disagreement (and corresponding outcomes) between the European Council of Ministers and the European Parliament concerning the Marine Strategy Framework Directive (European Union, 2008; Silva, 2008)..

Disputed Topic	European	European Council of	Outcome
Good environmental status (GES) definition rules	Proposed a certain degree of technical detail to assess the environmental status.	Argued that the required degree of technical detail was too high.	Evaluation must be done by region/sub-region, considering: (1) characteristics of marine waters (hydro-morphological, physicochemical and biological); (2) impacts and pressures on the environmental status; (3) economic and social aspects of water use and the cost of marine environment degradation.
Deadlines and costs	Proposed the achievement of GES by 2017.	Proposed the achievement of GES by 2021. Also proposed a new cost article stating that member states should not be obliged to take measures in situations where: (1) there are no significant risks to the environment or, (2) the costs of preparing management plans are disproportionately high compared to the environmental risks.	Member states must achieve GES by 2020. Member states are not required, except in the initial evaluation, to take specific measures if there are no significant risks to the marine environment, or if the costs are disproportionate with respect to the risks, and provided that environmental status does not decline.
Individual/collective responsibility for marine strategies implementation and regional cooperation	Proposed the term “collective responsibility” to develop a marine strategy per region/sub-region.	Did not agree with the term “collective responsibility” due to difficulties and/or jurisdictional implications. Also defended the use of existing structures of international cooperation, including marine regional conventions, in order to avoid duplication of effort.	Member states that share a region/sub-region must cooperate to ensure consistent and coordinated measures. To achieve such coordination, they must use the existing structures of regional institutional cooperation, including those covered by regional marine conventions.
Geographical delimitation between the MSFD and Water Framework Directive (WFD) – definition of “European waters”	All waters should be included, even when already covered by the WFD, enlarging the application to all tidal waters within the member states or in adjacent areas of their territories.	Argued that marine waters already covered by the WFD should only be included in the MSFD when relevant issues concerning the protection of the marine environment are beyond the scope of the WFD.	Waters, the seabed and subsoil on the seaward side of the baseline from which the extent of the territorial waters is measured extending to the outer edge of the area where a member state has and/or exercises jurisdictional rights (exclusive economic zones). Also covers coastal waters, their seabed and subsoil, as defined by the WFD, in which particular aspects of the environmental status of the marine environment are not already addressed through the WFD or other community legislation.
Marine Protected Areas (MPAs)	Recommended obligatory designation of MPAs.	Proposed optional designation of MPAs.	Programs of measures must include spatial protection measures that contribute to representative networks of MPAs.

INAG's experience in implementing the Water Framework Directive[8] (WFD) (Portuguese Water Institute, 2011) should now be put into practice for a smooth and integrated implementation of the MSFD, as both directives share similarities, as well as potential conflicts regarding the overlapping of their intervention area within coastal waters (Silva, 2008; Borja et al., 2010). In particular, the late transposition of the WFD into national law[9] caused a fragmentation of responsibilities and a delay in meeting deadlines. As a result, Portugal continues to face some difficulties in the implementation of the WFD concerning (1) the identification of pressures, (2) the assessment of pressures/risk impact on water bodies, (3) the preparation of measurement programs/validity, and (4) the duplication of efforts regarding monitoring programs (Rocha, 2009). Likewise, the MSFD implementation success will rely on a close collaboration, and coherent articulation among all institutions with authority and responsibility that are involved in the process. Additionally, according to Rocha (2009), there are three key aspects for a successful implementation of the MSFD: (1) the identification of authoritative/responsible entities; (2) the coordination within and between ministries; and (3) the contribution of the scientific community.

Only time will tell whether implementing the MSFD poses a bigger challenge for Portugal than implementing the WFD. At the present moment, the MSFD transposition into Portuguese national law is very recent (dating from 2010), and the implementation process is still in its early stages (see Soares, 2008). Nevertheless, an action plan has been established and the preparation of marine strategies scheduled to be accomplished by 2014 (Decree-Law No. 108, 2010).

---

[8] Directive 2000/60/EC of the European Parliament and of the Council, establishing a framework for the Community action in the field of water policy. Adopted in October 23, 2000. The main environmental objective of this Directive is to achieve or maintain "good environmental status" for all surface and ground waters by 2015 (European Union, 2000).

[9] The WFD, adopted at the EU level in 2000, was only transposed to the Portuguese internal law by 2005 - through the Law No. 58, from 2005, and further complemented by the Decree-Law No. 77, from 2006.

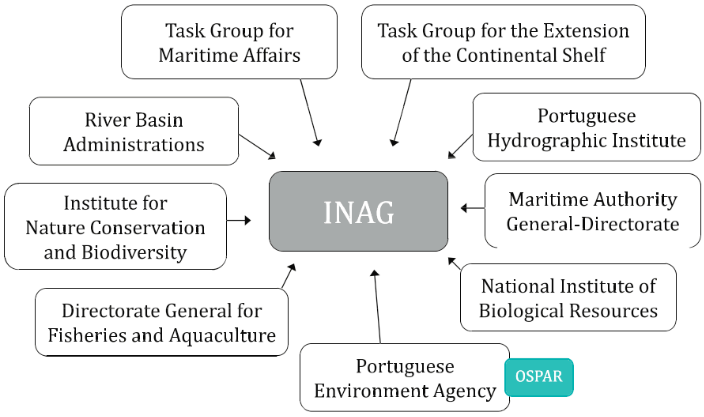

Figure 28 - Portuguese public entities that must provide relevant information and data to the Portuguese Water Institute (INAG) in the scope of the Marine Strategy Framework Directive implementation, according to the Portuguese Decree-Law No. 108, from 2010. In particular, the Portuguese Environment Agency has to provide additional information pertaining to the OSPAR Convention.

The following section reviews the long-term adequacy of the Directive implementation in Portugal with respect to its connection to (1) marine spatial planning, (2) climate change and (3) economic/financial crisis.

3.3. Long-term adequacy: links to marine spatial planning, climate change and the financial crisis

3.3.1. Marine spatial planning

Marine spatial planning is a continuous, iterative and adaptive process (Douvere, 2008) "that consists of data collection, stakeholder consultation and the participatory development of a plan" (European Commission, 2008), and the subsequent stages of implementation, monitoring, evaluation and revision of such plan. MSP is also an operational tool, or instrument for the management of human activities in the maritime space (from coastal watersheds to marine ecosystems) through the allocation of maritime space and uses.

A particular, and of major relevance, aspect of MSP is that EBM is its overarching principle. The entire planning process must always take into account the biophysical, socioeconomic and institutional aspects of a given ecosystem – its "total ecology" (Orbach, 1996) – making the necessary trade-offs to achieve socioeconomic development without compromising resource use for future generations.

Decision 2010/477/EU (European Commission, 2010) considers MSP as a mechanism to achieve the goals of the MSFD, thus clarifying the existing link between both. Referring to the general conditions for applying the criteria for GES of marine waters, the Decision states that in order to identify areas where marine ecosystems are adversely affected, a combined assessment of the scale, distribution and intensity of pressures and impacts, in addition to the extent, vulnerability and resilience of the different ecosystem components, is required. Also, the selection of the most appropriate indicators to assess progress towards the achievement of GES is encouraged. The Decision also states that the development of specific tools to support the EBM approach – which is required to achieve GES – is also facilitated by the aforementioned approach, and that included in such tools are "spatial and temporal distribution controls, such as maritime spatial planning" (European Commission, 2010).

Portugal has one of the largest EEZ among EU member states, currently with 1.7 million km2, which is approximately eighteen times the size of the country's terrestrial area, and a proposal was submitted in 2009 (Task Group for the Extension of the Continental Shelf, 2009) to increase its size by 2.15 million km2 (Figure 29).

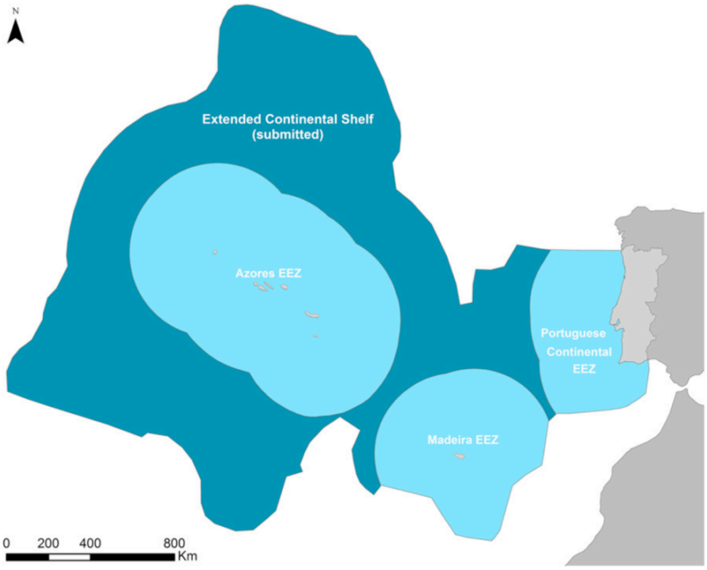

Figure 29 - Current Portuguese Exclusive Economic Zone (Continental, Azores and Madeira fractions) and submitted Extended Continental Shelf. Adapted from Task Group for the Extension of the Continental Shelf (2009).

The entire Portuguese EEZ is encompassed in the MSFD North-east Atlantic Ocean marine region and encloses two MSFD marine sub-regions: Macaronesian Biogeographic Region in the Atlantic Ocean, within the Azores and Madeira EEZs, and Bay of Biscay and Iberian Coast, in the continental EEZ (European Union, 2008). Due to the ocean strategic role and importance at a national level, and in accordance to the National Sea Strategy objectives (Rulling No 32277, 2008), Portugal began developing a marine spatial plan – Plano de Ordenamento do Espaço Marítimo (POEM) – for its EEZ, territorial waters and coastal waters in 2008 [9]. Properly managing present and future uses of the maritime space, in close connection with coastal zone management, the POEM aims to ensure and promote: (1) a sustainable use of the resources; (2) its protection and conservation; (3) an efficient, integrated and multisectoral approach to the use of the maritime space; and (4) the socioeconomic and environmental importance of the sea to the Portuguese context (Rulling No 32277, 2008). POEM, expected to be completed by the end of 2011 while the first plan review is scheduled to take place in 2013 (Calado et al., 2010).

A challenge lies in the ability to translate MSP principles into practice, as it happens with EBM and the MSFD, despite its acknowledged necessity, efficiency and utility. Coordination and communication among all entities responsible for marine and coastal areas management are required, although it is not always an easy process, especially among already established sectors in the maritime space (e.g., fisheries, marine protected areas, shipping routes, tourism). Managing such sectors together is the basis of the EBM concept, and if this process is properly accomplished the benefits from such approach will be evident for all involved parties. All things considered, in order to ensure the long-term adequacy of MSFD goals as well as the improvement of coastal/marine conservation and management in Portugal, such challenge must be overcome.

3.3.2. Climate change

Within the EU context, member states located in the Mediterranean region, such as Portugal, are expected to be more vulnerable to climate change impacts than the ones located in the north of Europe (Santos and Miranda, 2006). With regard to Portugal, climate change is likely to have an enormous impact due to the existence of an extensive shoreline inhabited by approximately 65% of the country's population, as well as to the major economic contribution of coastal areas to national GDP. During the 20th century, sea level rose 0.10-0.20 m along the Portuguese mainland coast and in extensive areas the shoreline has been retreating a few meters per year (Ferreira et al, 2008). Storm surge events are also possible along the Portuguese coastline, and might reach extreme values of 1 m in specific locations of the NW region (Santos and Miranda, 2006). Moreover, sediment input to the Portuguese coast has been reduced due to human management of river basins, intensifying coastal vulnerability to climate change. In fact, Santos et al. (2001) forecasted a risk of land loss in 67% of the coastal areas, and according to Santos and Miranda (2006) erosion rates are expected to increase 15-25% by the end of the 21st century. Since the MSFD considers coastal waters as an integral part of the marine environment, additional attention should be paid to sea level rise effects on the coasts, such as erosion and shoreline displacement, saltwater intrusion, inundation and flooding (Davidson-Arnott, 2005; Masterson and Garabedian, 2007; Purcell et al., 2010; Robichaud and Bégin, 1997).

The MSFD recognizes that it may not always be possible to meet environmental targets in all marine waters due to natural causes or force majeure. In fact, although member states have to take the necessary measures to achieve/maintain GES in the marine environment, the Directive goes farther and identifies the necessity to "assess serious environmental concerns, in particular those due to climate change", stating that "action may be required to ensure the environmental protection" (European Union, 2008). Such recommendations, although specifically addressed to Arctic Waters, may have an actual consequence not only in the final environmental status of some marine waters, but for measures taken with respect to all regions/sub-regions. The elements taken into account to assess the environmental status might, in several cases, suffer a shift in their patterns and/or in their relationships with each other due to climate change. From physical and chemical features (Andersen et. al., 2006; Coelho et al., 2007; Deutsch et al., 2011) to biological characteristics and habitat types (Hãder et al., 2007; Hicks et al., 2011; Millian et al., 2011), all marine waters and their dependent human uses may suffer climate change effects, with repercussions for their assessment and monitoring.

Finally, marine protected areas (MPA) management must also be an issue when addressing climate change, since modifications in ocean currents, upwelling patterns and other physical and chemical changes may impact biological populations and their interactions, as well as impact MPA design and establishment (Keller et al., 2009; Stram and Evans, 2009). In fact, the MSFD establishes that MPA will make important contributions towards achieving the goals of conserving habitats, protecting rare populations, preserving representative ecosystems and enhancing fish harvesting. In the last couple of decades, Portugal has defined and established some MPA within its waters (Institute for Nature Conservation and Biodiversity, 2011; Task Group for maritime affairs, 2011).

Overall Portugal is already experiencing the impacts of climate change and attendant sea level, thus increasing the need for dynamic management that will incorporate long-term modifications in the planning process.

3.3.3. Economic and financial crisis

According to Article 22 of the Directive 2008/56/EC, the programmes of measures drawn up by the member states to implement the MSFD "shall be co-financed by the EU in accordance with existing financial instruments". Such Community financial instruments are issued in due course and provide a secure funding. In fact, the EU defined the establishment of marine strategies as a priority, providing sources of funding such as the LIFE programmes, the FP7 - Seventh Framework Programme and the INTERREG IVC Programme (European Commission DG environment, 2010).

However, member states must also account for the implementation of the MSFD in their government budgets. Portugal's large external debt constrains the country's economy and thus may point to a difficult future for the Directive implementation. Despite these challenges, the Portuguese government presented a National Reform Programme (NRP) in accordance with the Europe 2020 Strategy, taking into account the priority of budgetary consolidation together with boosting competitiveness, growth and employment (European Commission, 2011; Portugal 2020 – National Reform Program, 2011).

Key areas of the Europe 2020 Strategy include the investment in Research and Development (R&D) and Innovation (European Commission, 2011, European Commission, 2004). R&D is crucial to achieve MSFD targets thus highlighting the importance of such key areas for the Directive implementation. In fact, among other (scientific) studies required [2]: (1) new tools to evaluate water quality must be developed; (2) tougher ocean monitoring programs must be implemented; (3) new in situ research must be established; (4) marine zones and their management plans must be defined under further ocean assessment; (5) criteria and methodological standards to ensure consistency and to allow for comparison between marine regions/sub-regions must be provided; and (6) fisheries management must be based on scientific advice.

To summarize, despite the economic downturn Portugal cannot afford to ignore issues relating to its marine environment. In fact, preventing future crises may depend on the attention paid by Portugal to environmentally sustainable marine management. Furthermore no member state can risk the implementation of the MSFD on its own EEZ without jeopardizing its implementation in the surrounding marine regions/sub-regions. For this reason, even under economic recession conditions, measures must be identified and established to guarantee the achievement of the MSFD goals.

4. Conclusions

The Marine Strategy Framework Directive is the environmental pillar of the European maritime policies. It applies an ecosystem-based approach to the management of human activities to achieve or maintain a good environmental status on the marine environment, from coastal watersheds to the entire EEZ.

The implementation process of this strategy is still in its early stages across EU member states, including Portugal. The success of the MSFD implementation will always depend on the close cooperation among the institutions involved in the process, as well as on the long-term adequacy of the process. The existing connection between the MSFD and relevant topics such as climate change, economy, and spatial planning of coastal and marine areas, is of the utmost importance for an adequate, long-term, management of the marine environment.

From Portugal's perspective, the MSFD builds on – and thus benefits from – the lessons learned within the WFD implementation process. In upcoming years, significant developments are expected to take place. Although MSFD poses a methodological challenge to the present Portuguese context, when entirely implemented it will contribute significantly to the improvement of coastal/marine conservation and management at the national level.

Chapter VI - *Marine spatial planning and oil spill risk analysis: Finding common grounds*[10]

[10] This chapter is published in the Marine Pollution Bulletin as: **Frazão Santos, C., Michel, J., Neves, M., Janeiro, J., Andrade, F., Orbach, M., 2013*. Marine spatial planning and oil spill risk analysis: Finding common grounds.* Marine Pollution Bulletin, 74, 73-81.**

Abstract

A flow of key information links marine spatial planning (MSP) and oil spill risk analysis (OSRA), two distinct processes needed to achieve true sustainable management of coastal and marine areas. OSRA informs MSP on areas of high risk to oil spills allowing a redefinition of planning objectives and the relocation of activities to increase the ecosystem's overall utility and resilience. Concomitantly, MSP continuously generates a large amount of data that is vital to OSRA. The Environmental Sensitivity Index (ESI) mapping system emerges as an operational tool to implement the MSP–OSRA link. Given the high level of commonalities between ESI and MSP data (both in biophysical and human dimensions), ESI tools (both paper maps and dynamic GIS-based product) are easily developed to further inform MSP and oil spill risk management. Finally, several other benefits from implementing the MSP–OSRA link are highlighted.

1. Introduction

Marine spatial planning (MSP) is commonly defined as ''a process (...) of analysing and allocating the spatial and temporal distribution of human activities in marine areas'' (from coastal areas to entire exclusive economic zones) (European Commission, 2010) that takes the ecosystem-based approach to the management of such activities as its overarching principle (Douvere, 2008; European Commission, 2008). Ecosystem-based management (EBM) is characterized by: (1) encompassing the biophysical, human and institutional dimensions of a given ecological–economic system; (2) recognizing the connectivity amongst all of its elements; and (3) ensuring the necessary trade-offs to achieve sustainability. MSP is increasingly being developed and implemented around the world due to its potential and relevance for coastal and ocean management and the development of corresponding policies. Encompassed in this spatial planning process is the need to identify and analyse existing conditions within a target area, as well as to map and quantify the impacts of human activities on its bio- physical ecosystems (Ehler and Douvere, 2009). In order to do so, suitable data and assessment methods must be available, and MSP implies the development of a strong data and knowledge base.

Risk analysis is also a requirement for a proper spatial planning process (Greiving and Fleischhauer, 2006), and in this context MSP is no exception. Hence, instruments such as hazard potential, vulnerability, and risk profiles/maps are crucial to support contingency planning, as well as decision-making and risk management (Abascal et al., 2010; Castanedo et al., 2009). Because oil spills can cause significant impacts to coastal/marine environments and resources, and in view of the international policies and guidelines pertaining to the reduction of marine pollution and its subsequent impacts (e.g. OSPAR Convention, MARPOL Convention), the existence of related preparedness and response tools is crucial for a sustainable management (IPIECA, 2008; Frazão Santos and Andrade, 2009).

In spite of their different purposes and contexts, oil spill risk analysis (OSRA) and MSP share a need for spatial information on key coastal and marine resources and habitats, as well as processes identification. To make the best use of spatial data collected, and given the relevance of both MSP and OSRA for a truly sustainable management of coastal and marine spaces, finding common ground between them and further combining their development and application are challenges of paramount importance. The present work highlights the link between MSP and OSRA by: (1) analysing both processes' frameworks and identifying commonalities between them and (2) proposing an operational model to implement the MSP–OSRA link.

2. Methods: analysing MSP and OSRA frameworks

2.1. Marine spatial planning: data on existing conditions

As a planning process, MSP involves a group of steps that must be implemented to ensure its proper development (Ehler and Douvere, 2009; Foley et al., 2010). It starts with the definition of planning principles, goals and objectives for a management area (step 1 in **Figure 30**), followed by the analysis of present environmental, socio- economic, and political conditions (step 2). Based on the latter information, scenarios are built to predict/define potential future conditions (step 3), and management alternatives are established and spatially explicit decisions are made (step 4). When a management alternative is selected, a spatial plan is then developed (step 5), implemented (step 6) and the results of both the plan and its implementation are monitored/evaluated (step 7). Finally, the plan is revised so that the entire planning process can be adapted in light of learned lessons (step 8 in **Figure 30**).

The definition and analysis of existing conditions (step 2 in **Figure 30**) is a key step of MSP because management scenarios/alternatives will build on such initial information.

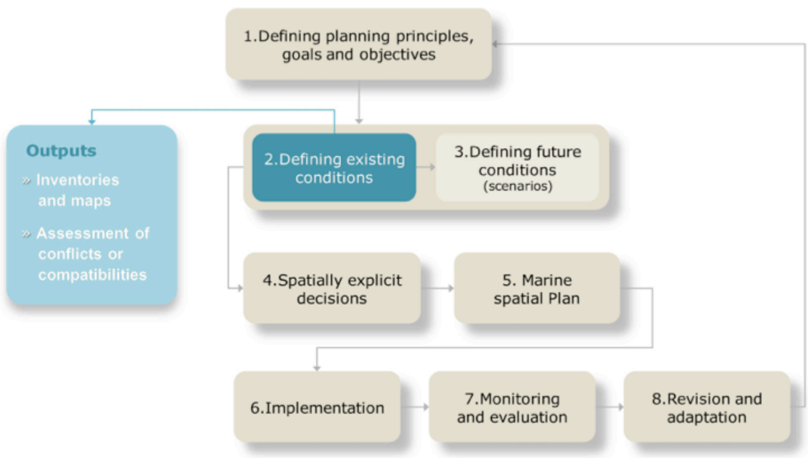

Figure 30 - Main steps in a full marine spatial planning process. Highlight is given to the expected outcomes from step 2 – ‘defining existing conditions’.

According to Ehler and Douvere (2009) there are two major outcomes from this step: (1) the development of 'inventories and maps' and (2) an 'assessment of potential conflicts and/or compatibilities', both among existing human uses and between them and the environment (effects that may risk or promote good environmental quality). Although the assessment of conflicts/compatibilities has a major relevance in MSP since it ultimately determines the need for a management plan[11], within the context of this paper special attention is given to the first outcome.

Because collecting, compiling and mapping spatial data tend to be high-cost and time-consuming processes yet constitute key components of planning and management activities (Beck et al., 2009; Ehler and Douvere, 2009), proper development of 'inventories and maps' is of paramount importance. MSP inventories/maps commonly pertain to the identification and mapping of two main types of information[12]: (1) important biological and ecological areas – i.e. areas to conserve/protect, as well as areas compatible with human activities – and (2) existing human activities and pressures – i.e. the spatial/temporal distribution and density of important human activities within an area. Data on important biological/ecological areas may be mapped using either qualitative or quantitative methods, depending on established goals and data constrains. In either case, however, entities involved in MSP (both decision-makers and stakeholders) must bear in mind that marine ecosystems' move, although sometimes at imperceptible speeds, and that their boundaries are more difficult to perceive and establish than terrestrial ones (Norse et al., 2005). For these reasons, there is a need for dynamic

[11] If no spatial overlaps are found among human activities/pressures, or between them and important biological/ecological areas, conflicts and compatibilities will not exist, and a management plan will (in fact) not be necessary; this situation is, however, very rare (Ehler and Douvere, 2009).

[12] A thorough list on information that can be included in MSP inventories and maps is found in Section 3 (Table VI).

mapping (and planning) to encompass the diversity of marine species and habitats in space and time (Crowder and Norse, 2008).

For data on human activities/pressures, the MSP process must recognize the complexity of human dimensions, as it does with the biophysical ones, and acknowledge that the set of existing processes and practices in place is ‘‘complex, integrated, and multi-scalar’’ (St. Martin and Hall-Arber, 2008). In fact, besides considering activities that directly take place in marine areas, MSP must consider effects from, or effects in, activities located ‘upstream’ (land) and ‘downstream’ (international waters) from the management area – e.g. links between offshore marine activities and on-shore communities and economies (Ehler and Douvere, 2009). Nevertheless, some direct activities (and areas) are always more relevant to identify and display than others, due to their social, economic or political value – e.g. fishing, energy production (Ehler and Douvere, 2009).

For both types of data, a key rule is that information must be ‘‘up-to-date, objective, reliable, relevant and comparable’’ (Ehler and Douvere, 2009) and should cover most of the planning area, instead of only small sub-areas (fine-scale data) that have little analytical utility for MSP (Beck et al., 2009). These authors further identify three main data sources: (1) scientific literature; (2) expert scientific opinion/advice; and (3) government sources. They further recognize that local knowledge and direct field measurements can be added but, because acquiring such new data is costly (especially when compared to integrating existing one), it should be kept to a minimum until significant data gaps are identified.

2.2. Oil spill risk analysis: features and phases

While there are many natural and man-made hazards that com- pose a threat to marine and coastal ecosystems, oil spills have earned a special status in the risk analysis framework given that they are one of the most damaging pollution events on such spaces, and have serious environmental and socioeconomic consequences (ITOPF, 2011a,b). Oil spill impacts vary according to a range of factors – e.g. spill conditions, specificities of the affected areas, types/ effectiveness of response and restoration actions taken place (Frazão Santos and Andrade, 2009) – and this is why there has been a growing concern on the importance of contingency planning and prevention actions (IPIECA, 2008; ITOPF, 2011c). Just as with other hazards, OSRA emerges as a way of dealing with uncertainty, providing decision-makers with fundamental information to support management and policy processes and to improve their quality (Botsford and Parma, 2005; Evans et al., 2006; Ricci et al., 2003).

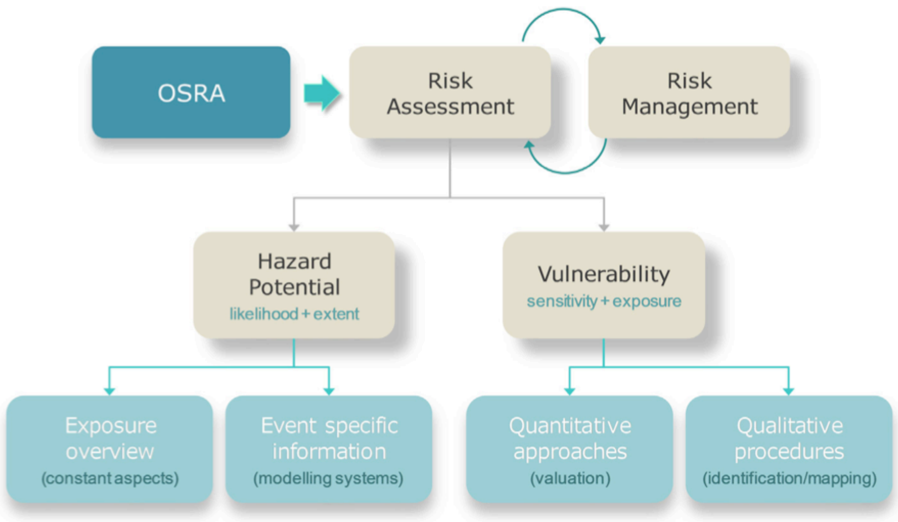

Figure 31 - Oil spill risk analysis (OSRA) framework.

Although a plethora of different 'risk' definitions and frame- works is available (e.g. ANZS, 2004; Cox and Ricci, 2005; ISO, 2009; Pine, 2009; Power and McCarthy, 1998), OSRA involves two essential phases: risk assessment (RA) and risk management (RM) (**Figure 31**). Oil spill RA estimates the extent of the damage that a spill may pose for a specific area, as well as the area's environmental and socioeconomic values. It encompasses (1) an 'exposure analysis', also called hazard potential analysis (**Figure 31**), where the likelihood/probability of the spill occurrence and the corresponding extent of damages on affected places are analysed; (2) a 'dose–response analysis', or vulnerability analysis (**Figure 31**), that correlates exposure levels and the actual impacts that will arise from the spill; and (3) a ‘risk characterization’ that combines the former two analyses (Field and Field, 2009; Pine, 2009). For these reasons, RA requires proper scientific data and assessment methodologies (Calow, 1998; Olfert et al., 2006; Power and McCarthy, 1998). European guidelines further suggest that methodologies that are focused on a single hazard and on a specific spatial context (e.g. coastal areas) allow for more accurate and reliable results (Kumpulainen, 2006; Schmidt-Thomé, 2005) thus representing the best assessment approaches.

On the other hand, oil spill RM focuses on the analysis of different planning/management options designed to cope with, or to minimize risk, and on the subsequent selection and implementation of the ‘best’ one(s) (Field and Field, 2009). Decision-making is, therefore, RM’s key element. In order to ensure informed and well-grounded RM decisions, RM should build on scientific knowledge gathered within RA. In fact, having quantitative RA results (Topuz et al., 2011) is key to facilitate both the development of management strategies (e.g. development of contingency plans in areas of high oil spill risk) and the decision-making process (e.g. information on high vulnerability areas will allow for an easier selection of protection priorities). If the information provided by RA is, however, characterized by a high level of uncertainty, entities responsible for RM must adopt a precautionary approach (Costanza et al., 1998; European Commission, 2000; Kriebel et al., 2001; Ricci et al., 2003) to ensure sustainable environmental management.

Both RA and RM must be connected in a continuous and adaptive process – (1) RA informs RM decision-making and (2) RM identifies information gaps and needs in RA – to ensure OSRA quality. In fact, two fundamental aspects must be present throughout OSRA (ANZS, 2004; Linkov et al., 2006): (1) monitoring and reviewing the entire process for continuous adaptation and improvement and (2) consulting and communicating with stakeholders. These are essential steps to ensure the quality of all stages of OSRA, without which achieving the previously mentioned sustainability objectives may become a utopia.

In the following sub-sections, the major specificities of (1) oil spill potential assessment, (2) coastal/marine vulnerability to oil spills assessment and (3) the

Environmental Sensitivity Index (ESI) mapping system will be discussed. The latter was a pioneer vulnerability assessment methodology and is highlighted here due to the important role it will further play in linking MSP and OSRA.

2.2.1. Hazard potential specificities

The likelihood of oil spill occurrences is not easily defined, and the extent of damage they may cause is not simple to assess with- out a certain degree of uncertainty. These make up the major reasons why a great number of oil spill potential assessment approaches were developed around the world during the last decade (e.g. Abascal et al., 2010; Guo and Wang, 2009; Inan, 2011; Janeiro et al., 2012; Skognes and Johansen, 2004).

The assessment of oil spill potential can be seen as having two sides (Frazão Santos et al., 2010a): (1) the first one, regarding aspects that are 'constant' throughout a period of time within a given marine/costal area, which can provide us with an approximation or overview of the area's 'exposure degree' to this hazard – e.g. the intensity of commercial vessels traffic crossing it, the proximity of commercial harbours, the volume and characteristics of oil products that are handled in both vessels traffic and harbours; (2) the second one, which corresponds to the singularity of each oil spill (**Figure 31**). This second type of information – which is 'event-specific' – will determine the type of impacts on a given marine/coastal area, as well as their probability, by considering aspects such as: (1) spill size (e.g. major spills over 700 tonnes, or smaller ones under 7 tonnes); (2) oil properties (from light oils, which are usually more toxic but that concomitantly dissipate faster, to heavy oils that can persist in the environment; ITOPF, 2011d); (3) the distance from the spill location to the shoreline (or from the spill to important marine sites, such as offshore aquaculture locations); and (4) hydrodynamic and weather conditions at the time of the spill (Frazão Santos and Andrade, 2009).

Because the fate of oil spilled in water is governed by complex, interrelated, physicochemical processes, dependent on previously mentioned factors (Mackay and McAuliffe, 1988), the necessary task of 'combining sides' is not simple (Frazão Santos et al., 2010a). In fact, while the use of a quantitative methodology, such as the development of a composite indicator, is possible for the first type of information, the second one, due to its event-specific nature, requires a different scale of analysis and, consequently, the application of different assessment procedures (Frazão Santos et al., 2010a).

To deal with such complexity, modelling of oil spills has been recognized as a valuable tool and is used by decision-makers not only to manage pollution crises, but also in planning and setting up contingency plans. Recent advances in remote ocean observation technologies and worldwide research initiatives that monitor the state of the ocean are allowing for the development of operational modelling systems that assimilate observed sea and atmospheric data and produce forecasts of ocean conditions. Coupling these models with algorithms that can simulate the oil weathering processes provides an effective tool to hindcast and forecast the trajectory and oil properties evolution during an oil spill accident (Janeiro et al., 2012).

The combination of model results with geographic information systems (GIS), integrating (1) different sources of geospatial information and (2) statistical analysis algorithms, further enhances the ability to assess oil spill risk (Guillen et al., 2004). The use of such dynamic mapping, which allows for an easy update and visualization of crucial spatial data, additionally benefits RM by providing effective operational tools to managers and stakeholders.

2.2.2. Vulnerability specificities

Broadly defined as the degree of fragility towards a specific hazard, and taking into account exposure level (damage potential) and sensitivity/resilience level (coping capacity) concepts, vulnerability can be seen as a set of conditions/processes resulting from bio-physical, environmental, social and economic factors that decrease resilience of a community/area (Kumpulainen, 2006). The assessment of coastal/marine vulnerability to oil spills has developed worldwide in recent years – just as it also happened with hazard potential – due to a variety of projects using a plethora of methodologies (e.g. Andrade et al., 2010; Castanedo et al., 2009; Frazão Santos et al., 2013; Mendoza-Cantú et al. 2011; Petersen et al., 2002; Schiller et al., 2005). Usually dynamic mapping (e.g. GIS) is used for displaying and analysing variation in space and time, again due to the ease of updating and visualizing crucial spatial data, which is a key aspect for these instruments (Andrade et al., 2010; Castanedo et al., 2009).

In general, vulnerability assessment can be carried out using two major approaches: (1) quantitative methodologies that usually attach relative vulnerability values to different coastal/marine units, thus assigning protection priorities to the ones with higher values; and (2) qualitative procedures, which identify and map the most vulnerable resources within a management area, presenting such information to decision-makers (**Figure 31**). Table V summarizes the analysis of the strengths, weaknesses, opportunities and threats (SWOT analysis) of each vulnerability assessment approach. Despite the advantages and disadvantages of each methodology, the combination of both seems to represent a 'step forward' in vulnerability assessment research. In fact, through the development of a multi-level scale assessment methodology using GIS technology, a quantitative approach could be applied at a larger spatial level (e.g. regions or municipalities; Frazão Santos et al., 2013), while at a fine-scale (i.e. more detailed level) vulnerable resources would be identified and mapped in a qualitative way (e.g. Petersen et al., 2002). This combined approach allows weaknesses and threats to be overcome since, in general, where one fails the other tends to succeed (e.g. in sensitivity maps, expert interpretation is required to define priority protection areas, potentially delaying the RM process, while in algorithm-based models, protection priorities are automatically established upon a scale of vulnerability values; Table V). The ultimate goal is always the development of the most effective vulnerability assessment tool to allow the assessment of risk, and further inform RM in coastal and marine spaces.

Table V - SWOT analysis on the two major assessment approaches of coastal/marine vulnerability to oil spills. This analysis builds on the information discussed by Santos and Andrade (2009) regarding the use of 'sensitivity maps' (qualitative procedure) versus 'algorithm-based sensitivity models' (quantitative method).

	Qualitative procedures	***Quantitative methodologies***
Strengths	Proven feasibility and effectiveness in a wide range of coastal areas ('mature' approach). Synthetic and objective way to provide crucial coastal/marine information to decision-makers.	Single and automatic vulnerability value for each coastal/marine unit, based on a group of ecological and socioeconomic criteria/variables. Automatic establishment of protection priorities based on relative vulnerability values.
Weaknesses	Lack of a pre-defined vulnerability rank for ecological and socioeconomic resources. Need for expert interpretation in order to define prioritized protection areas for each spill event.	The result (final vulnerability value) is an 'average' contribution of each criterion/variable, not the identification of important resources. Long process of quantification and numeric integration of criteria/variables due to high complexity level. Proper definition of homogeneous coastal/marine units is difficult. Non-adaptive (to decision-makers) vulnerability assessment process.
Opportunities	Information interpretation carried out by best experts. Development of general contingency plans before spill, and subsequent addition of event-specific information, make up an excellence decision-making tool.	Faster, and less subjective, assessment process due to relative vulnerability values. Identification of key criteria/variables behind each vulnerability value computed.
Threats	Information interpretation allows for subjective reading, if not carried by best experts. Slow response activity due to inexistence of contingency plans beforehand.	Automatic definition of protection priorities potentially generates conflicts amidst decision-makers. Misidentification of important ecological/socioeconomic values that would constitute a protection priority by themselves due to 'average contributions' for each unit.

2.2.3. ESI mapping system

ESI mapping (Petersen et al., 2002) began in the 1970s in the United States (Gundlach and Hayes, 1978), and evolved significantly in the next two decades with GIS and remote sensing technologies (Hayes et al., 1997; Jensen et al., 1998, 1990; Pavia et al., 1995).

Considered to be an assessment and prevention tool in oil spill RM, this system identifies and displays the coastal and marine resources most vulnerable to oil spills, as well as to disturbance caused by clean-up activities, thus allowing for the early definition of protection priorities and clean-up strategies. For over three decades, the ESI mapping system has shown an immense functionality and effectiveness for the assessment of coastal vulnerability to oil spills, and its broadness can further be proven by the amount of projects, developed worldwide, that either partially or thoroughly build on it (Frazão Santos and Andrade, 2009).

ESI tools (both paper maps and dynamic GIS-based products), which are normally focused on coastal, lacustrine, or riverine environments, always comprise and display three main types of information (Jensen et al., 1998; Petersen et al., 2002): (1) shoreline habitats; (2) biological resources; and (3) human-use resources[13]. The first type of information encompasses the 'sensitivity index' it-self, having an attached range of vulnerability values from 1 (less vulnerable) to 10 (most vulnerable). In fact, from exposed rocky shores to sheltered tidal flats or mangroves, shoreline vulnerability to oil spills is first classified and then mapped. The remaining two data types – sensitive biological resources and human-use resources – are simply compiled and mapped, and not classified as well. Because maps including the complete distribution of existing resources will have poor legibility, not being useful management tools, only resources with a higher vulnerability are displayed. Coral reefs, spawning and breeding areas, and endangered/rare species can, therefore, be found in the biological resources category, while high-use recreational beaches, archaeological sites, or

[13] A thorough list of the data typically included in ESI maps can be found in Table VI (Section 3).

recreational/commercial fishing areas are among human-use resources. The ultimate result is an extremely informative and 'easy to understand' map detailing the ecological and socioeconomic resources most sensitive to oil spills.

3. Results and discussion: linking MSP and OSRA

3.1. MSP and OSRA commonalities: a flow of key information

Although MSP and OSRA are two distinct processes, with different objectives and scopes of intervention, they can provide essential information to each other (**Figure 32**).

The importance of RA and RM for spatial planning has long been recognized (Olfert et al., 2006) and is expressed in several European Union laws, policies, and programmes (e.g. European Commission, 2011, 2009, 2004, 2001). OSRA will properly inform MSP on (1) areas of high sensitivity to oil spills and (2) areas where oil spills are more likely to occur, thus allowing the planning and management processes to carefully revise and redefine objectives as well as spatially explicit decisions and, therefore, relocate human activities to increase the ecological–economic system's overall utility.

In fact, in areas where sensitivity is high, activities that may increase the probability of oil spill occurrence/contamination should be avoided. This is the case of activities such as: boating (variable B05 from Table VI), marine transportation (B09), contaminated dredged material disposal (B12), crude pipelines (B13), and offshore oil exploration (B18). At the same time, where oil spill potential is high, presence of certain human activities/resources should be strategically discouraged because they may be compromised.

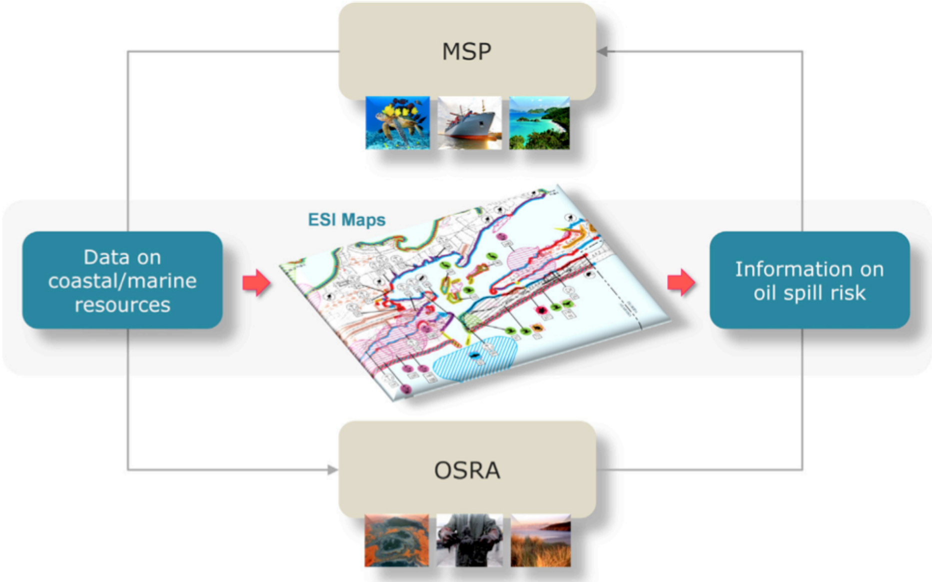

Figure 32 - Schematic representation of the connection between marine spatial planning (MSP) and oil spill risk analysis (OSRA). OSRA provides information on oil spill risk (both vulnerability and oil spill potential dimensions) to MSP, while MSP provides data on coastal/marine resources (both biophysical and human-use resources) to OSRA. Environmental Sensitivity Index (ESI) mapping emerges as an operational model to implement such connection.

This is especially important to infrastructure-based activities that are not easily or quickly relocated, as well as to non-removable resources – e.g. aquaculture (variable B08 from Table VI), water intake (B15) or cultural/historic conservation sites (B24). Other activities such as diving (B02), surfing (B03), use of recreational beaches (B04), recreational fishing (B06) or scientific re- search (B23), although being place-based as well (i.e. they occur in specific areas), are likely to suffer smaller impacts due to their more 'mobile' nature. Nevertheless, because there is a certain degree of uncertainty associated to OSRA – especially regarding the assessment of oil spill potential (Section 2.2.1) – entities responsible for MSP may still choose to allocate the aforementioned human activities to areas of high oil spill risk. In such cases, however, investing (beforehand) in proper preparedness/response mechanisms is especially important to cope with risk and minimize negative impacts[14]. On the other side, OSRA will benefit from the considerable amount of data continuously made available from MSP processes. Considering the difficulties identified in Section 2 regarding the collection and compilation of spatial data, the possibility of using MSP data in OSRA will save both time and money and will translate into an efficient use of available resources. Typical MSP information, such as important biological/ecological areas and existing/potential human activities and resources within a management area (Section 2.1), is also required to assess and manage oil spill risk. These kinds of data are, in fact, essential (1) to assess the vulnerability dimension (e.g. sensitive habitats such as coral reefs or, sensitive locations of intense recreational use), as well as (2) to inform the 'constant side' of oil spill potential assessment (e.g. vessels traffic and harbour location). However, MSP is unlikely to provide significant information to the event-specific side of oil spill potential assessment (see Section 2.2.1) because the data it requires is extremely specific for each spill event (e.g. data on spill size or oil properties), thus going beyond the MSP scope. A

An extra commonality between MSP and vulnerability assessment is the dichotomy between the use of qualitative and quantitative approaches to analyse and display data. In fact, while coastal/marine vulnerability to oil spills can be assessed with both quantitative and qualitative methods (as discussed in Table V and Section 2.2.2), Ehler and Douvere (2009) recognize that important biological/ecological values encompassed in MSP can be mapped either through the qualitative 'Ecologically or Biologically Significant Areas' approach (which maps only the most valuable areas) or the quantitative 'Biological Valuation Mapping' methodology (which calculates an intrinsic value for each zone/unity of a management area, and then represents it in a 'baseline map').

[14] The existence of prevention tools is further critical, especially under a precautionary approach, because even when the likelihood of occurrence is very low, oil spills can still occur and lead to daunting environmental and socioeconomic costs – e.g. Exxon Valdez or Deep Horizon accidents.

Table VI - Comparison between data required for a full marine spatial planning (MSP) process and data used to develop Environmental Sensitivity Index (ESI) tools. Information variables presented (A01–A19 and B01–B24) were defined by merging or adapting: examples from Ehler and Douvere (2009), information from specific MSP process (e.g. Portuguese Government, 2012) and examples/guidelines from Petersen et al. (2002). (●) Included. (○) Not referred.

		MSP	*ESI maps*
Code	***Information to include - biophysical dimension***	***Biological or ecological areas***	***Biological resources and coastal habitats***
A01	***Areas of higher biological diversity (e.g. habitats, species, genetic diversity)***	●	○
A02	***Areas of high endemism (species, populations or communities)***	●	●
A03	***Areas of high productivity (e.g. upwelling areas)***	●	○ [a]
A04	***Threatened, endangered, or rare species***	●	●
A05	***Aggregation/high concentration areas (e.g. staging, wintering, haul-out)***	●	●
A06	***Mating areas***	○	●
A07	***Spawning and breeding areas***	●	●
A08	***Nesting, pupping, and calving areas***	●	●
A09	***Nursery areas***	●	●
A10	***Feeding and foraging areas***	●	●
A11	***Migration stopover sites and routes***	●	●
A12	***Worm beds (intertidal/subtidal beds of structure-building worm species)***	○	●
A13	***Kelp forests and other algal beds***	○	●
A14	***Coral reefs***	●	●
A15	***Floating aquatic vegetation***	○	●
A16	***Seagrass beds and other submersed aquatic vegetation***	●	●
A17	***Hardbottom reefs***	○	●
A18	***Shoreline types (e.g. exposed/sheltered rocky cliffs, sand and gravel beaches, tidal flats)***	○	●
A19	***Wetlands (e.g. salt-water/ brackish-water marshes, mangroves)***	●	●
Code	***Information to include - human dimension***	***Human activities***	***Human-use resources***
B01	***Wildlife watching areas (e.g. birdwatching, whale watching)***	●	○
B02	***Scuba diving/snorkelling sites (e.g. artificial reefs)***	●	●
B03	***Surfing sites***	●	●
B04	***High-use recreational beaches***	●	●
B05	***Boating and sailing areas (e.g. high-use marine/estuarine facilities like marinas)***	●	●
B06	***Recreational fishing areas***	●	●
B07	***Commercial fishing areas***	●	●
B08	***Aquaculture areas***	●	●
B09	***Marine transportation areas (e.g. cargo vessel, tanker, cruise ship, ferry)***	●	○
B10	***Shoreline access sites (e.g. vehicular access, airport, helipad)***	○	●
B11	***Port and harbor operations' areas (e.g. dredging)***	●	○
B12	***Dredged material disposal sites***	●	○
B13	***Cables, pipelines, transmission lines***	●	○
B14	***Intertidal/subtidal mining areas (e.g. sand and gravel)***	●	●
B15	***Water intake sites***	○	●
B16	***Offshore renewable energy (e.g. wind farms, wave parks, tidal, currents)***	●	○
B17	***Offshore industrial production facilities***	●	○
B18	***Offshore oil and gas exploration***	●	○
B19	***Carbon sequestration sites***	●	○
B20	***Military operations' areas***	●	○
B21	***Strictly protected marine reserves (e.g. marine sanctuaries)***	●	●
B22	***Multiple use marine parks (e.g. national, state, regional parks)***	●	●
B23	***Scientific research areas***	●	○
B24	***Cultural and historic conservation sites (e.g. archaeological sites)***	●	●

[a] Although not mapped this information is considered as a criteria for shoreline type analysis.

Although the identification of common grounds is important to improve the efficiency of management, planning and policymaking processes, it is essential to determine 'how' to translate principles into practice. The following sub-section analyses how the link between MSP and OSRA can effectively be made operational.

3.2. ESI mapping system: an operational tool to implement the MSP– OSRA link?

The development of ESI tools emerges as a potential answer to implement the MSP–OSRA link. In effect, benefiting from the data that continuously flow from MSP processes, ESI data can be easily developed to further inform planning and management processes – either RM and/or MSP – on oil spill risk (**Figure 32**). The following discussion takes a deeper look into what relates ESI mapping to (1) OSRA and (2) MSP.

In view of the information already presented in Section 2.2.3, ESI mapping fits the group of qualitative methodologies to assess coastal/marine sensitivity to oil spills. Although qualitative approaches present limitations to vulnerability assessment (as dis- cussed in Section 2.2.2) they still provide a synthetic and objective way to present crucial information to coastal/marine managers and stakeholders. ESI maps can therefore be a vital part of OSRA, by ensuring the assessment of the vulnerability dimension of RA and further informing entities responsible for RM.

At the same time, ESI and MSP data share a need for information on key coastal and marine resources, habitat and processes identification and their distribution, despite having different objectives and spatial broadness (Frazão Santos et al., 2010b). By presenting the data required by MSP and the data usually included in ESI maps, Table VI allows for a comparison between both. For information on the biophysical dimension, eleven out of the nineteen variables considered (c. 58%) are common to MSP and ESI data (Table VI and **Figure 33**). This is the case of important ecological resources and areas, such as 'threatened, endangered or rare species' (variable A04 on Table VI), 'migration stopover sites and routes' (A11) or 'coral reefs' (A19). Only two variables (c. 11%) are exclusive to MSP – 'areas of higher biological diversity' (A01) and 'areas of high productivity' (A03) – while five variables (c. 32%) are exclusive to ESI maps – 'worm beds' (A12), 'kelp forests and other algal beds' (A13), 'floating aquatic vegetation' (A15), 'hardbottom reefs' (A17) and 'shoreline types' (A18) (Table VI and **Figure 33**). This exclusiveness is, in general, due to the different nature and broadness of MSP and ESI mapping processes: while MSP may need to assess the resilience of marine species/ecosystems as a whole using criteria not relevant for ESI mapping (e.g. a large number of species – variable A01 in Table VI – does not necessarily means a higher vulnerability if the existing species are resilient or if they have oil avoiding behaviours), ESI tools need to include data on very specific resources that may increase vulnerability but are not relevant for MSP. For example, although information on worm beds (variable A12 in Table VI) is important for ESI mapping because it can in- crease oil persistency and burial capacity, it is not especially relevant for MSP unless, for instance, when corresponding to rare or endangered species, which is already considered by variable A04.

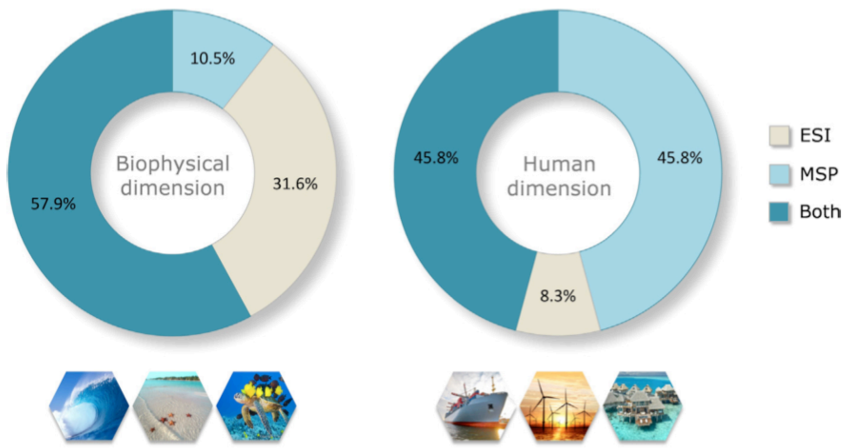

Figure 33 - Degree of commonality between variables from marine spatial planning (MSP) and from Environmental Sensitivity Index (ESI) mapping, according to data type (human dimension versus biophysical dimension). Percentage values are based on the total number of variables from Table VI that are: (1) exclusive to ESI mapping, (2) exclusive to MSP or, (3) common to both.

For the human dimension information, the percentage of common variables between MSP and ESI mapping decreases to c. 46% (eleven out of the twenty-four variables considered within this dimension; Table VI and **Figure 33**). Nevertheless, identification of recreational activities (e.g. diving (B02), surfing (B03), use of recreational beaches (B04), boating and sailing (B05) and fishing (B06)), commercial activities (namely, fishing (B07), aquaculture (B08), sand and gravel mining (B14)), and areas for ecological and/or cultural protection/conservation (e.g. full protection sanctuaries (B21), multiple use parks (B22) and archaeological sites (B24)), is common to both MSP and ESI mapping processes (Table VI). Within the human dimension, and contrarily to the biophysical one, there are more variables exclusive to MSP (c. 46%) than to ESI maps (c. 8%) (**Figure 33**). In fact, only the variables 'shoreline access points' (B10) and 'water intakes' (B15) are exclusive to ESI mapping, while MSP alone includes eleven variables that range from 'wildlife watching' (B01), to 'marine transportation' (B09) or to 'cables, pipelines, transmission lines' (B13) (Table VI). As with the biophysical dimension, the major differences found here are due to the different nature/broadness of MSP and ESI mapping processes. ESI tools are focused on coastal areas whereas MSP encompasses activities that occur in wider, open ocean areas (as is the case of off-shore activities from variables B16-B18). Furthermore, because MSP defines where/when human activities are to take place in marine/coastal environments, information on such activities needs to be more comprehensive than for ESI tools (which are focused on activities/resources that can be affected by oil spills). Finally, some features that are essential for ESI mapping due to its 'oil-spill oriented' nature – e.g. identification of vehicular access points, air- ports or helipads (variable B10) to be used for oil spill clean-up activities – are irrelevant for MSP. These also make up the major reasons why the number of common variables between MSP and ESI mapping is lower (46% versus 58%), and why the number of variables exclusive to MSP is higher (46% versus 11%) in the human dimension than in the biophysical one (**Figure 33**).

4. Final remarks

While the link between ESI mapping and OSRA seems to be clear and unequivocal, commonalities between ESI tools and MSP require further discussion. The percentage values showed in **Figure 33** and analysed in Section 3.2 are not 'absolute' values, i.e. they may change, especially according to the number of activities included in the MSP analysis. Information on ESI maps is more 'constant' deriving from a single, clear and objective guidelines document (Petersen et al., 2002), while MSP tends to be more flexible and vary according to its target area. Nevertheless, these relative values allow us to conclude that there is a high level of commonalities between ESI and MSP data, and that it varies with the type of information (human dimension versus biophysical dimension). This variation is mainly due to the fact that not all existing information in MSP and ESI mapping can be included (otherwise maps would not be informative) and only the most important data is selected according to the different objectives and scope of intervention of each process.

Another relevant aspect is that although MSP and ESI mapping include a large set of common data, and although we advocate that such MSP data can be used to develop ESI maps, the reverse situation does not seem to be equally valid. In fact, ESI data cannot be easily used directly in MSP because, even when common, they: (1) often have limited coverage and fall under the category of 'fine-scale data' (see Section 2.1); (2) are oil-spill oriented – e.g. data on marine mammals foraging areas may be adapted to oil spill RA and RM purposes, not covering the entire range of information that a broader MSP process requires. However, when ESI data are already available for an area, prior to MSP development (e.g. along the United States coast), they can draw MSP attention to important resources that are present and, therefore, should be considered when defining where activities will take place.

In addition to all previously stated, several benefits derive from using ESI tools to implement the MSP–OSRA link. First, available information on sensitivity to oil spills (provided by ESI mapping) decreases uncertainty and improves the understanding about the analysed ecological–economic system. Planning and management decisions – both in MSP and RM – are, then, more likely to encompass all interests and values at stake, ensure the necessary trade-offs to achieve sustainability and, thus, incorporate and implement EBM principles and goals.

Second, benefiting from the data gathered within MSP, a vulnerability assessment instrument of proven feasibility and effectiveness (ESI mapping) can be developed in a very efficient way, i.e. saving both time and monetary resources (Frazão Santos et al., 2010b). This higher efficiency is, in fact, one major benefit from finding common grounds between processes that, in spite of their differences, focus on the same areas (as is the case with OSRA and MSP).

Third, implementing the MSP–OSRA link (through ESI tools), although a challenging process, translates into a true integrated view of coastal zone management and marine planning, which managers and policymakers already recognized as the best practice to improve the quality of the overall system.

Finally, although ESI mapping is identified as an operational tool to implement the MSP–OSRA link, it should not be viewed as the only possible implementation model. In fact, there is still room for improvement given that ESI data are limited to providing information on the vulnerability dimension, while hazard potential is also required to fully characterize oil spill overall risk. Future re- search may, therefore, further identify alternative, and potentially more comprehensive and efficient ways to implement these commonalities, allowing for a 'stronger' flow of data to inform MSP and RM.

Chapter VII – *Integrating technologies for oil spill monitoring in the South Iberian Coast*

Abstract

To highlight the importance of integrating oil spill monitoring and response technologies in the south Iberia coast, an operational system implemented for the region was used to backtrack a CleanSeaNet oil detection in the marine environment. Taking advantage of regional operational products available, the system provides the necessary resolution to go from regional to coastal scales using a downscalling approach, while a multi-grid methodology allows the lagrangian based oil spill model spanning across model domains taking full advantage of the increasing resolution between the model grids. An extensive validation procedure using a multiplicity of sensors and with a good spatial and temporal coverage strengthens the operational system ability to accurately solve coastal scale processes. The lagrangian model is validated using available trajectories from satellite-tracked drifters. Errors found are included in the backtrack analysis allowing to identifying their possible origin by combining model backtrack results with ships trajectory supplied by Automated Identification System (AIS).

1. Introduction

Operational Ocean modelling has witnessed a very rapid evolution in recent years. Large-scale models covering the major ocean basins have improved their resolution and a new layer of high-resolution regional and local operational models is now arising, based on those larger models. This evolution is mainly due to improvements in numerical methods and computer performance, motivated by the need of accurate forecasts for research, for economic activities and for safety and security. The applications of such high-resolution operational models in the field of oil spill pollution are obvious, helping in prevention and during contention, clean-up and recovery phases (e.g. Sotillo et al. 2008; Broström et al. 2011; Janeiro et al. 2014).

The Portuguese mainland lies on one the busiest maritime routes of the globe and, despite numbers are difficult to obtain, tankers represent a significant part of the vessel traffic (Janeiro et al., 2012). Based on AIS data, Silveira et al. (2013) characterized the vessels traffic and studied the collision risk inside the Traffic Separation Schemes implemented off the coast of Portugal. From the methodology proposed in the study, and based on one month of AIS data, Silveira et al. (2013) estimated a total of 1766 collision candidates in the entire Portuguese coast. From this total, 355 collision candidates are tankers (Silveira et al. 2013). Based on 36 years of maritime casualties data (between 1971 and 2007), Gouveia et al. (2010) concluded that oil pollution in Portuguese coastal and maritime areas is significant, identifying over 2000 accidents. It is the authors' opinion that this value is underestimated, as the lack of surveillance during several years could encourage illegal discharges that would lead to a significant increase in this number.

Sea conditions may also represent a source of risk to local navigation and, therefore, contribute to the oil spill risk. Located in the South of Portugal, the Algarve region is the transition between two different wave climates. According to IPMA (2009), in the western coast of the Algarve, from Cape Sao Vicente northwards, the wave climate is dominated by waves from NW and N with Significant Wave Heights (H1/3) ranging from approximately 1 m, during summer time, to 2 m during winter. Waves from SW can be higher, reaching up to 7 m, but are less common and usually associated to wintertime. The maritime risk can be significantly increased in case concomitant incoming NW waves are present, generating crossed seas (Toffoli et al. 2005). Protected from most of the energy incoming from NW and N seas, the rough seas in the southern portion of the Algarve are associated to SW events, in which H1/3 may reach 3 m, and SE events, with H1/3 reaching over 2.5 m. Events of SE may be especially dangerous to navigation due to its fast growth (Toffoli et al. 2005).

The local economy is closely linked to the sea, depending mainly from both tourism and fisheries Janeiro et al., 2012. Environmentally it encompasses several important natural parks, being the most important ones the Ria Formosa Natural Park and the Natural Park of the Sudoeste Algarvio and Costa Vicentina. With a combined area of 92500 ha and 160 Km of coastline, both are filled with wide biodiversity of different species, natural habitats and act as nursery grounds for several marine species (Janeiro et al. 2012). So far, the oil spill hazard in the coast of the Algarve has been restricted to maritime transportation. However, eight concessions for offshore oil exploration have been create into the limits of the Algarve coast (DGEG, 2014).

The EU Member States saw amplified their surveillance capability with the creation of the European Maritime Safety Agency CleanSeaNet program in 2007, which aims on identifying possible marine oil spills through satellite remote sensing. By combining the oil spill detections with vessel information from SafeSeaNet and using backtracking models from national and regional centres, this is a valuable service to help detected and identify the source of pollution (EMSA, 2014).

In this context, an operational response and monitoring modelling system, with the ability to supply sea state and oil spills trajectories forecasts for the Algarve coast is presented in this paper. The goal of this research is to show how model downscaling methods can be used to backtrack CleanSeaNet oil detections in the marine environment, identifying their possible origin by combining model backtrack results with ships trajectory supplied by Automated Identification System (AIS). The article is structured as follows: (1) the operational system and downscaling methodology will be described; (2) model validation results, obtained against in-situ measurements from several type of sensors are presented; (3) the capability of our system to backtrack an oil spill was tested to a real event in the Algarve coast; finally (4) the main results will be discussed and conclusions gathered regarding the model implementation and ability to respond to oil pollution emergencies in the region.

2. Methods

As mentioned above, the methodology adopted in this study follows the proposed by Janeiro et al. (2014) for the Tuscany Archipelago (Italy) where an operational system was developed to aid in the response to oil spill accidents in the scope of the ARGOMARINE (Automatic Oil-Spill Recognition and Geopositioning integrated in a Marine Monitoring Network) project. The operational system proposed, hereby SOMA (Algarve Operational Modelling and Monitoring System), encompasses a hydrodynamic model and oil spill model. For the hydrodynamics, due to its system architecture, which allows the use of its several modules communicating in real time among them during a simulation, the MOHID water modelling system (Martins et al., 2001; Balseiro et al., 2003; Leitão et al. 2005) was considered a suitable and robust tool to be adopted with this kind of downscaling methodologies (Janeiro et al. 2014) and therefore was used in this study. It encompasses two grid levels of increasing resolution (Figure 34) built using bathymetry data retrieved from the European Marine Observation and Data Network (EMODNET - http://www.emodnet.eu). Level 1 is a three-dimensional model, with a constant horizontal resolution of 3 km, 11 sigma layers in the first 20 m depth and a resolution of 75 cm at the surface layer. From the 20 m to the bottom 35 unevenly spaced Z coordinate levels vertically discretize the model. A time discretization of 30 s is used at this level. At the boundary, a Blumberg and Kantha (1985) condition is applied to the water level and a Flow Relaxation Scheme (FRS) Martinsen and Engedahl (1987) is used for the velocities, salinity and temperature. This allows for a slow forcing of the model and a weighting of internal and external solution to prevent an overshoot of the dynamic equilibrium. In the outer grid cells a sponge layer was applied to attenuate reflected spurious baroclinic flow oscillations.

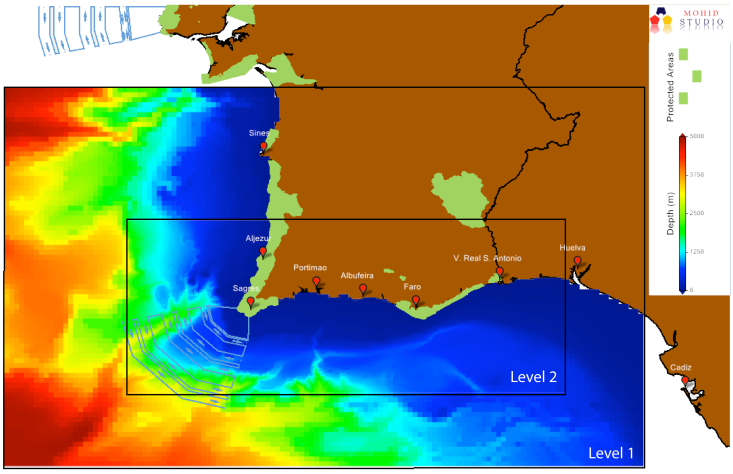

Figure 34 – The spatial coverage and grid limits for the two levels that composed SOMA. The ship traffic separation corridors are presented in blue while in green are the Protected areas encompassed in the model domain.

Level 2 is a three-dimensional model with a regular 1 km spatial resolution grid covering the Algarve coast. It has the same vertical resolution of Level 1 and a time discretization of 15 s. The communication between Levels 1 and 2 is made by relaxation of the zonal and meridional horizontal velocity components, through an eight cells band adjacent to the lateral boundary. The FRS is also used to pass the information from Level 1 to Level 2. The use of these boundary conditions is consistent with the conclusions of Blayo and Debreu (2005). Turbulent diffusion coefficients are computed in MOHID using its embedded version of the General Ocean Turbulence Model (GOTM) (Burchard et al. 1999; Umlauf and Burchard, 2005). The mixing-length scale parameterization proposed by Canuto et al. (2001) is used. Boundary conditions for temperature, salinity, tide and current velocities are being supplied by the Portuguese Coast Operational Modelling System (PCOMS) (Mateus et al. 2012; Campuzano et al. 2014, Ascione et al., 2014). Atmospheric forcing conditions are supplied by the regional weather forecasting system SKIRON, developed for operational use at the Helenic National Meteorological Service (Kallos, 1997; Papadopoulos et al., 2001). It provides hourly data of wind U and V components, air temperature, specific humidity, total cloud cover, sea level pressure, total precipitation, upward and downward long wave flux, evaporation, latent heat flux and sensible heat flux at a resolution of 5 km. SKIRON results are used in the operational system as atmospheric forcing fields for the hydrodynamic, wave and lagrangian models.

To simulate the oil spill trajectories and weathering processes, the multi-mesh Lagrangean model Fernandes et al., 2013 implemented in MOHID is used together with its oil weathering model Janeiro et al., 2008. Here, the spatial evolution of the particles is computed integrating the definition of velocity (Equation 3 and Equation 4) explained further in Janeiro et al. (2014).

MOHID multi-mesh approach ensures that the lagrangean model uses the best available hydrodynamics to force the lagrangean tracers. MOHID integrative architecture allows that both hydrodynamic model and lagrangean model run in real time with further advantages in the accuracy of the computed trajectories, as suggested by Janeiro et al. (2014). The Stokes drift will not be considered in this study. While identified as a relevant mechanism affecting the trajectory of oil spills Janeiro et al., 2014, at this stage, there was no regional product available to supply wave data to the operational system. This will change in the near future as work is being done to implement a dedicated wave model in the region that will integrate SOMA. A detailed description of the lagrangean model formulations considered in this study can be found in Janeiro et al. (2014). In what regards the oil weathering processes, MOHID oil module Janeiro et al., 2008 calculates the physical processes of the oil (density and viscosity) and the weathering processes (e.g. evaporation, dispersion, emulsification, dissolution) that affect them, updating the lagrangian module in each timestep.

3. Results

SOMA validation was accomplished using several data sources from different data providers. The validation dataset included data from tide gauges, moored buoys, vertical profiles (CTD, XBT, Argos), ADCP, High-Frequency Radars (HFR), remote sensing and drifter's buoys. To evaluate the model performance, as suggested by O'Donncha et al. (2015), an absolute and a relative error measure were considered. The Root Mean Square Deviation (RMSD) and Willmott (1981)

Model Skill Score (MSS) where, respectively, the error methodologies used to access the model results in this study. Defined as:

$$RMSD = \sqrt{\frac{\sum_{i=1}^{n}(x_{model} - x_{obs})^2}{n}}$$

Equation 14

$$MSS = 1 - \frac{\sum_{i=1}^{n}(x_{model} - x_{obs})^2}{\sum_{i=1}^{n}\left(\left|x_{model} - \overline{x}_{obs}\right| + \left|x_{obs} - \overline{x}_{obs}\right|\right)^2}$$

Equation 15

x_{model}, x_{obs} are the model predicted and observed values respectively, while $\overline{x}_{obs}$ is the mean of the observed values. While the RMSD is a dimensional variable providing an absolute measurement of the error between the datasets, the MSS is non-dimensional and provides a deeper insight into the predictive abilities by overcoming the sensitivity of the correlation statistics to differences in the predicted mean and variances (O'Donncha et al., 2015). MSS varies between 0 (total disagreement between model and observations) and 1 (total agreement between model and observations). Five stations where used to validate the operational system for medium to long-term features of a study area: two tidal gauges (Lagos and Huelva); two wave buoys Datawell MK2 (IH Sines Buoy) and MK3 (IH Faro Buoy); and multiparameter ocean buoy SeaWatch Directional Ocean-Met in the Gulf of Cádiz. The distribution of the sensors in the model domain is presented in Figure 35.

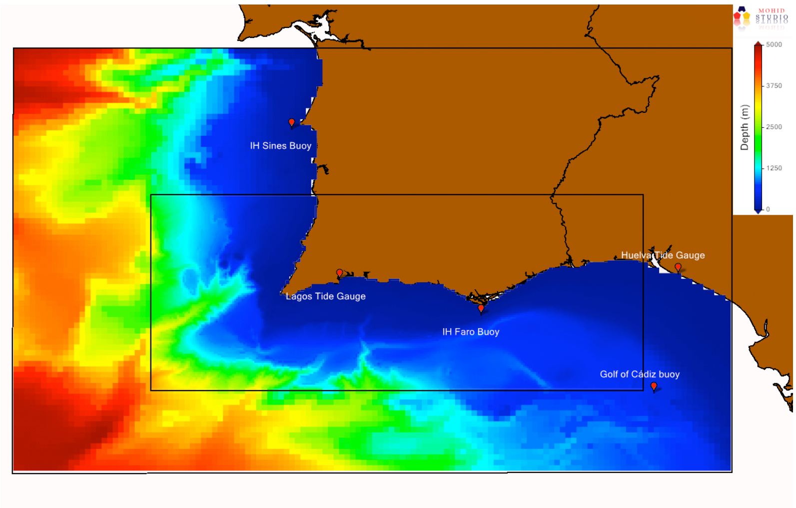

Figure 35 – Distribution of the sensors providing time series observations used in the validation of SOMA. The grid levels implemented in the system are enclosed in black.

Due to data availability two different periods were considered in our analysis. The tidal observations from Lagos and Huelva tide stations were compared with model results for a twenty day long period in May 2012, while the validation using IH and Gulf of Cadiz buoys was done, for the same amount of days, in October 2013. IH buoys (Faro and Sines), due to the high frequency of data available (every 10 minutes) were subject to a post-processing phase in which, both time series were filtered to eliminate frequencies above tide by means of a Cosine-Lanczos low-pass filter with half power point at 6 hours spanning 50 hours. The results obtained for the time series analysis are summarized in Table VII.

A good level of agreement between observations and model predictions was accomplished. With the exception of temperature at IH Sines Buoy, which has an error in temperature of 0.98 ºC, and salinity at Cádiz Buoy that presented an error of 0.21, all other properties/stations had MSS very close to one (perfect agreement).

Table VII- Errors obtained for the validation of the model against time series observations.

Station	Property	RMSD	MSS
Lagos Tide Gauge	*Water Level*	0.13 m	0.99
Huelva Tide Gauge	*Water Level*	0.10 m	0.99
IH Sines Buoy	*Temperature*	0.98ºC	0.63
IH Faro Buoy	*Temperature*	0.50 ºC	0.96
Cadiz Buoy	*Temperature*	0.36 ºC	0.96
	Salinity	0.21	0.31
	Current velocity	0.12 ms^{-1}	0.98
	Current direction	82.7º	0.91

Level 1 sea surface temperature (SST) was compared with satellite images from MODIS Aqua and METOP-A in three different seasonal conditions (Winter, Spring and Summer) during 2012 and 2013. Data from MODIS Aqua was retrieved from NASA's Ocean colour webpage (NASA, 2014) and it consisted on a dataset of 5 days during August 2013 for MODIS binned 4 km (night time 11 µm) daily images. Only "good data" (FLAG 0) was considered. Covering winter and spring conditions, available images from METOP-A were retrieved from OSI-SAF webpage (OSI-SAF, 2014) and matched with Level 1 results. METOP-A provides 1km resolution daily SST images in six spectral bands in the range of 0.58 - 12.5 µm. To allow comparison, only nigh time images were. The results obtained are presented in Figure 36. Qualitatively, the results obtained emphasize the model ability to reproduce the main spatial distributions of the SST found from space.

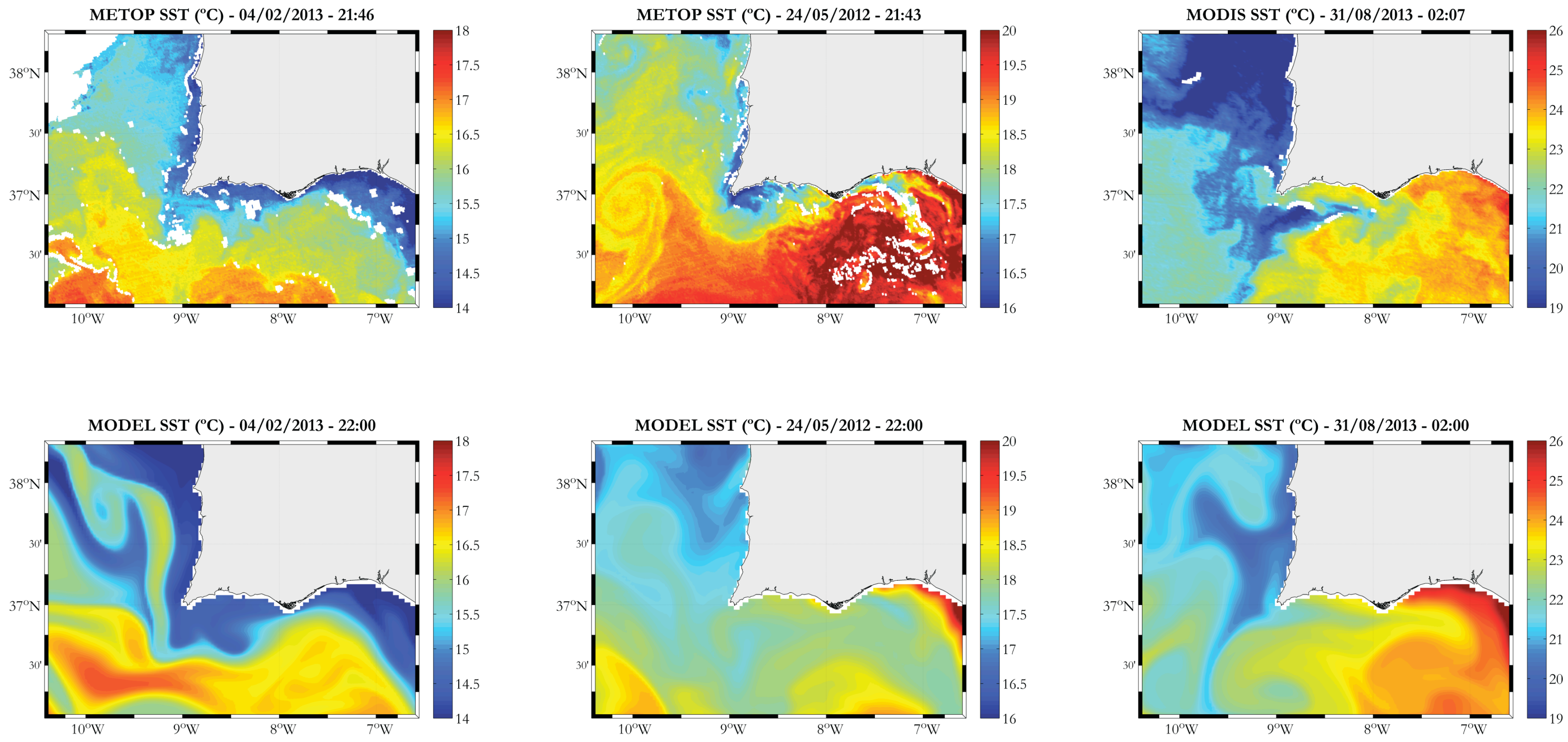

Figure 36 – Assessment of Level 1 (bottom) seasonal SST model performance by using available images (top) from both METOP-A and MODIS-AQUA satellites. From left to right: winter, spring and summer situations.

Although for the three periods considered a small bias can be found, the spring scenario seems to be the on presenting greater differences when relating model results with satellite image.

The model ability to reproduce vertical variations in temperature, salinity, and density was evaluated by using profiles available for the study area. Profiles from ARGO buoys, expendable bathythermographs (XBT's) and CTD where employed. Two ADCP transects were also used to validate the model current velocity components in depth. Due to data availability and to ensure a good geographical coverage on both model levels', the data spanned between the years of 2011, 2012 and 2013. In Figure 37 the distribution of the stations used is indicated.

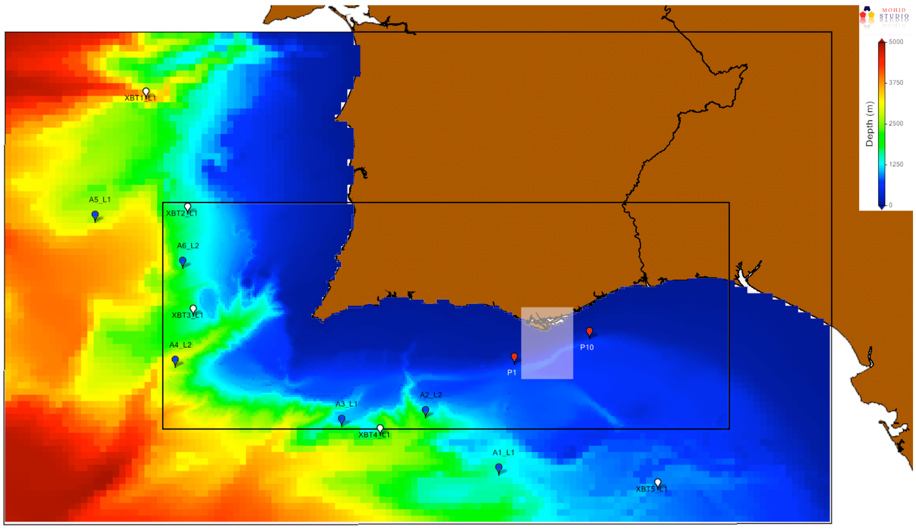

Figure 37 – Distribution of the vertical profiles used in the validation process in the model domain. Argo buoys profiles (blue), XBT profiles (white) and CTD profiles (red). The white filled rectangle represent the area were the ADCP transects were made while the grid levels implemented in the system are enclosed in black.

ARGO and XBT profiles were collected and made freely available by the Coriolis project and programmes contributing to it (http://www.coriolis.eu.org) for 2013 and 2011 respectively. Profile depths ranged the 1000 meters in each station. Both CTD profiles and ADCP transects were carried out during September 2012 in the scope of the EU programme Eurofleets using a SeaBird SBE 911plus CTD and a hull mounted RDI OS 75 kHz ADCP. Results obtained for the several vertical profiles are presented in Table VIII.

Table VIII - Errors obtained for the validation of the model against vertical profiles.

Station	***Property***	***RMSD***	***MSS***
A1_L1	*Temperature*	0.38 ºC	0.99
	Salinity	0.08	0.99
A2_L2	*Temperature*	0.54 ºC	0.95
	Salinity	0.20	0.90
A3_L2	*Temperature*	0.61 ºC	0.99
	Salinity	0.23	0.98
A4_L2	*Temperature*	0.7 ºC	0.94
	Salinity	0.25	0.95
A5_L1	*Temperature*	0.33 ºC	0.99
	Salinity	0.1	0.99
A6_L2	*Temperature*	0.6 ºC	0.96
	Salinity	0.16	0.90
XBT1_L1	*Temperature*	1.02 ºC	0.88
XBT2_L2	*Temperature*	0.73 ºC	0.97
XBT3_L2	*Temperature*	0.45 ºC	1.00
XBT4_L1	*Temperature*	0.47 ºC	0.99
XBT5_L1	*Temperature*	0.36 ºC	0.99
P1	*Temperature*	0.48 ºC	0.99
	Salinity	0.07	0.97
	Density	0.12 kg/m^3	0.99
P10	*Temperature*	0.64 ºC	0.99
	Salinity	0.14	0.96
	Density	0.15 kg/m^3	0.99

A good agreement between model results and vertical profiles was achieve throughout the model domain and in both grid levels, with MSS values very close to 1 (perfect agreement). Model validation results against two ADCP transects are presented in Figure 38.

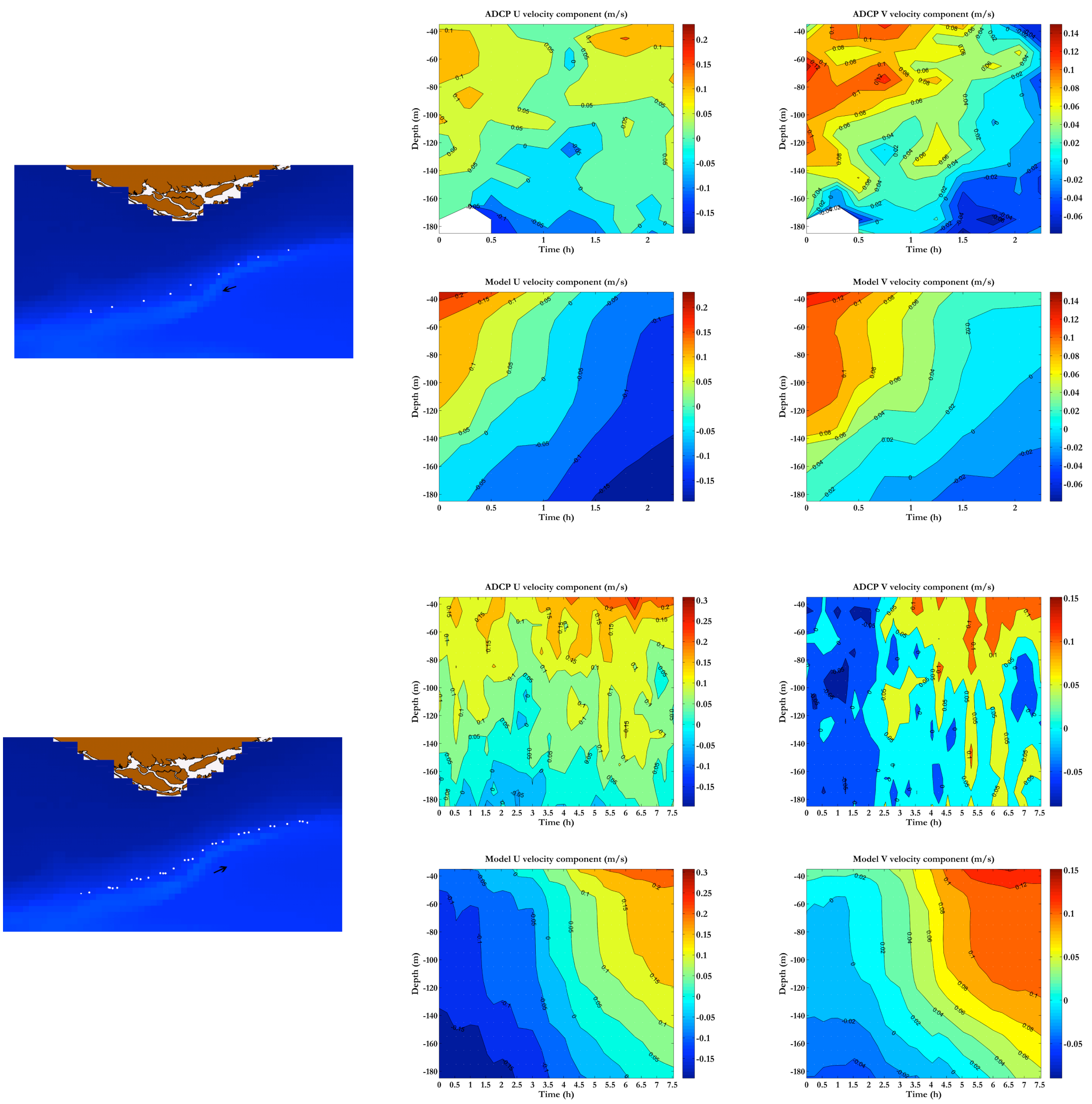

Figure 38 – Model validation against ADCP transects. The U and V components of the model are compared with the ones measured using the ADCP. The direction of the boat during each transect is represented by a black arrow.

The ADCP data was pre-processed using the CODAS (Common Ocean Data Access System) processing software (http://currents.soest.hawaii.edu/docs/doc/)

The two ADCP transects were recreated from model data by extracting, in each time step, the velocity components (U and V) corresponding to the bin depth. The different vertical resolution between model and ADCP bins required depth, and consequently, velocity interpolations in order to allow comparisons. Due to the differences in resolution, both horizontal and vertical, only a qualitative analysis was performed to the results. Although the model doesn't capture the high variability presented in the ADCP transects, in general terms, the results obtained show a good reproduction of the ADCP transects by the model. This is especially true for the V component of the velocity.

HFR technology has been rapidly expanding over last decade for measuring surface currents (Yaremchuk and Sentchev, 2011). The Portuguese Instituto Hidrográfico (IH) with the Spanish Puertos del Estado, since 2013, have been implementing a joined network of HFR Codar SeaSonde antennas to monitor sea surface currents and waves in the Gibraltar Strait and at the boundary area between Spain and Portugal (Mazagon and Monte Gordo respectively). This HFR network provides hourly data with a maximum range of 75km and a resolution of 1.3km. These observations were used to validate the model surface currents. In Figure 6 the results obtained for the comparisons between HFR and model (Level1 and Level2) are presented. Qualitatively, the results obtained show a good reproduction - in both levels of the model - of the surface velocity field near the coast, with the main features present in the HFR map being well reproduced by the model. Especially the increase in the velocity modulus from Level 1 to Level 2 closer to the coast near Faro, in agreement to what is observed in the HFR map.

Drifter buoys have been applied by several authors (e.g. Caballero et al., 2008; Janeiro et al., 2014; Price et al., 2006, 2003; Reed et al., 1988; Verjovkina et al., 2010) to validate oil spill models, as model simulated drifter trajectories can be directly compared with independent drifter experiments (Barron et al., 2007; Thompson, 2003). In this research 5 drifting buoys trajectories, drogued at depth of 15m, were used to validate the lagrangian model.

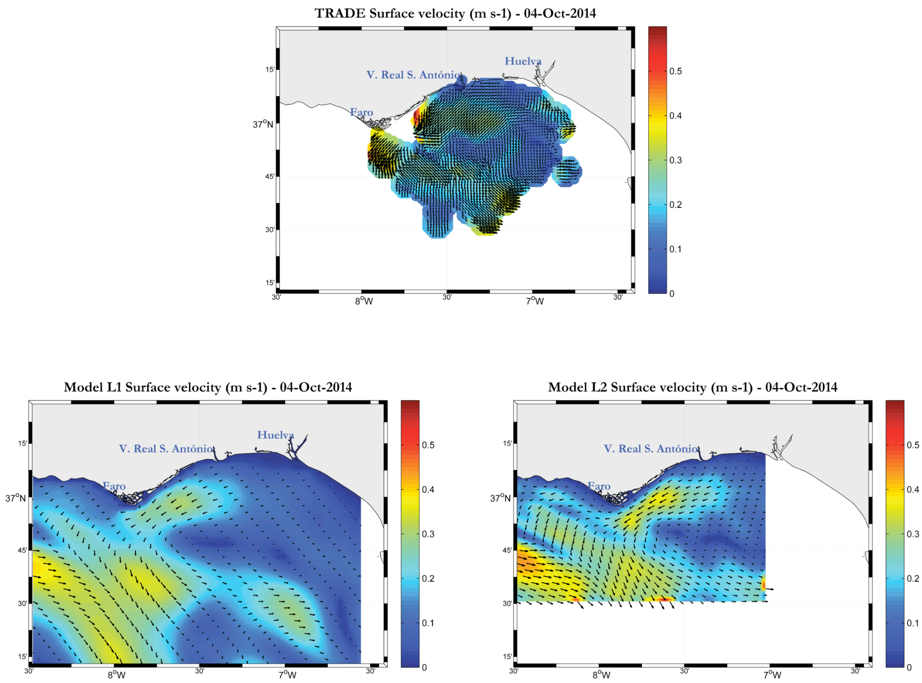

Figure 39 - Validation of model results, for both Level 1 (L1) and Level 2 (L2), against HFR observations in the eastern coast of Algarve.

The data, part of the Surface Drifting Program (SVP), was available by the Coriolis project covering periods from 2011 till 2014. Model drifters were released in the location where satellite-tracked drifters were observed, and their separation distance is a direct measurement of the trajectory model skill. The buoys positions were compared with the simulated trajectory of 200 lagrangian particles during 40 hours. The total release may be envisaged as a particle "cloud" which represents the probability of the buoy position, being thus described as a "probability cloud". In this approach a particle cannot be subdivided and is unable to interact with other particles. The multi-mesh approach ensures that the high-resolution hydrodynamics (Level 2) is used whenever the particles move into its geographical boundaries.

Turbulent diffusion coefficients were adjusted to better represent the drifters spreading. To compare the buoy trajectory with the model results, the centre of mass of the lagrangian particles outputted by the model was calculated

(Equation 12) according with the described in Janeiro et al, (2014). The errors were estimated using the Lagrangian trajectory-based non-dimensional index (Equation 13) proposed by Liu and Weisberg (2011) by which a total agreement is reflected by an *s* value equal to zero. In a first approach, a model scenario assuming the release of 200 particles at 15 m depth (anchor depth of the drifters) was simulated (Sim 1). The trajectories results are presented in Figure 40 while Table IX show the *s* values obtained for the simulations. With this approach four of the five drifters show comparisons with high *s* values with the exception of Drifter D (*s* = 0.45). This fact was also reported by Janeiro et al. (2014) with the authors suggesting several factors that might explain the discrepancies found. Among them, the change in anchor depth due to deterioration of the drifter's sock and the fact the velocity affecting the drifter is an integration of the current velocities from the surface to the anchor depth, along the connecting cable, considering that velocities in depth will have more weight than the ones at the surface due to the drifter's sock, rather than the current velocity at the drifters depth.

Table IX – Values obtained for s considering the five drifters studied and three simulation scenarios: Sim 1 – Depth of the lagrangian particles equal to depth of the drifter sock (15m); Sim 2 – Lagrangian particles imposed at the surface: Sim 3 – Lagrangian particles imposed at the surface plus a 3% wind velocity.

Scenarios	***s* Index**				
	Drifter A	*Drifter B*	*Drifter C*	*Drifter D*	*Drifter E*
Sim 1	0.79	1.08	0.96	0.45	1.16
Sim 2	0.77	0.48	0.86	0.69	1.30
Sim 3	0.77	0.48	0.86	2.90	0.48

To address these problems a simulation with the lagrangean particles located at the surface was developed (Sim 2).

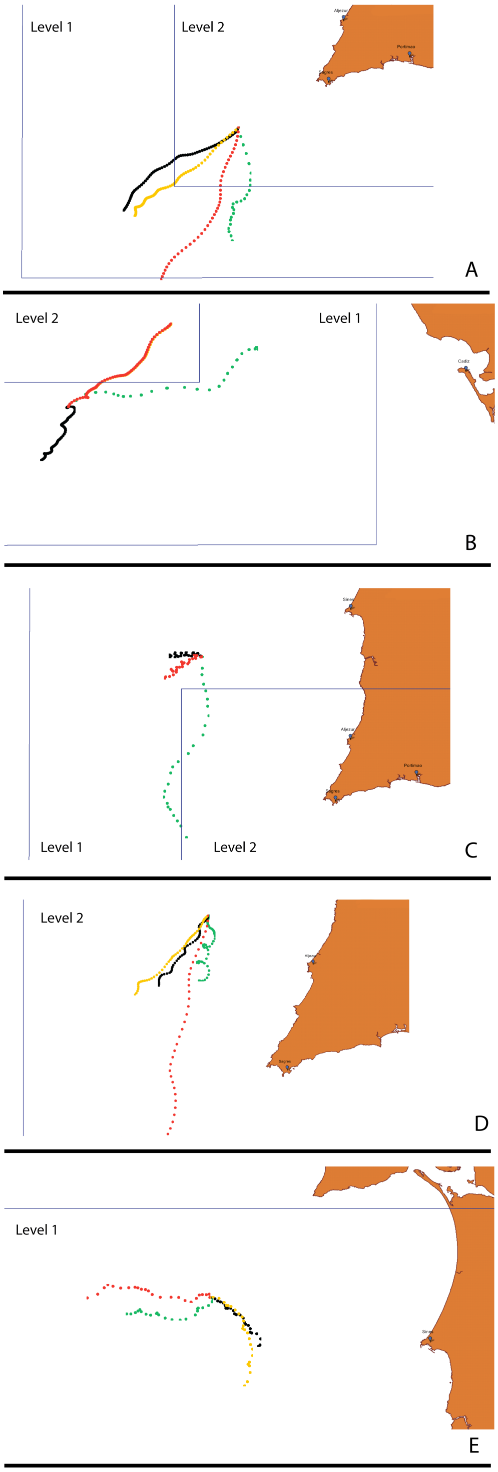

Figure 40 – Validation of the lagrangian model. Trajectories for satellite-tracked drifters (green) are compared with the centre of mass of the lagrangian cloud of particles for: Sim 1 corresponds to the release of 200 particles at 15 m depth (black), Sim 2 corresponds to the release of 200 particles at the surface (yellow), Sim 3 corresponds to the release of 200 particles at the surface but considering 3% of the wind velocity affecting the lagrangian particles (red). The limits of the two grid levels are also presented.

The results obtained show that the trajectories of the centre of mass at the surface or at 15 m didn't have a significant change, in fact in some cases (Drifters C and E) both trajectories were in the opposite direction of the drifters' (Figure 40). A final simulation (Sim 3) was developed combining the surface scenario with 3% of the wind velocity affecting the lagrangian particles (Figure 40). Although the results for the *s* index (Table X) didn't show substantial improvements from the surface scenario (only Drifter E presenting a lower *s* value) the wind correction seem to affect the trajectories of the particles in the model, which now follow the observed ones. The wind correction also induced an overestimation of the velocities affecting the lagrangian particles, which also explain the s values, obtained.

Table X– Values obtained for s considering the five drifters studied and three simulation scenarios: Sim 1 – Depth of the lagrangian particles equal to depth of the drifter sock (15m); Sim 2 – Lagrangian particles imposed at the surface: Sim 3 – Lagrangian particles imposed at the surface plus a 3% wind velocity.

Scenarios	***s* Index**				
	Drifter A	*Drifter B*	*Drifter C*	*Drifter D*	*Drifter E*
Sim 1	0.79	1.08	0.96	0.45	1.16
Sim 2	0.77	0.48	0.86	0.69	1.30
Sim 3	0.77	0.48	0.86	2.90	0.48

4. Backtracking

Following the validation procedure, SOMA was used in hindcast mode to backtrack a CleaSeaNet detection in the study area, occurring 65 km south Cape São Vicente during on the 20th of September 2012. MOHID backtracking feature (Fernandes et al., 2013) allows to simulate an oil spill back in time, with the purpose of detecting likely release sites, illegal discharges and potential polluters. This was done by backtracking a CleaSeaNet detection during 40 hours and combining the results obtained with AIS data for the period of the simulations. To minimize the trajectory errors associated to the backtracking simulation, the absolute distances between model-drifter, obtained during the validation procedure, were analyzed for the five drifters considering the scenario Sim 3 (Figure 41).

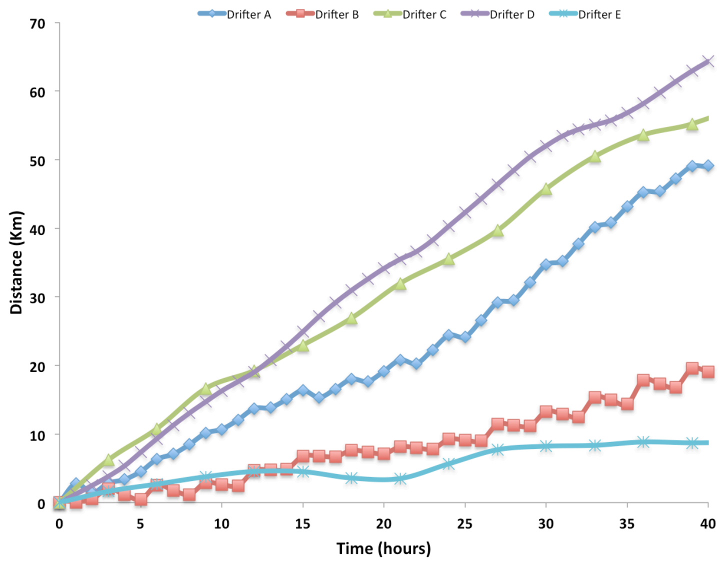

Figure 41 – Absolute distances between model and satellite-tracked drifter for each of the drifters considered in the study and for scenario Sim 3**.**

This is accordingly to the proposed by Price et al. (2006) and later by Abascal et al. (2009), that found the separation distance between model and satellite-tracked drifter trajectories during short time scales, a useful way to assessing applications related to oil spill trajectories. In the event of a spill, looking at the results from Figure 41, after 40 hours the estimated error of the model forecasted trajectory (based on all drifters) would be a radius of approximately 40 km from the forecasted position, while this value decreases to 23 km if a 24 hours forecast would be supplied. This approach was followed to identify possible sources for the pollution event. The model backtracked trajectory and AIS positions of the ships were divided in 8 hours blocks to ease the interpretation of the results. For each block, AIS positions were categorized using a temporal and a spatial filter in order to include the model trajectory errors. From the results presented in Figure 41, we choose 5 hours as temporal filter. This value allowed a good resolution when filtering the AIS data, with a higher degree of confidence in the model predictions, as the five drifters average for the absolute difference between model-drifter is approximately 5 km. The spatial filter used was then 5 km. Figure 9 resumes the results obtained. For each 8 hour block, ships that passed in a radius of 5km from the backtracked position and in a time period of ± 5 hours, where considered potential candidates to the pollution event. To add further information to this analysis, the identified ships were classified by type of boat using available online information from AIS databases.

5. Discussion

Based on the results obtained, in the overall, SOMA was considered well validated with its results showing good accuracy to be used as a forecasting tool to respond to oil pollution in the region. This is strengthened by the extensive validation procedure, with both a good spatial and temporal coverage (covering conveniently both model grids) while spread along a multiplicity of sensors.

Although errors found are in general low, differences between model and observations were found. These can be due a multiplicity of factors, as pointed out by Price and Bush (2004), including numerical errors (e.g. forcing fields, model implementations and boundary conditions methods) and observation errors (e.g. satellite-tracked drifters may contain location errors due to their long period at the sea).

Remote sensing observations provide a good tool to validate regional and coastal models, especially in regions characterized by strong temperature gradients like the study area. Time series observations provide a good insight on the model ability to correctly reproduce the evolution of properties in time. From the results obtained from Table VII, this was done accurately for all properties considered, with temperature at Sines buoy and salinity at Cadiz buoy being the ones with lower MSS (0.63 and 0.31 respectively). Sines is located in a region of high variability regarding SST due to the seasonal upwelling events occurring at the west coast. Especially in the month of October where in general these mesoscale features are more intense, stronger bias may occur if the model doesn't completely reproduce these features.

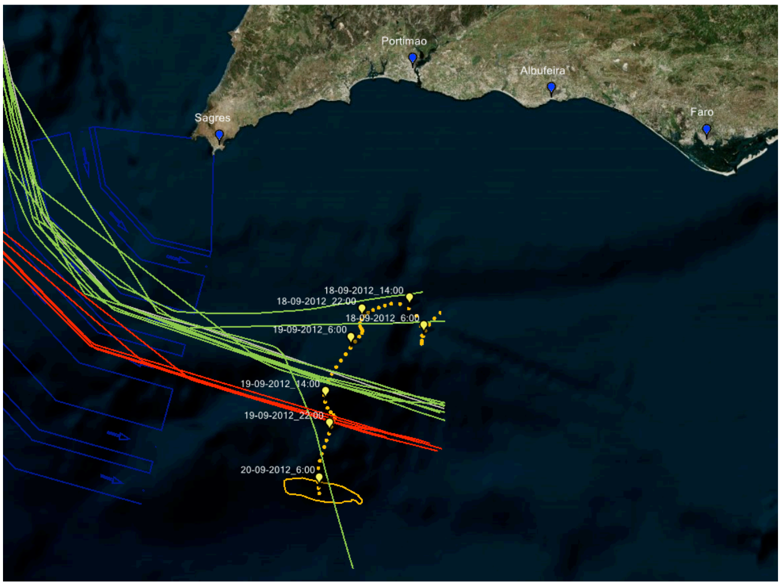

Figure 42 – Backtracking results for a CleaSeaNet detection in the southern Portuguese coast. The backtracked trajectory was combined with AIS positions for the ships in the region during the simulated period contributing to identify the potential source of this pollution event. The type of ship was colour classified: tankers (red), cargo (green) and unknown type (grey).

A small bias was also found in Figure 36 for the SST spatial distribution from satellite. Regarding the low value of MSS for the salinity obtained at Cadiz buoy, these also can be explained if we considered that the freshwater water balance (Evaporation-Percipitation-Runof) was not implemented in SOMA so far. The discharges of the rivers Guadalquivir, Odiel e Tinto (all discharging in the coast between Huelva and Cadiz) may explain this differences in salinity at the surface at Cadiz buoy. To support this, results obtained for the vertical profiles (Table VIII) all present low errors (MSS values very close to 1) for both temperature and salinity, with all stations being located in areas with few influence from freshwater discharges (Figure 37). The model current velocities where validated at the surface (HF Radar), in depth (ADCP) an as a time series (Cadiz Buoy) with results, analysed both quantitatively and qualitatively, for distinctive time periods. In the overall the model show good reproductions of the observed velocities. This is especially true when looking at the validation results obtained for the time series at Cadiz Buoy (Table VII), with MSS varying from 0.98 for the current velocity and 0,91 for the current direction. Also, HF Radar results (Figure 39) show that, not only the model manage to reproduce the current field observed, but there is a clear improvement on the surface velocity when we look at the high resolution results of Level 2. This highlights the advantages of the downscalling methodology in coastal areas where the bathymetry gradients are important shaping mechanism of the current field. Velocity comparisons for the ADCP transects are also considered good validation results, with a relevant difference between the zonal and meridional components. Looking at Figure 38, the difference in vertical resolutions between comparisons is detectable. The vertical geometry developed for SOMA allows higher resolution in the first 20 m depth, in order to better represent the surface layer and consequently oil spills trajectories, while decreasing it in depth to save computational time. The high resolution ADCP transects, starting at 35 m depth, are then being compared with the model results calculated with lower grid resolution, what explains some of the differences found. Thus, turbulence can also be a factor to consider when trying explaining these differences. Although no validation has been done to the turbulence model implemented in SOMA, turbulence is a quantity difficult to simulate. This is due not only to the limitations of the physics describing turbulent processes, and consequently the numerics, but also due to the high vertical resolution needed to solve turbulent motions.

The final dataset used for validation of SOMA were the satellite-tracked drifters. Although not an oil spill, it is an available method to validate the simulated trajectories and estimate model errors that should integrated future forecasts for oil trajectories. Three distinct scenarios were simulated in order to understand and explain the differences obtained. In this study the top layer is less than a meter thick which is considered high resolution enough to solve the Ekman boundary layer and so, as suggested by Janeiro et al. (2014) the drift velocity due to the wind was not considered initially. Nevertheless the results obtained in Figure 7 only show improvement when considering 3% of the wind speed in the lagrangian simulations, leaving us to believe that the model is not currently solving the Ekman layer properly. The improvements are only reflected in the direction of the trajectory, as from Table IX, the *s* values obtained for the error analysis of each simulated drifter scenario are high for the majority of the drifters. Considering that the model doesn't solve the Ekman layer disagrees with the velocity results presented and discussed above, showing very good comparisons, especially at the surface, for the model current field. With this in mind, boundary conditions arise as a possible explanation, as they introduce a relevant source of variability to the operational system that can explain the differences obtained from the drifter experiments.

Both ocean and atmospheric boundaries are themselves, operational model results with errors affecting its solutions. Although errors exist in the hydrodynamic solution being imposed at the open boundaries, these are minimized inside the model domain due to the Flow Relation Scheme implemented and explained above. Also, inside the model domain, the circulation at the surface is mainly wind driven, particularly in the study area, known by its high mesoscale variability (Haynes et al., 1993; Peliz et al., 2002, 2005; Serra and Ambar, 2002; Torres et al., 2003; Relvas and Barton, 2005). All the above points out for wind forcing being the plausible explanation for the results obtained in the drifters validation. An effort to test this assumption was made by using the observations from Cadiz buoy to validate both wind and current velocity for the entire simulation period of Drifter B. This drifter was the only that could be considered due to its location, the nearest to Cadiz buoy (approximately 60 km). Unfortunately the buoy dataset for the simulation period was not complete with values only covering the first 6 hours of each day, thus not being considered suitable to use.

The validation procedure confirmed the suitability of SOMA to simulate oil spill in the region. By combining remote detection technologies and numerical modelling, the backtracking of a CleanSeaNet spill detected south of Cape São Vicente was successfully completed. The methodology applied allow to include the errors found with the drifters during validation, leading to a more accurate detection of the ships that potentially might have been responsible for the pollution event. Although this is only a test of concept, this type of methodologies are considered useful to access responsibilities during oil pollution events. By tighten the legislation towards the use AIS, making it compulsory, and by increasing the current AIS coverage with the use of satellites, an international effort was given towards increasing the security and safety of maritime transportation. The combination of these technologies is seen as a step further in the response to oil pollution.

6. *Final Remarks*

SOMA was considered a fully validated operational system with the ability to forecast oil spill trajectories in the South Iberian coast. Discrepancies found during the validation procedure where identified and possible solutions are now suggested as future work:

- The bias identified in the SST comparisons should be addressed to better solve the natural variability of the study area. This is done being including in SOMA methods that allow data assimilation from operational monitoring stations (e.g. mooring buoys HF Radar, SST from satellite and altimetry) available for the region.
- Results obtained from drifters' experiments raise the question whether wind forcing fields, used operationally in SOMA, might be responsible for the discrepancies found. This hypothesis wasn't tested due to constrains' in the observations at Cadiz Buoy. Nevertheless, attention should be given to this issue and SKIRON results should be tested using available wide-ranging methods (e.g ASCAT) that allow a good coverage of the study area.
- Although waves weren't used as a forcing mechanism in this study, SOMA wave component is under development. Based on a SWAN (Simulating WAves Nearshore model) implementation, a 2-D phase-averaged wave model adapted to coastal areas (Booij et al., 1999) is being implement for the region. The domain

coincided with the SOMA Level 1, with a spatial resolution of 2.5-km while being forced with parametric boundary conditions made available by the Institut Français de Recherche pour l'Exploitation de la MER (IFREMER).

The results for the backtracking were encouraging. A robust methodology was proposed to derive possible pollution candidates from AIS positions, while incorporating model trajectory errors calculated during the validation procedure.

Chapter VIII – ***Mesoscale patterns and their role on oil spill trajectories in the Southwest Iberian coast***

Abstract

Several mesoscale processes, including upwelling filaments and fronts, characterize the Southwest Iberia oceanography. These mesoscale features are tied up to the large-scale climatological variability between the Azores high-pressure cell and the Iceland low. This climatological variability presents seasonal patterns from spring to late summer and during winter, which influence and characterize the Iberia coast circulation. The region lies on the main maritime route from the Mediterranean Sea and Southern Hemisphere to the North of Europe with tankers representing a significant part of the vessel traffic. The occurrence of an oil spill has thus a strong probability to happen. The present research study analyses the effects of regional mesoscale patterns in the evolution of oil spill trajectories. Five years of SST images, retrieved form both MODIS Aqua and METOP-A satellites are used to identify five typical mesoscale patterns at the Southwest Iberian Coast. An operational oil spill model implemented for the region was used to simulate several oil spill hypothetical scenarios along dense navigation routs. Results obtained show the model ability to correctly reproduce the observed regional sea surface patterns, highlighting the importance of accurate atmospheric forcing to solve the regional mesoscale variability. The importance of regional mesoscale features in the dynamics of oil spills is emphasized, not only by their direct effect in driving 'event-specific' spills but also the potential use of its seasonal patterns in the regional 'exposure degree' to oil spills. This study reinforces the discussion regarding the importance of these regional mesoscale features in the scale of human activities, while opens ways for a possible integration of this knowledge and this techniques in future regional planning and response operations for oil spills.

1. Introduction

Several research studies have focused on the western Iberian oceanography (e.g. Oliveira et al., 2004; Peliz et al., 2005; Relvas et al., 2007, Santos et al., 2011, Pires et al., 2013). With an overall circulation related to all other Eastern Boundary Current System (e.g. Benguela, Humbolt and California), here, the discontinuity imposed by the Mediterranean Sea together with the seasonality of the large scale atmospheric circulation have a profound impact on the regional oceanography.

However, as shown by Álvarez-Salgado et al. (2003), time scales of a few tens of days explain more than 70% of the variability of the coastal alongshore wind stress, a major factor governing the regional coastal circulation. The region's continental shelf, with less than 10 km wide south of Lisbon, 30–40 km wide off central Portugal and somewhat narrower again off northern Portugal and Galicia, is filled by topographical features, such as prominent capes, promontories and submarine canyons, whose spatial scales are tens to hundreds of kilometres (Relvas et al., 2007). The entire above highlight the importance of sub-seasonal temporal scales and sub-basin spatial scales, which explain the observed oceanographic patterns. Relvas et al. (2007) presented an extensive review on the physical oceanography of the western Iberia system and characterize the main mesoscale features described for the region. They include a succession of mesoscale structures such as jets, meanders, ubiquitous eddies, upwelling filaments and counter currents, superimposed on the more stable variations at seasonal timescales has suggested by several authors (e.g. Haynes et al., 1993; Peliz et al., 2002, 2005; Serra and Ambar, 2002; Torres et al., 2003; Relvas and Barton, 2005).

Focusing on the southwest coast of the Iberia Peninsula including the south coast and the northern Gulf of Cadiz (Figure 43), this mesoscale variability impacts directly the human coastal activities developed along a 450 km coastline. Among the activities, the maritime corridor passing between land and the Gorringe Ridge seamount, the Northwest area offshore of the Cape São Vicente, which concentrates shipping routes from the Mediterranean Sea and Southern

Hemisphere to Northern Europe, is of special concern due to its high traffic of oil tankers Janeiro et al., 2012.

The motivation behind this work is to investigate how oil trajectories respond to this mesoscale variability in Southwest Iberian coast in case of a tanker accident. Alvarez-Salgado et al. (2006) combining hydrographic, meteorological and dynamic data (remote sensing, drifting/moored buoys) showed how regional mesoscale features had an impact on the trajectories of the Prestige oil spill accident in the North Iberia.

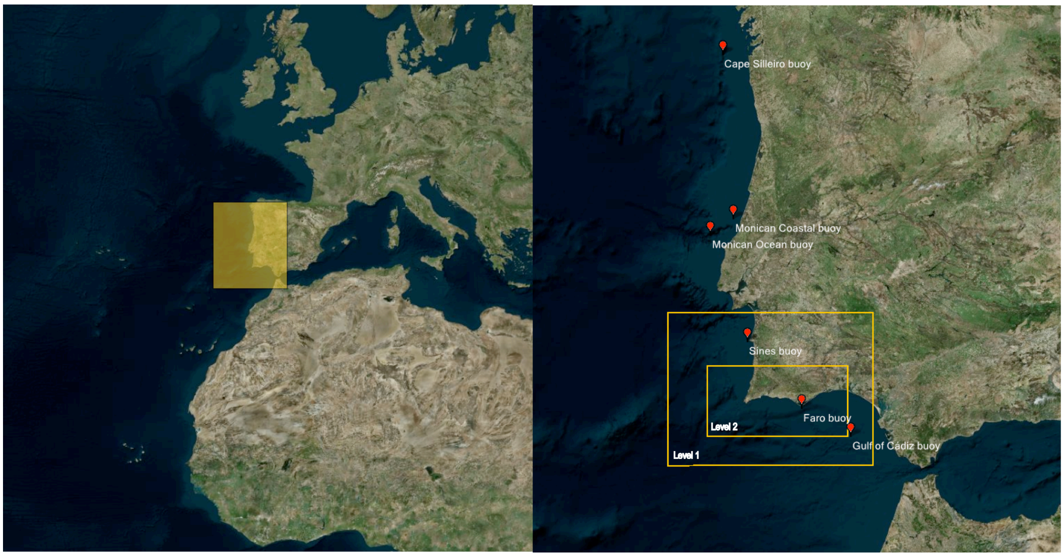

Figure 43 - Map of the study area displaying the location of the operational buoys used during the validation of the model and grid level comprising the operational system.

The authors concluded that the combination between the Iberian poleward current (IPC) and the convergence front between the IPC and the Western Iberian Buoyant Plume (WIBP) waters, prevented the entry of Prestige oil patches into the Galician Rías Baixas (Alvarez-Salgado et al., 2006). In this study, focusing at the surface, we looked for sea surface temperature (SST) patterns captured by remote sensing techniques, and relate them with the trajectory of hypothetical oil spills using an operational model already setup for the region (Janeiro et al., 2012).

Satellite SST images, nowadays an available operational product with resolutions ranging one kilometer, provide a good coverage at the regional and coastal scale. By relating them with the trajectory of oil spills, factors like the seasonality of these events and their inertia can provide an additional set of valuable information to both oil spill responders and planners in the region. The research paper is organized in the following way: the methodology used to derive the most important regional mesoscale patterns from SST images is presented followed by results of the model simulations preformed to reproduce these patterns and to drive hypothetical oil spills. Finally the results obtained are analyzed and discussed. Finally the main conclusions are presented, along with perspectives for future work.

2. *Methods*

Seasonal mesoscale features shape the regional ocean surface circulation of the South Iberian coast. These events affect the physical, chemical and biological processes (Relvas & Barton 2002; Cravo et al., 2010; Cardeira et al., 2013; Lopes et al., 2014) that occur at the surface layer also being a driving mechanism in the evolution of oil spills trajectories. To investigate the role of these regional features in the fate of oil spills a methodology combining remote sensing imagery, mooring buoy time series and model hindcasts was applied in the Southern Iberian coast.

2.1. Mesoscale Patterns

To look for seasonal mesoscale circulation patterns, five years of satellite images from both MODIS Aqua and METOP-A satellites were selected between 2009 and 2013. MODIS satellite data was retrieved from NASA's Ocean color webpage (NASA, 2014) consisting in a dataset of 470 MODIS binned 4 km (night time 11μm) images (Figure 44A).

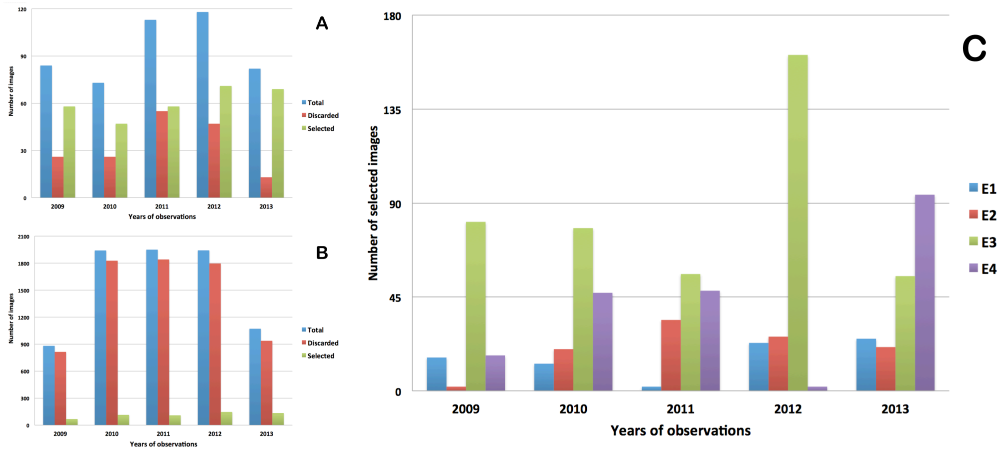

Figure 44 - Distribution of the SST satellite images considered in this study to define regional mesoscale patterns: (A) MODIS-Aqua; (B) METOP-A; (C) Distribution of the representative mesoscale events during the study period.

The data was visually selected and only swaths with relevant coverage were downloaded. From this dataset of images a quality control was applied. Based on the flagging methodology only "good data" (FLAG 0) was considered. The METOP-A dataset comprised approximately 7800 daily world SST images with 1km resolution and was retrieved from OSI-SAF webpage (OSI-SAF, 2013) for the period of interest (Figure 44B). The data was pre-processed applying a filter to select the images covering the geographical limits of the study area. To identify the several events, a visual review of the combined MODIS – METOP SST image dataset was done. Based on the SST images, Figure 45 resumes the five topologies of mesoscale events considered the most representative of the South Iberian coast.

The first mesoscale pattern defined, hereby E1, is associated with the meander of the southward upwelling jet to the west, near Cape S. Vicente, alongside occurring the development of upwelling filaments. Pattern E2 is depicted by the southwards flow of the upwelling jet overpassing the Cape S. Vicente forming an extended meridional filament. A clear signal of cool water throughout the southern Iberian coast without detachment is what defines pattern E3, which after further reviewing the SST image dataset, was subdivided into two sub-patterns.

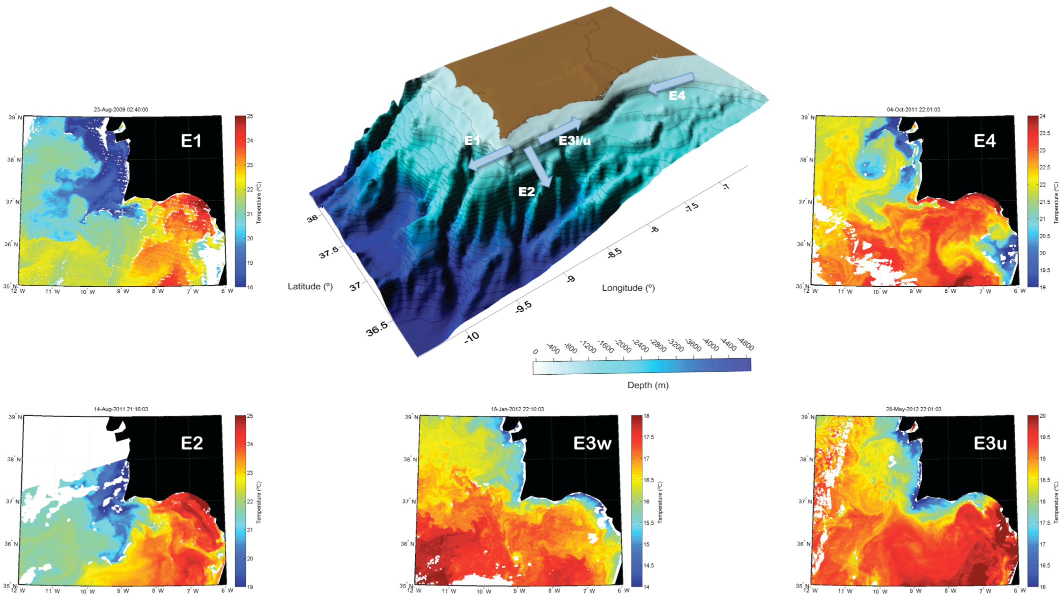

Figure 45 - Mesoscale events considered the most representative of South Iberian coast and classified from the available MODIA-Aqua e METOP-A SST images.

When the signal of cool water throughout the southern Iberian coast was associated with a small thermal gradient between adjacent Gulf of Cadiz water we classified it as E3w. In the satellite image dataset, this event is more frequent during winter with the warm water along the Iberian shelf edge and slope being associated with the upsurge of a poleward flow (Peliz et al., 2005), a direct effect of the shift in wind direction verified during wintertime. In E3u a significant thermal gradient with adjacent Gulf of Cadiz waters can be noticed. The cool water signal was associated with the upwelling jet turning Cape S. Vicente while flowing through the south Iberian coast. Finally, in pattern E4, a warm counter-current (Relvas and Barton, 2005; García-Lafuente et al., 2006; Teles-Machado et al., 2007) establishes near the south Iberian coast turning Cape S. Vicente flowing northwards near the coast. Figure 44C summarizes the distribution of the several events in the studied five-year period.

2.2. Model Simulations

Following the classification of the SST dataset into representative events, this information was used to generate a battery of simulations with the objective of assessing how effectively could the model simulate the mesoscale features. The simulations were performed by SOMA in hindcast mode. The system encompass a hydrodynamic model and an oil spill model running online and exchanging information in real-time, this is considered a more suitable method of simulating complex processes like the evolution of oil spills at sea Janeiro et al., 2014. The hydrodynamic model is composed by a set of two nested model implementations (Figure 43), assimilating boundary conditions from regional operational models available, while delivering high-resolution 3D hydrodynamic results with a horizontal spatial resolution of one kilometer in Level 2 and three kilometers in Level 1. In the vertical direction, the discretization is accomplished using a generic vertical coordinate divided in Cartesian layers at depth and high-resolution sigma layers in the first 20 m. The objective is to better describe the atmosphere-wave-ocean interface, while maintaining horizontality of the layers at higher depths. Hydrodynamic boundary conditions are provided daily by the Portuguese Coast Operational Modelling System (PCOMS) (Mateus et al. 2012; Campuzano et al. 2014, Ascione et al., 2014) including the day plus three days forecast of temperature, salinity, tide and velocities with a time step of 900 s.

The regional weather forecasting system SKIRON, developed for operational use at the Helenic National Meteorological Service (Kallos, 1997; Papadopoulos et al., 2001) provides 7 days forecasts with hourly data of wind U and V components, air temperature, specific humidity, total cloud cover, sea level pressure, total precipitation, upward and downward long wave flux, evaporation, latent heat flux and sensible heat flux at a resolution of 5 km. SKIRON results are used in the operational system as atmospheric forcing fields for the hydrodynamic and lagrangian models. The oil spill model is Lagrangian based and uses a multi-grid methodology allowing spanning across model domains Janeiro et al., 2014. A more detailed description of the operational system can be found in the research paper of the Chapter VII together with the validation results, performed using several types of observations. From the SST database, dates for each of the classified events were crossed with the available historical forcing data to initialize the model. This was considered a limitation in this study, as several well-defined events had to be disregarded due to the absence of forcing conditions.

A quantitative assessment of model ability to correctly reproduce the events simulated was done relating the model results of SST with operational observations from several buoys along the study area (Figure 43). This was done following the suggestions from O'Donncha et al. (2015). The Root Mean Square Deviation (Equation 14) and Willmott (1981) Model Skill Score (MSS) (Equation 15) error methodologies where applied. While the RMSD is a dimensional variable providing an absolute measurement of the error between the datasets, the MSS is non-dimensional and provides a deeper insight into the predictive abilities by overcoming the sensitivity of the correlation statistics to differences in the predicted mean and variances (O'Donncha et al., 2015). MSS varies between 0 (total disagreement between model and observations) and 1 (total agreement between model and observations). The BIAS between model results and observations was also calculated as:

$$BIAS = \frac{1}{n}\sum_{i=1}^{n}(e_i - m_i)$$

Equation 16

where n is the number of observations and e and m are, respectively, the model results and observations. This error assessment was done for the entire period of each simulated event. Table I resumes the findings. From Table XI, in general, the model presents a reasonable ability to reproduce the events, with an average of 0.5 for the MMS results. Nevertheless, there is a noteworthy bias in most of the comparisons. This is particular true for the results obtained in Sines buoy where it exceeds 1ºC in 4 of the 5 events simulated, reaching 4 ºC in event E4. Also, the bias doesn't show a clear tendency, with the model overestimating and underestimating the SST for different events and locations.

Due to the strong bias obtained for several events, in order to better identify and relate the SST patterns from both satellite images and model, in each event, an average bias for the three buoys was calculated and retrieved from the model SST. An exception was made for the maximum value of the bias, verified in Sines during event E4, which was not considered in the average. In Figure 46, the results obtained for the SST model simulations are presented and compared with the correspondent satellite image available.

Table XI - Assessing errors from simulations by matching model results with SST observations from three operational buoys along the study area. During event E1 there was no data available for Cadiz buoy.

Events	**Buoys**								
	Cadiz			***Faro***			***Sines***		
	BIAS (ºC)	RMSD (ºC)	MSS	BIAS (ºC)	RMSD (ºC)	MSS	BIAS (ºC)	RMSD (ºC)	MSS
E1	-	-	-	-1.2	1.3	0.5	1.1	1.1	0.4
E2	-0.01	0.1	0.9	2.6	2.6	0.2	3	3.1	0.3
E3w	-0.6	0.6	0.1	0.4	0.5	0.6	1.3	1.3	0.2
E3u	-0.6	0.7	0.5	-0.3	1	0.9	-0.2	0.3	0.9
E4	1.1	1.1	0.3	0.2	0.4	0.8	4	4	0.3

In event E1 the MODIS image gives a clear picture of the upwelling jet flowing southward, meandering when it encounters Cape São Vicente and creating a well-defined upwelling filament stretching westward. Northwards, around 38ºN, a second upwelling filament can be observed with possible origin in Cape Sines. Part of the upwelling jet bends Cape São Vicente reaching the south Portuguese coast as far as 8ºW.

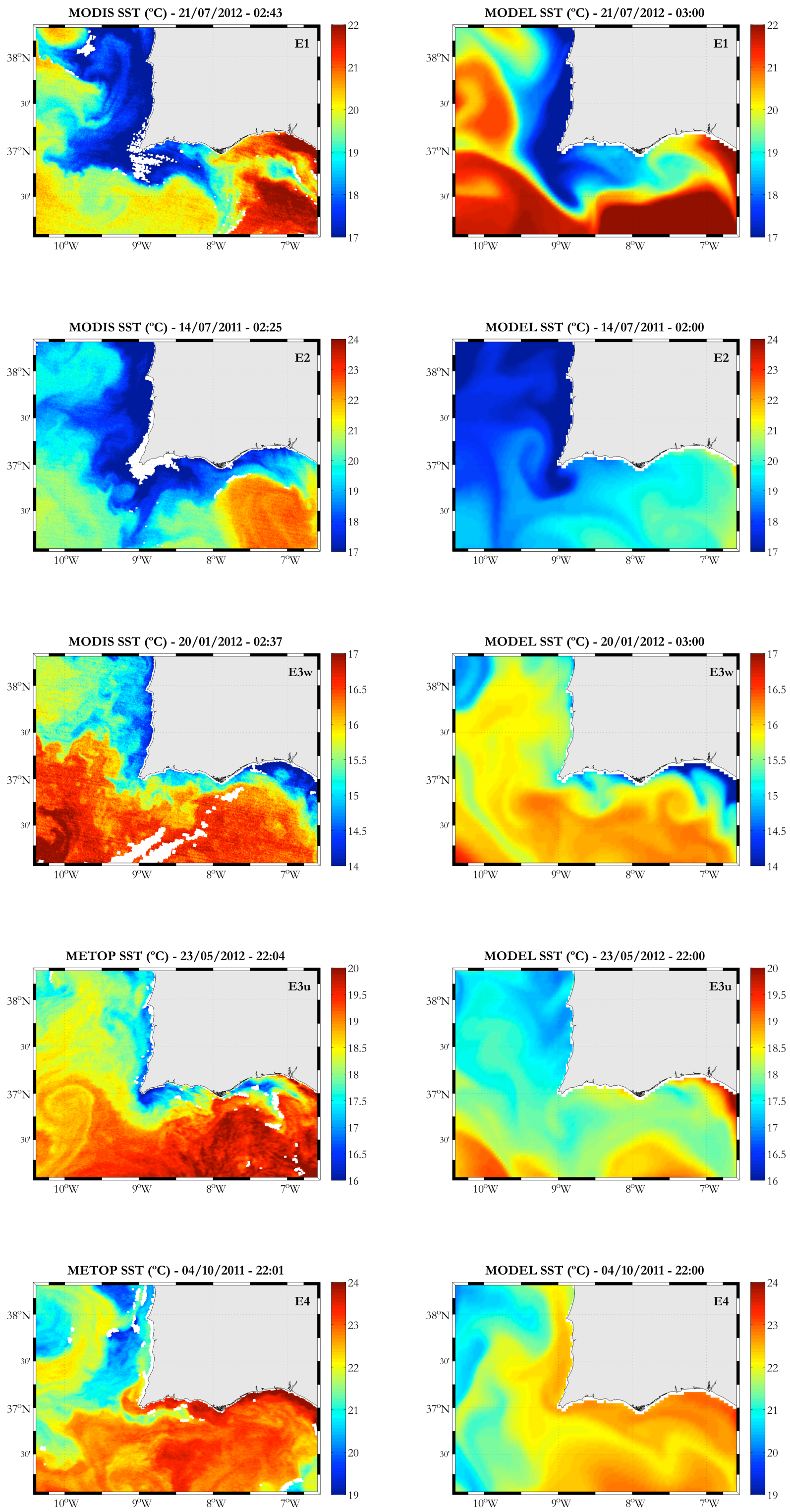

Figure 46 – Mesoscale events considered in the study derived from both MODIS and METOP-A SST dataset. For each particular event model results are presented in the right while SST images in the left.

Here a warm coastal counter-current flowing westwards balances the upwelling front, with the cool water jet shifting its directions northwards creating a well defined thermal front. The cool water pocket in the Gulf of Cadiz suggests that the upwelling jet reached further east. A rapid relaxation of favorable upwelling winds may explain the advance of the warmer Gulf of Cadiz water that intercepted the upwelling jet separating this patch. In the model simulation the major features described above are present. The upwelling filaments near Sines and Cape São Vicente, although present, are not well developed by the model. Instead of a westward flow when reaching Cape São Vicente, part of the upwelling jet flows southwards. As in the satellite image, the upwelling jet turns Cape São Vicente flowing eastwards where it further encounters the warm counter-current and a balance is reached near the longitude of 8ºW. Off the coast, the cool water signal reveals that the upwelling jet was further east like observed in the satellite image, with warmer water from the coastal counter-current enfolding the remain of that cool water.

During event E2, part of the upwelling jet flows straight southward of Cape São Vicente to around 36º. At Cape São Vicente, the remaining part turns eastwards, flowing along the coast till 7ºW. The model succeeds in reproducing the upwelling jet going south Cape São Vicente, although underestimating its southern reach. There is also a cooler water jet flowing eastwards around the coast although the difference in temperatures is not so marked as it is in the satellite image.

The warm water signal associated with the poleward flow, a distinctive winter feature in the region (Peliz et al., 2005), can be well identified in the satellite image in event E3w. Along the coast, a cool water signal is noticeable from the Gulf of Cadiz till Sines. The model reproduces to a good extent the E3w pattern. Especially in the west coast the bias in SST is still perceptible, nevertheless the presence of warmer water in the Gulf of Cadiz opposing with the cool water signal along the south coast distinctly mark this E3w event in the model results.

During event E3u, the upwelling jet flowing south shifts eastwards after Cape São Vicente reaching 9.5ºW. Possibly due to the persistence of northwesterly wind, a second upwelling event occurs eastwards Cape Santa Maria extending into the Gulf of Cadiz till 7ºW piercing into the warmer Gulf of Cadiz waters. While E3u pattern features are present in the satellite image, there were period's far more representative of E3u events in the SST images database but those dates could not be used due to the lack of forcing conditions for the model. Though an overall bias occurs, especially in the warmer Gulf of Cadiz waters, most of the features existing in the satellite image can be observed in the model simulations. The upwelling in the west coast seems to be starting in response to the intensification of the wind while east of Cape Santa Maria an incipient upwelling front is developing into the Gulf of Cadiz. A weak signal of the warm Gulf of Cadiz waters can be seen near shore from Faro to Sagres, where it recirculates south in Cape São Vicente.

Finally, event E4, presents the evolution of the warm coastal counter-current that is established when the relaxation of upwelling favorable winds occur. There is a clear signal of its warm water from the Gulf of Cadiz to Cape São Vicente, where it flows poleward after turning the Cape. Its signal can be traced as far as 38ºN near Sines. In the model simulations obtained for this period, the same pattern can be observed, although an important difference in the magnitude of the event, both in longitude and latitude, exists. This difference in magnitude explains the 4ºC bias obtained in Sines buoy.

2.3. Oil trajectories

To assess the influence of the identified regional mesoscale features in the trajectories of oil spills, several hypothetical spills were simulated during two days in the period of each event. The position of each spill was choose based on the major shipping routes crossing the study area and the presence of major ports. The oil spills are only influenced by the hydrodynamics, which accounts for the wind effect. Figure 47 resumes the results obtained.

During event E1 there is a clear influence of the upwelling jet flowing southwards on the trajectories of the spills located in the west coast.

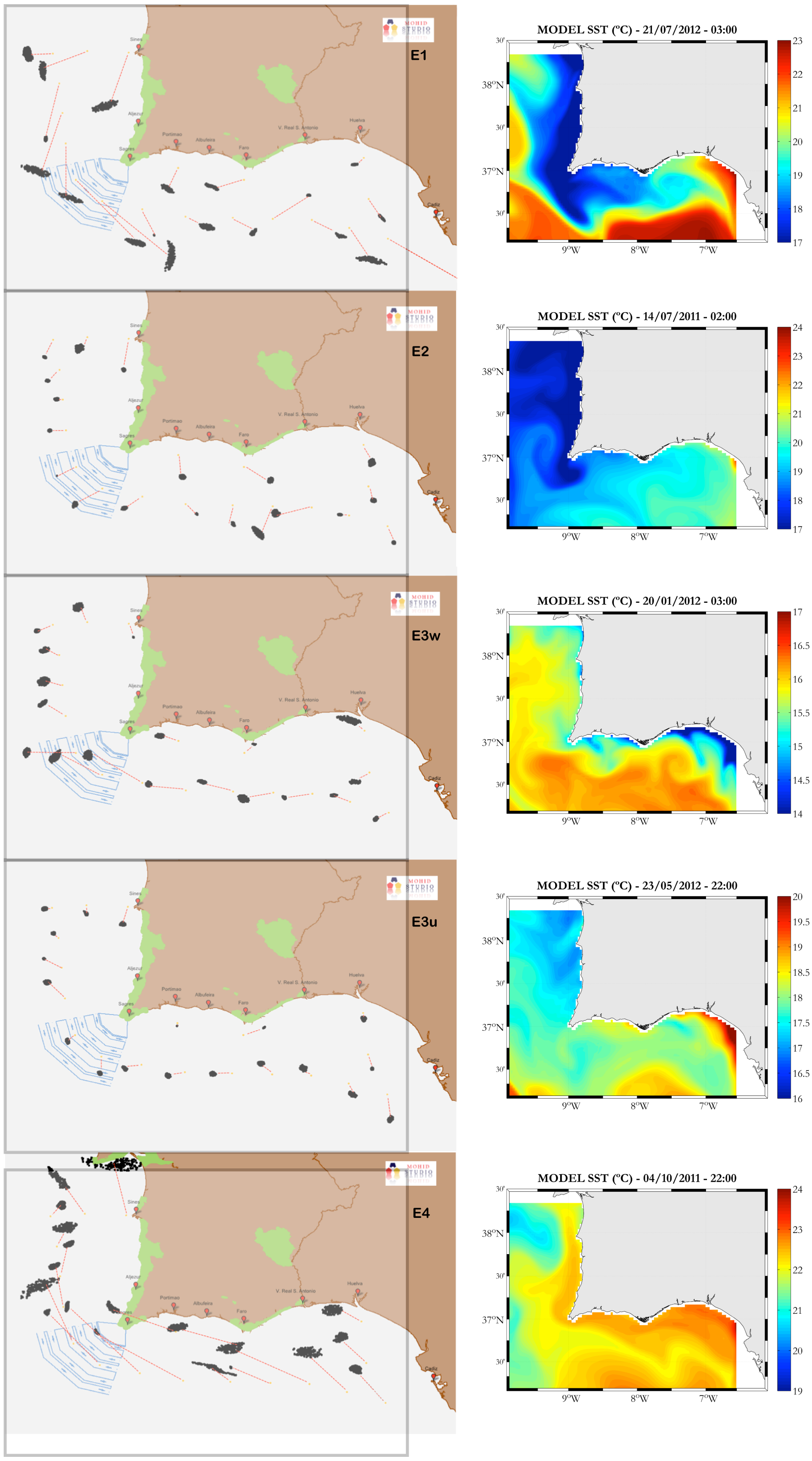

Figure 47 - Oil spill scenarios simulated for each classified upwelling event (left). The orange dots correspond to the initial position of the spill while the red line shows the trajectory associated with each spill and in black the final position of the spill. The grey rectangle marks the Northern and Eastern limits of level 1, the outer model grid. Green areas represent protected areas. To the right the correspondent simulated SST distribution in the study area is presented

Two spills off Sines travel away from the coast influenced by the upwelling filament that, although not so obvious in the SST simulations, it's clear from the satellite image (Figure 46). The two spills located inside the shipping corridor, off the coast of Sagres, follow the upwelling jet that shifts eastwards in Cape São Vicente. This jet further impacts on the trajectories of all other spills located southwards offshore, transporting then eastwards, with one of the spills located offshore Cadiz leaving the model domain. When this happens the model is driven by the PCOMS hydrodynamic forcing conditions, with the spill not being extinct inside the outer model domain. Nevertheless, further on, results outside the model domain (grey rectangle) will not be discussed. Near the coast, the spills respond to the warm coastal counter-current and to more localized circulation patterns.

Through event E2 the south flowing upwelling jet drives the trajectories of the four spills closest to Sines. Near Aljezur, an upwelling filament, present both in the satellite image and in the model results, drives two of the spills west. In the vicinity of Cape São Vicente, the upwelling jet continues south, driving the trajectories of the three spills closest to the shipping corridor. Part of the upwelling jet, flowing eastwards along the coast after turning Cape São Vicente, enters the Gulf of Cadiz and drives the trajectory of the spills more close to the shore. The Gulf of Cadiz thermal front circulation seems to be associated with the different trajectories of the offshore spills, which flow westwards. The thermal front established between the warmer Gulf of Cadiz waters and the cool waters near the coast, very clear in the satellite images and distinct in the model simulations, affects the trajectories of the two spills offshore Faro, driving them southwards.

In event E3w, the more offshore oil trajectories noticeably follow the thermal fronts established between the warmer poleward circulation and the cool waters near the shore. Along the southern and western Iberian coast, oil trajectories are towards west, while closest to shore, the spills respond to more local hydrodynamic forcing's, but possible to detect in the SST distribution. Near Sines the spill trajectory is southwards in response to the re-circulation of the poleward flow near the coast, nevertheless this feature is considered an overestimation by the model, since it is not visible in the satellite image. Near the ports of Portimão, Faro and Huelva, the spills also respond to the thermal gradients established locally, visible in both model and satellite image SST signatures. It is also interesting to notice how the spill closest to Faro has an eastward trajectory following shore and associated to the vortex established off Cape Santa Maria. This vortex is also not visible in the satellite image, although there are some clouds in the region that may be affecting the results.

Looking at the results during event E3u, again the SST distribution seems to be in a good agreement with the modeled oil trajectories. In the west coast, between Sines and north of Sagres, spill trajectories are driven by: 1) a south flowing upwelling jet in formation, 2) the poleward flow. In the vicinity of Sagres, the trajectories of the two spills inside the ship corridor appear to be related with the warm patch of water that recirculates south when it encounter Cape São Vicente. This feature doesn't seem to be present in the satellite image (Figure 4) where the developed upwelling jet turns Cape São Vicente, impinging against the warmer waters of the Gulf of Cadiz. Offshore, from Sagres to V. Real S. António, the spill trajectories seem related with the warmer patch of water from Gulf of Cadiz, flowing westwards. Closest to shore the small upwelling region forming east of Cape Santa Maria, creates a pressure gradient driving the spill near Faro eastwards, while the upwelling jet flowing southeast, directly influence the four spill trajectories closer to Huelva and Cadiz.

Though the coastal counter-current is being overestimated in the model, this feature of event E4 is the key driver of all spills simulated. This overestimation is especially true at the exit of Cape São Vicente, explaining the larger influence on the spills more offshore, while in the satellite image the coastal counter-current jet seems to be more confined to the shore, although its real dynamical influence is unknown. From the modeled events, only E4 produced spills reaching the shore during the two days simulated period. This happened firstly with the spill located near Portimão, which arrived to shore near Sagres turning Cape São Vicente and flowing north. The spill nearest to Sines, being transported northwards, also arrives the shore in Setúbal during the two days period, though it leaves the level 1 model grid prior to that. Based on the results obtained, increasing the simulation time would potentially have a direct effect on the number of spill reaching shore during this event.

3. Discussion

The main mesoscale features present in the region, observed and described by several authors, were clearly identified by observing the remote sensing SST data. Also, the temporal coverage of the database, combining both MODIS and METOP-A satellites, allowed us to perceive the mesoscale patterns that occur in the region. This is regarded as useful information not only for the present work, but also for future research focused on relating and explaining these regional patterns with the main driving forcing mechanism defining the oceanography of the Iberian Peninsula.

In what respects to SST, the southwest and south coast are two well-distinguished areas. This is clear from satellite images but also from in situ observations, with the majority of the patterns observed being produced by the dynamic equilibrium between these two areas. Looking at the results obtained, differences in SST exist between satellite images and model results, nonetheless, in general the model represents to a good extend the major features observed from space. These differences occur both in the magnitude and direction of each of the events, with each of the simulations presenting different temperature bias when compared to in-situ observations. This points out for the important weight that regional natural variability may have in the overall error. This variability is included in the model throughout its boundaries, both ocean and atmospheric.

Although errors exist in the hydrodynamic solution being imposed at the open boundaries of the model, these are minimized inside the model domain due to the Flow Relation Scheme implemented and further explained in the previous chapter. To explore the role of atmospheric boundary conditions in the quality of the simulated SST patterns, the SKIRON historical forcing conditions for each one of the events simulated were compared with data from METOP-A ASCAT Level2 ocean surface wind product, optimized for Coastal Ocean. With a 12.5 km sampling resolution, this EUMETSAT product differs from the standard ASCAT datasets in that it utilizes a spatial box filter, rather than the Hamming filter, to generate a spatial average from the Level1B retrievals. This enhanced method allows ASCAT winds to be computed as close to ~15 km from the coast, as compared to the static ~35 km land mask in the standard 12.5 km dataset. Verhoef and Stoffelen (2011) present a more detailed description of the methods used and validation results for this ASCAT product. The accuracy of both model and ASCAT datasets was matched against observations from four operational meteo-oceanographic buoys along the Iberian Coast (Figure 43). As a first step, it was selected for each of the simulated events, the times when ASCAT and buoy observation coincide at the buoys locations. Finally a regression was done between ASCAT/buoy and SKIRON/buoy for those specific times. To estimate the quality of the comparisons, quantification of the differences was performed for both wind speed and direction using the Pearson correlation coefficient (Equation 11). The results obtained are summarized in Table XII.

Looking at the results obtained in Table XII, there is a clear difference in accuracy between ASCAT and SKIRON if we consider wind speed or wind direction. While for ASCAT, R is in general constant between both parameters (but in the overall still presenting a better correlation for wind speed than for wind direction), when considering SKIRON the results obtained show a better correlation between wind speed (in most cases better than ASCAT) while a poor correlation for wind direction. In fact, only looking at Cadiz buoy, the results obtained for the MMS, presented in Table XI, correlate with the lowest value of R for wind direction in Table XII. The parallel can't be established between the other buoys as their location differs significantly from the study area. In this way, the differences in wind direction observed between observations and the SKIRON dataset were considered significant to influence the simulation results. This was also suggested as a possible explanation for the differences found in the previous chapter during the validation using drifting buoys, where errors in the wind forcing affected the model performance.

Table XII– Pearson coefficient values for the comparison between wind speed and direction measured by meteo-oceanographic buoys along the Iberian coast and ASCAT and SKIRON results. Data for buoy MONICAN combines both Coastal and Ocean buoy due to individual data availability for the simulated periods. Results from the coastal buoy are marked with *. The location of the buoys can be observed in **Figure 43**.

Event	Cape Silleiro			
	Wind Speed		Wind Direction	
	ASCAT	*SKIRON*	*ASCAT*	*SKIRON*
E1	0,59	0,81	0,64	0,15
E2	0,59	0,76	0,65	-0,06
E3i	0,58	0,82	0,42	-0,26
E3u	0,41	0,67	0,31	0,43
E4	0,41	0,82	0,04	-0,27

Event	Monican - Ocean/Coast			
	Wind Speed		Wind Direction	
	ASCAT	*SKIRON*	*ASCAT*	*SKIRON*
E1	0,67*	0,76*	0,62*	0,53*
E2	0,62	0,91	0,36	-0,35
E3i	0,56*	0,83*	0,53*	-0,12*
E3u	0,67*	0,91*	0,65*	-0,14*
E4	0,6	0,87	0,31	0,02

Event	Cádiz			
	Wind Speed		Wind Direction	
	ASCAT	*SKIRON*	*ASCAT*	*SKIRON*
E1	0,75	0,81	0,72	0,68
E2	0,71	0,71	0,73	0,51
E3i	0,37	0,59	0,56	-0,03
E3u	0,46	0,41	0,66	-0,02
E4	0,7	0,6	0,75	0,12

This study reinforces the discussion for the importance of these regional mesoscale features in the scale of human activities. Despite the differences obtained, the methodology applied highlighted the good agreement between SST features, presenting seasonal patterns in the study area, with the trajectory of oil spills. This opens way for a possible integration of this oceanographic features in future regional planning and response operations for oil spills.

A successful response to an oil spill accident in a defined geographical area involves, in its baseline, an oil spill risk analysis (OSRA) for that specific area (**Figure 31**). As identified by Santos et al. (2013) OSRA, which deals with the uncertainty associated to these pollution events, is a combination of two key phases: risk assessment (RA) and risk management (RM). Part of the RA phase encompasses a hazard potential analysis of the likelihood/probability of the spill occurrence and the corresponding extent of damages on affected places This analysis includes aspects that are ‘constant’ throughout a period of time within a given marine/costal area, but also ‘event-specific’ characteristics that will determine the type of impacts on a given marine/coastal area, as well as their probability Santos et al., 2013. With this study, the importance of regional mesoscale features in the dynamics of oil spills is emphasized, not only by their direct effect in driving ‘event-specific’ spills but also the potential use of the patterns associated with these events in the regional ‘exposure degree’ to oil spills. All the above highlight the importance to better understanding these mesoscale patterns, identified as a key challenge by Relvas et al. (2007), and their further response to externalities like climate changes Pires et al., 2013.

4. Conclusions

The importance of regional mesoscale features, identified by several authors in the last decades, has been related with oil spill trajectories by using a combination of remote sensing with operational modeling. Although other hydrodynamic modeling implementations do exist, focus on explaining some of the physical processes identified in this work, while providing more accurate results, we highlight the limitations in accuracy linked to the ability of providing operational results. In the field of operational oceanography, not only the question of computational power arises as a limitation, but also the dependence of other operational products, as shown. Nonetheless, the results obtained in this study reinforce the discussion regarding the importance of these features in the scale of human activities, while opens ways for a possible integration of this knowledge in the oil spill risk assessment process.

Chapter IX – Conclusion and future work

In this work a methodology to downscale regional operational products to the coastal scale was successfully applied in two European regions most sensitive to oil pollution. In each, an operational model capable to simulate and forecast the fate of oil spills at sea was implemented and fully validated. Two main advantages arise from the use of the methodology presented. The first is related to the capability of reaching the resolutions required to focus on the coastal scale without compromising the time frame of the operational system, always a key issue due to computational limitations. The second is related to the ability to improve the system based on the increasing advances in operational products available both in Europe and worldwide. In fact, operational oceanography has been growing in importance in the past decade, with new and improved regional products being constantly available, providing improved boundary conditions to coastal systems like the ones presented here.

Research work on the interaction between waves/currents/wind and their importance in improving the accuracy of oil spill forecasts was done with the objective to contribute to the understanding of how ocean physical processes affect the trajectory of oil spills. Likewise, regional mesoscale features have been related with oil spill trajectories reinforcing the discussion regarding the importance of these features in the scale of human activities, suggesting a possible integration of this knowledge in the oil spill risk assessment process. The influence of coastal processes was demonstrated and indicated as relevant in most cases to improve the simulated trajectories. Consequently, the need to have accurate atmospheric boundary conditions was shown of vital importance and it is considered a limitation of the method. When increasing the resolution, small scale processes start to become important leading to the need of even higher resolution atmospheric boundary conditions to accurately solve the high variability obtained. This brings the paradox: increasing the resolution may actually degrade the quality of the results. This happens, externally to the operational system, with atmospheric forcing, but also, internally. To increase the resolution emphasizes the role of turbulence in the quality of the results. This is also a challenge, not only due to the limited background knowledge available on turbulent quantities but also due to the scales necessary to effectively simulate turbulent flows.

Knowledge was also gather on the decision making process involved in the management of ocean resources and response to oil spills. This was of paramount importance to achieve a more comprehensive tool, with the ability to provide answers to the next societal challenges concerning these issues in both regions. In fact, both operational system were also integrated with detection and monitoring (both *in situ* and remote) technologies in order to improve the response and management to oil pollutions events. The methodology discussed in this work proved its ability to respond during the emergency of Costa Concordia in Giglio Island (Italy), pointing out the importance of integrating this operational tools in the planning and response actions.

Although the main focus of this thesis is oil spills, the challenges that affect the coastal regions are far broader. Nowadays, coastal activities (leisure, industry, transport, governance) require further information not only about present and future state of the sea, but also the study of scenarios or to understand past events, in order to improve their competitiveness but also to better manage their activities. Understanding this, the development of operational tools which ensure information for a multiplicity of applications was also understand as of utmost importance. This is seen as the main priority regarding future work. The integration of more data providers in the operational system widening the availability of boundary conditions (for both hydrodynamics, waves and atmosphere) would be of priority. This will safeguard not only a potential increase of accuracy in the results (dependent on the quality of the forcing's) but above all to ensure redundancy. Data assimilations methods are also a key issue and a future implementation foreseen. Especially in the Southwest Iberian coast, where the surface variability was seen important, to assimilate SST, altimetry, and observations from the available operational moorings in place in the region, would potentially provide an increase of accuracy. Closest to shore, the presence of freshwater discharges was pointed out as a potential explanation to the differences found between modelled temperature and salinity, with salinity always presenting the lowest comparisons with observations. To address this, to include the freshwater cycle on both operational models is also pointed as future work.

References

Abascal, A.J., Castanedo, S., Medina, R., Liste, M., 2010. Analysis of the reliability of a statistical oil spill response model. Mar. Pollut. Bull. 60, 2099–110. doi:10.1016/j.marpolbul.2010.07.008

Abascal, A.J., Castanedo, S., Mendez, F.J., Medina, R., Losada, I.J., 2009. Calibration of a Lagrangian Transport Model Using Drifting Buoys Deployed during the Prestige Oil Spill. J. Coast. Res. 251, 80–90. doi:10.2112/07-0849.1

Abdulla, A., Gomei, M., Hyrenbach, D., Notarbartolo-di-Sciara, G., 2008. Challenges facing a network of representative marine protected areas in the Mediterranean: prioritizing the protection of underrepresented habitats. ICES Journal of Marine Science 66, 22-28

Albers, S., 1995. The LAPS wind analysis. Weather Forecast, 10, 342-352

Allen, C. M., 1982. Numerical simulation of contaminant dispersion in estuary flows. Proceedings Royal Society of London, A381, 179-194.

Alvarez A., Caffaz A., Caiti A., Casalino G., Gualdesi L., Turetta A. and Viviani R., 2009. Folaga: A low-cost autonomous underwater vehicle combining glider and AUV capabilities, Ocean Engineering, Vol. 36, No. 1, pp 24-38.

Alvarez-Salgado, X. a, Herrera, J.L., Gago, J., Otero, P., Soriano, J. a, Pola, C.G., García-Soto, C., 2006. Influence of the oceanographic conditions during spring 2003 on the transport of the Prestige tanker fuel oil to the Galician coast. Mar. Pollut. Bull. 53, 239–49. doi:10.1016/j.marpolbul.2005.09.031

Álvarez-Salgado, X.A., Figueiras, F.., Pérez, F.., Groom, S., Nogueira, E., Borges, A.., Chou, L., Castro, C.., Moncoiffé, G., Ríos, A.., Miller, A.E.., Frankignoulle, M., Savidge, G., Wollast, R., 2003. The Portugal coastal counter current off NW Spain: new insights on its biogeochemical variability. Prog. Oceanogr. 56, 281–321. doi:10.1016/S0079-6611(03)00007-7

AM&WFG, 2010. Atmospheric modelling and Weather Forecast Group, University of Athens, http://forecast.uoa.gr/. Accessed: 14/07/2010

Andersen, H.E, Kronvang, B., Larsen, S.E., Hoffmann, C.C., Jensen, T.S., Rasmussen, E.K., 2006. Climate-change impacts on hydrology nutrients in a Danish lowland river basin. Sci. Total Environ.; 365: 223–237.

Andrade, M.M.N., Szlafsztein, C.F., Souza-Filho, P.W.M., Araújo, A.R., Gomes, M.K.T., 2010. A socioeconomic and natural vulnerability index for oil spills in an Amazonian harbor: a case study using GIS and remote sensing. J. Environ. Manage. 91, 1972-1980.

ANZS, 2004. Risk management guidelines: companion to AS/NZS 4360:2004. Australia and New Zealand Standards, 116p. ISBN: 0733759602.

Ardhuin, F., Bertotti, L., Bidlot, J., Cavaleri, L., Filipetto, V., Lefevre, J., & Wittmann, P., 2007. Comparison of wind and wave measurements and models in the Western Mediterranean Sea. Ocean Engineering, 34(3-4), 526-541

ASCE task committee on modeling of oil spills of the water resources engineering division, 1996. State-of-the-art review of modeling transport and fate of oil spills. ASCE, J. Hydraul. Eng., 122 (11), 594-609.

Ascione Kenov, I., Campuzano, F., Franz, G., Fernandes, R., Viegas, C., Sobrinho, J., de Pablo, H., Amaral, A., Pinto, L., Mateus, M., Neves, R., 2014. Advances in Modeling of Water Quality in Estuaries, In: Remote Sensing and Modeling, C.W. Finkl & C. Makowski (Eds.). Springer International Publishing, 237-276.

Balseiro, C.F., Carracedo, P., Gómez, B., Leitão, P.C., Montero, P., Naranjo, L., Penabad, E., Pérez-Muñuzuri, V., 2003. Tracking the Prestige oil spill: An operational experience in simulation at MeteoGalicia. Weather, 58(12), 452-458

Barron, C.N., Smedstad, L.F., Dastugue, J.M., Smedstad, O.M., 2007. Evaluation of ocean models using observed and simulated drifter trajectories: Impact of sea surface height on synthetic profiles for data assimilation. J. Geophys. Res. Ocean. 112, 1–11. doi:10.1029/2006JC003982

Bebiano, M. J., (1995) Effects of pollutants in the Ria Formosa Lagoon, Portugal. Science of The Total Environment 171: 107-115. doi: 10.1016/0048-9697(95)04672-9

Beck, M.W., Ferdaña, Z., Kachmar, J., Morrison, K.K., Taylor, P., 2009. Best practices for marine spatial planning. Arlington, VA: The Nature Conservancy, 25p.

Blayo, E., Debreu, L., 2005. Revisiting open boundary conditions from the point of view of characteristic variables. Ocean Model. 9, 231–252.

Blumberg, A.F., Kantha, L.H., 1985. Open boundary condition for circulation models. Journal of Hydraulic Engineering, ASCE, 111, 237-2555.

Booij, N., Ris, R.C., Holthuijsen, L.H., 1999. A third-generation wave model for coastal regions, Part I: Model description and validation. Journal of Geophysical Research, 104 (C4), 7649-7666

Borja A., Elliot, M., Carstensen, J., Heiskanen, A-S., van de Bund, W., 2010. Marine management – towards an integrated implementation of the European Marine Strategy Framework and the Water Framework Directives. Mar. Pollut. Bull; 60: 2175–2186.

Botsford, L.W., Parma, A.M., 2005. Uncertainty in marine management, in: Norse, E.A., Crowder, L.B. (Eds.), Marine conservation biology: the science of maintaining the sea's diversity. Island Press, pp. 375-392.

Broström, G., Carrasco, A., Hole, L.R., Dick, S., Janssen, F., Mattsson, J., Berger, S., 2011. Usefulness of high resolution coastal models for operational oil spill forecast: the "Full City" accident. Ocean Sci. 7, 805–820. doi:10.5194/os-7-805-2011

Buchard, H., Bolding, K., Villarreal, M.R., 1999. GOTM, a General Ocean Turbulence Model. Theory, implmentation and test cases. Report EUR18745 EN, European Comission, 103 pp., 1999.

Caballero, A., Espino, M., Sagarminaga, Y., Ferrer, L., Uriarte, A., González, M., 2008. Simulating the migration of drifters deployed in the Bay of Biscay, during the Prestige crisis. Mar. Pollut. Bull. 56, 475–82. doi:10.1016/j.marpolbul.2007.11.005

Calado, H., Ng., K., Johnson, D., Sousa, L., Phillips, M., Alves, F., 2010. Marine spatial planning: lessons learned from the Portuguese debate. Mar. Policy; 34: 1341–1349

Calow, P. (Ed.), 1998. Handbook of environmental risk assessment and management, Blackwell Science, UK. 590p.

Campuzano, F.J., Kenov, I., Brito, D., Juliano, M., Fernandes, R., Pinto, L., Neves, R., 2014. Numerical evaluation of the river nutrients for the Western Iberian coastal region, in: 3 Jornadas Da Engenharia Hidrográfica. Instituto Hidrográfico, Lisbon, Portugal, pp. 263–266.

Canuto, V. M., A. Howard, Y. Cheng, and M. S. Dubovikov, 2001. Ocean turbulence. Part I: One- point closure model—momentum and heat vertical diffusivities, J. Phys. Oceanogr., 31, 1413–1426

Cardeira, S., Rita, F., Relvas, P., Cravo, A., 2013. Chlorophyll a and chemical signatures during an upwelling event off the South Portuguese coast (SW Iberia). Cont. Shelf Res. 52, 133–149. doi:10.1016/j.csr.2012.11.011

Carracedo, P., Torres-López, S., Barreiro, M., Montero, P., Balserio, C.F., Penabad, E., Leitão, P.C., Pérez-Muñuzuri, V., 2006. Improvement of pollutant drift forecast system applied to the Prestige oil spills in Galicia Coast (NW of Spain): Development of an operational system. Marine Pollution Bulletin 53, 350-360

Castanedo, S., Medina, R., Losada, I.J., Vidal, C., Méndez, F.J., Osorio, A., Juanes, J.A., Puente, A., 2006. The Prestige oil spill in Cantabria (Bay of Biscay) Part I: operational forecasting system for quick response, risk assessment and protection of natural resources. Journal of Coastal Research 22(6), 1474–1489

Castanedo, S., Juanes, J.A., Medina, R., Puente, A., Fernandez, F., Olabarrieta, M., Pombo, C., 2009. Oil spill vulnerability assessment integrating physical, biological and socio-economical aspects: application to the Cantabrian coast (Bay of Biscay, Spain). J. Environ. Manage. 91, 149-159.

Cavaleri, L., Sclavo, M., 2006. The calibration of wind and wave model data in the Mediterranean Sea. Coastal Engineering, 53(7), 613-627

Coelho, C., Silva, R., Veloso-Gomes, F., Taveira-Pinto, F., 2009. Potential effects of climate change on northwest Portuguese coastal zones. ICES J. Mar. Sci.; 66: 1497–1507

Collard F., Mouche A., Chapron B., Danilo C. and Johannessen J.A., Routine High Resolution Observation of Selected Major Surface Currents from Space, Proc. of SeaSAR, (2008)

Costanza, R., Andrade, F., Antunes, P., Van den Belt, M., Boersma, D., Boesch, D.F., Catarino, F., Hanna, S., Limburg, K., Low, B., Molitor, M., Pereira, J.G., Rayner, S., Santos, R., Wilson, J., Young, M., 1998. Principles for sustainable governance of the oceans. Science 281, 198-199.

Costanza, R., D'Arge, R., de Groot, R., Farber, S., Grasso, M., Hannon, B., Limburg, K., Naeem, S., O'Neill, R. V, Paruelo, J., Raskin, R.G., Sutton, P., van den Belt, M., 1997. The value of the world's ecosystem services and natural capital. Nature 387, 253–260.

Cox Jr., L.A., Ricci, P.F., 2005. Causation in risk assessment and management: models, inference, biases, and a microbial risk–benefit case study. Environ. Int. 31(3), 377-397.

Craig, P. D., and M. L. Banner, 1994. Modeling wave-enhanced turbulence in the ocean surface layer, J. Phys. Oceanogr., 24, 2546–2559

Cravo, A., Relvas, P., Cardeira, S., Rita, F., Madureira, M., Sánchez, R., 2010. An upwelling filament off southwest Iberia: Effect on the chlorophyll a and nutrient export. Cont. Shelf Res. 30, 1601–1613. doi:10.1016/j.csr.2010.06.007

Crowder, L., Norse, E., 2008. Essential ecological insights for marine ecosystem-based management and marine spatial planning. Mar. Policy 32, 772-778.

Daniel P., 1996. Operational forecasting of oil spill drift at METEO-FRANCE. Spill Science & Technology Bulletin 3: 53-64. doi:10.1016/S1353-2561(96)00030-8

Daniel, P., Dandin, P., 2005. Benefits and use of operational oceanography systems for drift forecasts, in: International Oil Spill Conference. Miami, pp. 1–4.

Daniel, P., F. Marty, P. Josse, C. Skandrani and R. Benshila, 2003. "Improvement of Drift Calculation in MOTHY Operational Oil Spill Prediction System", in Proceedings of the 2003 International Oil Spill Conference , American Petroleum Institute, Washington, D.C.

Davidson-Arnott, R., G., D., 2005. Conceptual model of the effects of sea level rise on sandy coasts. Journal of Coastal Research, 21: 1166-1172+1193.

Deutsch, C., Brix, H., Ito, T., Frenzel, H., Thompson, L., 2011. Climate-forced variability of ocean hypoxia. Science, 333 (6040): 336-339.

Dobricic, S., Pinardi, N., Adani, M., Bonazzi, A., Fratianni, C., Tonani, M., 2005. Mediterranean Forecasting System: An improved assimilation scheme for sea-level anomaly and its validation. Quarterly Journal of the Royal Meteorological Society 131: 3627-3642

Dobricic, S., Pinardi, N., Adani, M., Tonani, M., Fratianni, C., Bonazzi, A., Fernandez, V., 2006. Daily oceanographic analyses by the Mediterranean basin scale assimilation system. Ocean Science 3: 1977-1998

Douvere, F., 2008. The importance of marine spatial planning in advancing ecosystem-based sea use management. Mar. Policy 32, 762-771.

Douvere, F., Ehler, C., N., 2009. New perspectives on sea use management: initial findings from European experience with marine spatial planning. Journal of Environmental Management, 90: 77-88.

Dias, J.A., 1988. Aspectos geológicos do Litoral Algarvio. Geonovas 10, 113–128.

Ehler, C., Douvere, F., 2009. Marine spatial planning: a step-by-step approach toward ecosystem-based management. Paris: UNESCO, Intergovernmental Oceanographic Commission and Man and the Biosphere Programme, IOC Manual and Guides 53, ICAM Dossier 6, 99p.

Espinosa-Romero, M., J., Chan, K., M., A., McDaniels, T., Dalmer, D., M., 2011. Structuring decision-making for ecosystem-based management. Marine Policy, 35: 575-583.

Etkin, D. S, 2004. Modelling Oil Spill Response and Damage Costs. Proc. 5th Biennial Freshwater Spills Symposium

European Commission, 2000. Communication on the precautionary principle. Brussels: COM (2000) 1 final, 28p.

European Commission, 2001. Communication on the sixth environment action programme and proposal for a Decision on laying down the community environment action programme 2001-2010. Brussels: COM (2001) 31 final, 81p.

European Commission, 2004. Proposal for a Regulation on the European regional development fund. Brussels: COM (2004) 495 final, 19p.

European Commission, 2008. Roadmap for maritime spatial planning: achieving common principles in the EU. Brussels: COM (2008) 791 final, 11p.

European Commission, 2009. A Community approach on the prevention of natural and man-made disasters. Brussels: COM (2009) 82 final, 9p.

European Commission, 2010. Maritime spatial planning in the EU – achievements and future development. Brussels: COM (2010) 771 final, 10p.

European Commission, 2011. Implementation plan of the EU strategy for supporting disaster risk reduction in developing countries 2011-2014. Brussels: SEC (2011) 215 final, 14p.

European Commission. Commission Decision 2010/477/EU of 1 September 2010 on criteria and methodological standards on good environmental status of marine waters. Brussels: Official Journal of the European Union, L232: 14-24.

European Commission DG Environment. Scoping study on the requirements for economic assessment in the Marine Strategy Framework Directive - Final report. Denmark: COWI; 2010. 78pp.

European Commission. Europe 2020. In http://ec.europa.eu/europe2020/index_en.htm, accessed in 01/11/2011.

European Commission. Facing the Challenge - The Lisbon strategy for growth and development. Luxembourg: Office for Official Publications of the European Communities, Report from the High Level Group chaired by Wim Kok; 2004. 51pp.

European Commission. International Conventions. In http://ec.europa.eu/environment/water/marine/conventions_en.htm, accessed in 17/11/2011.

European Union. Directive 2000/60/EC of the European Parliament and of the Council of 23 October 2000, establishing a framework for community action in the field of Water Policy (Water Framework Directive). Official Journal of the European Communities, L327: 1-72.

European Union. Directive 2005/35/EC of the European Parliament and of the Council of 7 September 2005, on ship-source pollution and on the introduction of penalties for infringements. Official J. Eur. Union, L255: 11–21

European Union. Directive 2008/56/EC of the European Parliament and of the Council of 17 June 2008, establishing a framework for community action in the field of marine environmental policy (Marine Strategy Framework Directive). Official Journal of the European Union, L164: 19-40.

European Union. EU institutions and bodies. In http://europa.eu/about-eu/institutions-bodies/index_en.htm, accessed in 08/09/2011.

Evans, J., Wood, G., Miller, A., 2006. The risk assessment–policy gap: an example from the UK contaminated land regime. Environ. Int. 32(8), 1066-1071.

Fernandes, R., Neves, R., Viegas, C., Leitão, P., 2013. Integration of an Oil and Inert Spill Model in a Framework for Risk Management of Spills at Sea–A Case Study for the Atlantic Area, in: 37th AMOP Technical Seminar on Environmental Contamination and Response. p. 28.

Ferraro G., Bernardini A., Meyer-Roux S. and Tarchi D., 2006. Satellite monitoring of illicit discharges from vessels in the French environmental protection zone (ZPE) 1999–2004, European Commission, EUR 22158 EN.

Ferraro, G., Meyer-Roux, S., Muellenhoff, O., Pavliha, M., Svetak, J., Tarchi, D., Topouzelis,K., 2009. Long term monitoring of oil spills in European seas. International Journal of Remote Sensing, 30:3, 627-645

Ferreira, O., Dias, J., Taborda, R., 2008. Implications of sea-level rise for continental Portugal. Journal of Coastal Research, 24 (2): 317-324.

Field, B.C., Field, M.K., 2009. Environmental economics: an introduction, fifth ed. McGraw-Hill, New York. 493p.

Foley, M.M., Halpern, B.S., Micheli, F., Armsby, M.H., Caldwell, M.R., Crain, C.M., Prahler, E., Rohr, N., Sivas, D., Beck, M.W., Carr, M.H., Crowder, L.B., Duffy, J.E., Hacker, S.D., McLeod, K.L., Palumbi, S.R., Peterson, C.H., Regan, H.M., Ruckelshausm, M.H., Sandifer, P.A., Steneck, R.S., 2010. Guiding ecological principles for marine spatial planning. Mar. Policy, 34: 955–966.

Frazão Santos, C., Carvalho, R., Andrade, F., 2013. Quantitative assessment of the differential coastal vulnerability associated to oil spills. J. Coast. Conserv. 17: 25-36.

García-Lafuente, J., Delgado, J., Criado-Aldeanueva, F., Bruno, M., del Río, J., Miguel Vargas, J., 2006. Water mass circulation on the continental shelf of the Gulf of Cádiz. Deep Sea Res. Part II Top. Stud. Oceanogr. 53, 1182–1197. doi:10.1016/j.dsr2.2006.04.011

Gouveia, J.A. V., Soares, C., Guedes Soares, C., 2010. Oil spill incidents in Portuguese waters, in: Advanced Ship Design for Pollution Prevention. CRC Press, London, UK, pp. 217–223. doi:doi:10.1201/b10565-27

Greiving, S., Fleischhauer, M., 2006. Spatial planning response towards natural and technological hazards. Natural and technological hazards and risks affecting the spatial development of European regions, Geological Survey of Finland, Special Paper 42, 109-123.

Guillen, G., Rainey, G., Morin, M., 2004. A simple rapid approach using coupled multivariate statistical methods, GIS and trajectory models to delineate of common oil spill risk. J. Marine Syst. 45, 221-235.

Gundlach, E.R., Hayes, M.O., 1978. Vulnerability of coastal environments to oil spill impacts. Mar. Technol. Soc. J. 12(4), 18-27.

Guo, W.J., Wang, Y.X., 2009. A numerical oil spill model based on a hybrid method. Mar. Pollut. Bull. 58, 726-734.

Hacket, B., Comerma, E., Daniel, P. and Ichikawa, H., 2008. Marine pollution monitoring and prediction. GODAE Final Symposium, Nice (France)

Häder, D-P., Kumar, H., D., Smith, R., C., Worrest, R., C., 2007. Effects of solar UV radiation on aquatic ecosystems and interactions with climate change. Photochemical & Photobiological Sciences, 6: 267-285.

Hansen, S. E., Stel, J. H., 1997. SEAWATCH. Performance and future. In "Operational Oceanography. The challenges for European Cooperation", Proceedings of the 1st International. Conference on EuroGOOS

Hayes, M.O., Michel, J., Montello, T.M., 1997. The Reach Sensitivity Index (RSI) for mapping rivers and streams. Proc. 1997 Intl. Oil Spill Conference, API Publ. No. 4651, American Petroleum Institute, Washington, D.C., 343-350.

Hicks, N., Bulling, M., T., Solan, M., Raffaelli, D., White, P., C., L., Paterson, D., M., 2011. Impact of biodiversity-climate futures on primary production and metabolism in a model benthic estuarine system. BMC Ecology, 11: 7.

Holthuijsen, L.H., Booij, N., Padilla-Hernandez, R., 1997. A curvi-linear, third-generation coastal wave model. Conference of Coastal Dynamics, Plymouth (United Kingdom): 128–136

Inan, A., 2011. Modeling of oil pollution in Derince harbor. J. Coast. Res. SI64, 894-898.

INE - Instituto Nacional de Estatística (2008) Statistical Yearbook of the Algarve Region, INE, Lisbon.

International Oil Pollution Compensation Funds (2009) Prestige report. http://www.iopcfund.org/prestige.htm. Accessed 29 January 2010

Institute for Nature Conservation and Biodiversity. List of Protected Areas of the National Network of Protected Areas. In http://portal.icnb.pt/NR/rdonlyres/395B1D6E-3D46-4D87-8E2B-7241C80A3AD9/0/AP_UOIA_RNAP_14JUL2011.pdf, accessed in 08/09/2011.

IOC, IHO and BODC, 2003, "Centenary Edition of the GEBCO Digital Atlas", published on CD-ROM on behalf of the Intergovernmental Oceanographic Commission and the International Hydrographic Organization as part of the General Bathymetric Chart of the Oceans; British Oceanographic Data Centre, Liverpool.

IPIECA, 2008. Oil spill preparedness and response – report series summary. London: International Petroleum Industry Environmental Conservation Association, IPIECA Report Series 1990-2008, 42p.

IPMA, 2009. Caracterização Climática 2009. Relatórios Anuais, Clima em Portugal.

ISO, 2009. Risk management – Vocabulary. ISO GUIDE 73:2009(E/F). Switzerland: International Organization for Standardization, 15p.

ITOPF, 2011a. Effects of oil pollution on the marine environment. UK: The International Tanker Owners Pollution Federation, ITOPF Technical Information Paper 13, 11p.

ITOPF, 2011b. Fate of marine oil spills. UK: The International Tanker Owners Pollution Federation, ITOPF Technical Information Paper 2, 11p.

ITOPF, 2011c. Contingency planning for marine oil spills. UK: The International Tanker Owners Pollution Federation, ITOPF Technical Information Paper 16, 11p.

ITOPF, 2011d. Effects of oil pollution on social and economic activities. UK: The International Tanker Owners Pollution Federation, ITOPF Technical Information Paper 12, 7p.

Janeiro, J., Fernandes, E., Martins, F., Fernandes, R., 2008. Wind and freshwater influence over hydrocarbon dispersal on Patos Lagoon, Brazil. Mar. Pollut. Bull. 56, 650–65. doi:10.1016/j.marpolbul.2008.01.011

Janeiro, J., Martins, F., Relvas, P., 2012. Towards the development of an operational tool for oil spills management in the Algarve coast. J. Coast. Conserv. 16, 449–460. doi:10.1007/s11852-012-0201-8

Janeiro, J., Zacharioudaki, A., Sarhadi, E., Neves, A., Martins, F., 2014. Enhancing the management response to oil spills in the Tuscany Archipelago through operational modelling. Mar. Pollut. Bull. 85, 574–89. doi:10.1016/j.marpolbul.2014.03.021

Janjic, Z. I., Gerrity Jr., J. P., Nickovic, S., 2001. An Alternative Approach to Nonhydrostatic Modeling. Monthly Weather Review, 129, 1164-1178.

Jensen, J.R., Halls, J.N., Michel, J., 1998. A systems approach to Environmental Sensitivity Index (ESI) mapping for oil spill contingency planning and response. Photogramm. Eng. Rem. S. 64(10), 1003-1014.

Jensen, J.R., Ramsey, E.W., Holmes, J.M., Michel, J., Savitsky, B., Davis, B.A., 1990. Environmental sensitivity index (ESI) mapping for oil spills using remote sensing and geographic information system technology. Int. J. Geogr. Inf. Syst. 4(2), 181-201.

Johannessen J.A., Collard F., Chapron B., Kudryavtsev V., Mouche A., Akimov D., and Dagestad K.F., 2008. Combined Backscatter and Doppler Shifts from SAR Images: Observations and Simulations, Proc. of SeaSAR.

Kallos, G., 1997. The Regional weather forecasting system SKIRON. Proceedings, Symposium on Regional Weather Prediction on Parallel Computer Environments, Athens, Greece, 9 pp

Kallos, G. and the SKIRON group, 1998. The SKIRON forecasting system: VOL. I: Preprocessing, ISBN 960–8468–15–9; VOL. II: Model description, ISBN 960– 8468–16–7; VOL. III: Numerical techniques, ISBN 960–8468–17–5; VOL. IV: Parallelization, ISBN 960–8468–18–3; VOL. V: Postprocessing, ISBN 960–8468–19–1; VOL. VI: Procedures, ISBN 960–8468–20–5

Keller, B., D., Gleason, D., F., McLeod, E., Woodley, C., M., Airame, S., Causey, B., D., Friedlander, A., M., Grobber-Dunsmore, R., Johnson, J. E., Miller, S., L., Steneck, R., S,. 2009. Climate change, coral reef ecosystems, and management options for marine protected areas. Environmental Management, 44 (6): 1069-1088.

Kriebel, D., Tickner, J., Epstein, P., Lemons, J., Levins, R., Loechler, E.L., Quinn, M., Rudel, R., Schettler, T., Stoto, M., 2001. The precautionary principle in environmental science. Environ. Health Persp. 109(9), 871-876.

Kumpulainen, S., 2006. Vulnerability concepts in hazard and risk assessment. Natural and technological hazards and risks affecting the spatial development of European regions, Geological Survey of Finland, Special Paper 42, 65-74.

Lardner, R. W., Zodiatis, G., Loizides, L., Demetropoulos, A., (1998) An operational oil spill model in the Levantine Basin (Eastern Mediterranean Sea). International symposium on Marine Pollution, Monaco (France)

Leitão, P., Coelho, H., Santos, A., Neves, R., 2005. Modelling the main features of the Algarve coastal circulation during July 2004: A downscaling approach. J. Atmos. Ocean Sci. 10, 421–462. doi:10.1080/17417530601127704

Linkov, I., Satterstrom, F. K., Kiker, G., Batchelor, C., Bridges, T., Ferguson, E., 2006. From comparative risk assessment to multi-criteria decision analysis and adaptive management: Recent developments and applications. Environ. Int. 32(8), 1072-1093.

Liu, Y., Weisberg, R.H., 2011. Evaluation of trajectory modeling in different dynamic regions using normalized cumulative Lagrangian separation. J. Geophys. Res. 116, 1–13. doi:10.1029/2010JC006837

Long, R., 2011. The Marine Strategy Framework Directive: A new European approach to the regulation of the marine environment, marine natural resources and marine ecological services. Journal of Energy and Natural Resources Law, 29 (1): 1-44.

Longuet-Higgins, M.S., 1953. "Mass Transport in Water Waves", Philosophical Transactions of the Royal Society of London, Series A 245 (903), pp. 535–581

Longuet-Higgins, M. S., Stewart, R. W., 1960. Changes in the form of short gravity waves on long waves and tidal currents. Journal of Fluid Mechanics, 8, 565–583

Lopes, J.F., Ferreira, J. a., Cardoso, A.C., Rocha, A.C., 2014. Variability of temperature and chlorophyll of the Iberian Peninsula near costal ecosystem during an upwelling event for the present climate and a future climate scenario. J. Mar. Syst. 129, 271–288. doi:10.1016/j.jmarsys.2013.07.002

Lyard, E., Lefevre, F., Letellier, T., 2006. Modelling the global ocean tides, modern insights from FES2004. Ocean Dynamics 56, 394 – 415

Mackay, D., McAuliffe, C.D., 1988. Fate of hydrocarbons discharge at sea. Oil Chem. Pollut. 5, 1-20.

Maes, F, 2008. The international legal framework for marine spatial planning. Marine Policy, 32: 797-810.

Magne, R., Ardhuin, F., 2009. Wave hindcasting in the Mediterranean Sea. 11th International Workshop on Wave Hindcasting and Forecasting, Halifax, Canada

Martins, F., Leitão, P., Silva, A., Neves. R., 2001. 3D modelling in the sado estuary using a new generic vertical discretization approach. Oceanologica Acta 24, S51-S62

Martinsen, E. A., Engedahl, H., 1987. Implementation and testing of a lateral boundary scheme as an open boundary condition in a barotropic ocean model. Coastal Engineering 11, 603-627

Masterson, J., P., Garabedian, S., P., 2007. Effects of sea-level rise on ground water flow in a coastal aquifer system. Ground Water; 45(2): 209-217.

Mateus, M., Riflet, G., Chambel, P., Fernandes, L., Fernandes, R., Juliano, M., Campuzano, F., de Pablo, H., Neves, R., 2012. An operational model for the West Iberian coast: products and services. Ocean Sci. 8, 713–732. doi:10.5194/os-8-713-2012

Maya N.J., Jason L. and Yang G., 2008. Advances in Remote Sensing for Oil Spill Disaster Management: State of the Art Sensors Technology for oil Spill Surveillance, sensors, Vol.8, pp 236-265

Meiner A., 2010. Integrated maritime policy for the European Union – consolidating coastal and marine information to support maritime spatial planning. Journal of Coastal Conservation, 14: 1-11.

Mendoza-Cantú, A., Heydrich, S.C., Cervantes, I.S., Orozco, O.O., 2011. Identification of environmentally vulnerable areas with priority for prevention and management of pipeline crude oil spills. J. Environ. Manage. 92(7), 1706-1713.

Milligan, S., R., Holt, W., V., Lloyd, R., 2011. Impacts of climate change and environmental factors on reproduction and development in wildlife. Philosophical Transactions of the Royal Society B, 364 (1534): 3313-3319.

Miranda R., P.C. Leitão, H.S. Coelho, H. Martins and R. Neves, 1999. "Transport and Mixing Simulation along the Continental Shelf Edge Using a Lagrangian Approach", Bol. Inst. Esp. Oceanogr, 15(1-4): pp. 39-60

NASA (2012). National Aeronautics and Space Administration, http://oceancolor.gsfc.nasa.gov/. Accessed 25/06/2012

Neves R., Leitão P., Braunschweig F., Martins F., Coelho H., Santos A., and Miranda R., 2000. The advantage of a generic coordinate approach for ocean modeling, In: Water Studies, Ed. W.R. Blain & C.A. Brebbia, WITpress, Vol. 7, pp 25-34

Nittis, K., Zervakis, V., Perivoliotis, L., Papadopoulos, A., Chronis, G., 2001. Operational monitoring and forecasting in the Aegean Sea: system limitations and forecasting skill evaluation. Marine Pollution Bulletin 43:154–163. doi:10.1016/S0025-326X(01)00055-8

NOAA (2000). ADIOSTM (Automated Data Inquiry for Oil Spills) version 2.0. Seattle: Hazardous Materials Response and Assessment Division, NOAA. Prepared for the U.S. Coast Guard Research and Development Center, Groton Connecticut

Norse, E.A., Crowder, L.B., Gjerde, K., Hyrenbach, D., Roberts, C.M., Safina, C., Soulé, M.E., 2005. Place-based ecosystem management in the open ocean, in: Norse, E.A., Crowder, L.B. (Eds.), Marine conservation biology: the science of maintaining the sea's diversity. Island Press, pp. 302-327.

O'Donncha, F., Hartnett, M., Nash, S., Ren, L., Ragnoli, E., 2015. Characterizing observed circulation patterns within a bay using HF radar and numerical model simulations. J. Mar. Syst. 142, 96–110. doi:10.1016/j.jmarsys.2014.10.004

OECD, 2003. Pollution abatement and control expenditure in OECD countries: a report for theWorking Group on Environmental Information and Outlooks. OECD Environment Directorate Working Paper ENV/EPOC/SE(2003)

Olfert, A., Greiving, S., Batista, M.J., 2006. Regional multi-risk review, hazard weighting and spatial planning response to risk – results from European case studies. Natural and technological hazards and risks affecting the spatial development of European regions, Geological Survey of Finland, Special Paper 42, 125-151.

Oliveira, P.B., Peliz, Á., Dubert, J., Rosa, T.L., Santos, A.M.P., 2004. Winter geostrophic currents and eddies in the western Iberia coastal transition zone. Deep Sea Res. Part I Oceanogr. Res. Pap. 51, 367–381. doi:10.1016/j.dsr.2003.10.016

Orbach, M., 1996. Social science contributions to managing ecosystems. In Cicin-Sain B (editor). Improving interactions between coastal science and policy: proceedings of the Gulf of Mexico Symposium. Washington DC: National Academy Press, 37-49.

OSPAR Commission, 2010. OSPAR regional implementation framework for the EU Marine Strategy Framework Directive - MSFD Road Map. London: OSPAR Commission; Publication No. 501/2010; 19pp.

Papadopoulos, A., Katsafados, P., Kallos, G., 2001. Regional weather forecasting for marine application. Global Atmosphere Ocean Systems, 8, 219-237

Pavia, R., Michel, J., Petersen, J., Birk-Risheim, S., 1995. An integrated program for sensitive environment mapping. Proc. 1995 Intl. Oil Spill Conference, API Publ. No. 4620, American Petroleum Institute, Washington, D.C., 73-76.

Pawlowicz, R., Beardsley, B., Lentz, S., 2002. Classical tidal harmonic analysis with errors in matlab using t-tide. Computers & Geosciences, 28, 929–937

Peliz, Á., Dubert, J., Santos, a. M.P., Oliveira, P.B., Le Cann, B., 2005. Winter upper ocean circulation in the Western Iberian Basin—Fronts, Eddies and Poleward Flows: an overview. Deep Sea Res. Part I Oceanogr. Res. Pap. 52, 621–646. doi:10.1016/j.dsr.2004.11.005

Petersen, J., Michel, J., Zengel, S., White, M., Lord, C., Plank, C., 2002. Environmental sensitivity index guidelines version 3.0. Seattle: U.S. National Oceanic and Atmospheric Administration, Technical Memorandum NOS OR&R 11, 89p.

Pinardi, N., Allen, I., Demirov, E., De Mey, P., Korres, G., Lascaratos, A., Le Traon, P.-Y., Maillard, C., Manzella, G., Tziavos, C., 2003. The Mediterranean ocean forecasting system: first phase of implementation (1998–2001). Ann. Geophys. 21, 3–20. doi:10.5194/angeo-21-3-2003

Pine, J.C., 2009. Natural hazards analysis: Reducing the impact of disasters, CRC Press, Taylor & Francis Group, 285p.

Pires, A., Nolasco, R., Rocha, A., Dubert, J., 2013. Assessing future climate change in the Iberian Upwelling System. J. Coast. Res. 1909–1914. doi:10.2112/SI65-323.1

Portugal 2020 - National Reform Program; 2011. 70pp. In http://www.eurocid.pt/pls/wsd/wsdwcot0.detalhe_area?p_cot_id=6578, accessed in 01/11/2011 [in Portuguese].

Portuguese Government, 2012. The POEM Spatialization Document. POEM: Volume 2 - Plano de Ordenamento do Espaço Marítimo, Tomo 1 - Espacialização. Portugal: Ministério da Agricultura, do Mar, do Ambiente e do Ordenamento do Território, 25p [in Portuguese].

Portuguese Water Institute. In http://www.inag.pt, accessed in 06/08/2011 [in Portuguese].

Power, M., McCarthy, L., 1998. A comparative analysis of environmental risk assessment/risk management framework. Environ. Sci. Technol. 32, 224A-231A.

Price, J.D., Bush, M.R., 2004. Comparisons between Model Forecast and Observed Boundary Layer Profiles and Related Comments on Cloud Prediction. Weather Forecast. 19, 959–969. doi:10.1175/822.1

Price, J. D., Bush, M. R., 2006. Comparisons between Model Forecast and Observed Boundary Layer Profiles and Related Comments on Cloud Prediction. Weather and Forecasting, 19(6), 959-969

Price, J., Ji, Z., Reed, M., Marshall, C.F., Howard, M., Guinasso Jr, N., Johnson, W.R., Rainey, G.B., 2003. Evaluation of an oil spill trajectory model using satellite-tracked, oil-spill-simulating drifters, OCEANS 2003. San Diego, California.

Price, J., Reed, M., Howard, M., Johnson, W., Ji, Z., Marshall, C., Guinassojr, N., Rainey, G., 2006. Preliminary assessment of an oil-spill trajectory model using satellite-tracked, oil-spill-simulating drifters. Environ. Model. Softw. 21, 258–270. doi:10.1016/j.envsoft.2004.04.025

PriceWaterhouseCooper, 2006. Main Report Socio-Economic Benefits Analysis of GMES. ESA contract number 18868/05, October 2006

Purcell, K., M., Klerks, P., L., Leberg, P., L., 2010. Adaptation to sea level rise: does local adaptation influence the demography of coastal fish populations? Journal of Fish Biology, 77 (6): 1209-1218.

Ratsimandresy, A., Sotillo, M., Carreteroalbiach, J., Alvarezfanjul, E., Hajji, H., 2008. A 44-year high-resolution ocean and atmospheric hindcast for the Mediterranean Basin developed within the HIPOCAS Project. Coastal Engineering, 55(11), 827-842

Reed, M., Turner, C., Odulo, A., 1994. The role of wind and emulsification in modelling oil spill and surface drifter trajectories. Spill Science & Technology Bulletin, 1(2), 143–157

Reed, M., Turner, C., Spaulding, M., Jayko, K., Dorson, D., Johansen, O., 1988. Evaluation of satellite-tracked surface drifiting buoys for simulating the movement of spilled oil in the marine environment. Reston, Virginia.

Relvas, P., Barton, E.D., 2002. Mesoscale patterns in the Cape São Vicente (Iberian Peninsula) upwelling region. J. Geophys. Res. 107, 3164. doi:10.1029/2000JC000456

Relvas, P., Barton, E.D., 2005. A separated jet and coastal counterflow during upwelling relaxation off Cape São Vicente (Iberian Peninsula). Cont. Shelf Res. 25, 29–49. doi:10.1016/j.csr.2004.09.006

Relvas, P., Barton, E.D.D., Dubert, J., Oliveira, P.B., Peliz, A., Dasilva, J., Santos, a. M.P., Peliz, Á., da Silva, J.C.B.C.B., Silva, J.C.B., 2007. Physical oceanography of the western Iberia ecosystem : Latest views and challenges. Prog. Oceanogr. 74, 149–173. doi:10.1016/j.pocean.2007.04.021

REMPEC, 2002: Protecting the Mediterranean against Maritime Accidents and Illegal Discharges from Ships, Malta 2002

Ricci, P.F., Rice, D., Ziagos, J., Cox Jr, L.A., 2003. Precaution, uncertainty and causation in environmental decisions. Environ. Int. 29(1), 1-20.

Riflet, G., Juliano, M., Fernandes, L., Leitão, P. C., Neves, R., 2008. Operational Ocean forecasting of the Portuguese waters. Mercator Ocean Quarterly Newsletter 30: 20-32

Robichaud, A., Bégin, Y., 1997. The effects of storms and sea-level rise on a coastal forest margin in New Brunswick, Eastern Canada. Journal of Coastal Research, 13: 429-439.

Rocha, F., 2009. Aspects of the implementation of the Water Framework Directive in Portugal for transitional and coastal waters. Presentation from the workshop "Marine Strategy Framework Directive: A new challenge for the sustainable management of oceans and seas". Portugal: Task Group for Maritime Affairs [in Portuguese].

Rulling No. 32277. Despacho no. 32277/2008, de 18 de Dezembro, Diário da República, 2.ª série, 244: 50546-50547 [in Portuguese].

Salem F., and Kafatos P.M., 2001. Hyperspectral image analysis for oil spill mitigation, Proc. ACRS — 22nd Asian Conference on Remote Sensing, Singapore, Vol. 1, 748– 753.

Santoro, F. M., Stel, J. H., 2005. Can Operational Oceanography support decision-making in the coastal zones? Proceedings of the Fourth International Conference of EuroGOOS, 6-9 June, France, 37 - 42

Santos, C.F., Andrade, F., 2009. Environmental sensitivity of the Portuguese coast in the scope of oil spill events – comparing different assessment approaches. J. Coast. Res. SI56, 885-889.

Santos, C.F., Carvalho, R., Andrade, F., 2010a. Quantitative assessment of the differential risk associated to oil spills for the Portuguese coast. Portugal: International Conference on Coastal Conservation and Management'10, 11-17 April, Book of abstracts, 117p.

Santos, C.F., Carvalho, R., Andrade, F., 2010b. Marine spatial planning and environmental sensitivity index maps – benefits and complementary aspects of an integrated use. Portugal: International Conference on Coastal Conservation and Management'10, 11-17 April, Book of abstracts, 127.Schiller, H., van Bernem, C., Krasemann, H.L., 2005. Automated classification of an environmental sensitivity index. Environ. Monit. Assess. 110, 291-299.

Santos, F., D., Forbes, K., Moita, R., 2001. Climate change in Portugal - Scenarios, impacts and adaptation measures - Project SIAM. Executive Summary and Conclusions. Lisboa: Gradiva.

Santos, C.F., Michel, J., Neves, M., Janeiro, J., Andrade, F., Orbach, M., 2013. Marine spatial planning and oil spill risk analysis : Finding common grounds. Mar. Pollut. Bull. 74, 73–81.

Santos, F. D., Miranda, P., editors, 2006. Climate change in Portugal – Scenarios, Impacts and Adaptation Measures – Project SIAM II. Lisbon: Gradiva; 505p [in Portuguese].

Santos, F., Gómez-Gesteira, M., DeCastro, M., Álvarez, I., Res, C., 2011. Upwelling along the western coast of the Iberian Peninsula: dependence of trends on fitting strategy. Clim. Res. 48, 213–218. doi:10.3354/cr00972

Schiller, H., van Bernem, C., Krasemann, H.L., 2005. Automated classification of an environmental sensitivity index. Environ. Monit. Assess. 110, 291-299.

Schmidt-Thomé, P. (ed), 2005. The spatial effects and management of natural and technological hazards in Europe – final report of the European spatial planning and observation network (ESPON) project 1.3.1. Geological Survey of Finland, 197p.

Silva, M. C., 2008. Marine Strategy Framework Directive: presentation and back- ground. Public presentation session of the Marine Strategy Framework Directive. Portugal: Portuguese Environment Agency [in Portuguese].

Silveira, P. a. M., Teixeira, A.P., Soares, C.G., 2013. Use of AIS Data to Characterise Marine Traffic Patterns and Ship Collision Risk off the Coast of Portugal. J. Navig. 66, 879–898. doi:10.1017/S0373463313000519

Skognes, K., Johansen, O., 2004. Statmap – a 3-dimensional model for oil spill risk assessment. Environ. Modell. Softw. 19, 727-737.

Small, C., Nicholls, R.J., 2003. A global analysis of human settlement in coastal zones. Journal of Coastal Research, 19, (3), 584-599.

Soares C. V., 2008. The challenges of a scientifically consistent approach to the implementation of the Marine Strategy Framework Directive. Public presentation session of the Marine Strategy Framework Directive. Portugal: Portuguese Environment Agency [in Portuguese].

Sobanski T., Szczurek A., Nitsch K., Licznerski B.W. and Radwan W., 2006. Electronic nose applied to automotive fuel qualification. Sensors and Actuators, B, Vol. 116, 207–212

Sobey, R. J., Barker., C. H., 1997. Wave-Driven Transport of Surface Oil. Journal of Coastal Research, 13(2), 490–496

Sotillo, M., Aznar, R. & Valero, F., 2008. The 44-year Mediterranean HIPOCAS wind database: A useful tool to analyse offshore extreme wind events from a long-term regionalperspective. Coastal Engineering, 55(11), 930-943

Sotillo, M.G., Fanjul, E.A., Castanedo, S., Abascal, A.J., Menendez, J., Emelianov, M., Olivella, R., García-Ladona, E., Ruiz-Villarreal, M., Conde, J., Gómez, M., Conde, P., Gutierrez, A.D., Medina, R., 2008. Towards an operational system for oil-spill forecast over Spanish waters: initial developments and implementation test. Mar. Pollut. Bull. 56, 686–703. doi:10.1016/j.marpolbul.2007.12.021

Soukissina, T., Chronis, G., 2000. Poseidon: A marine environmental monitoring, forecasting and information systems for the Greek seas. Mediterranean Marine Science 1: 71-78

St Martin, K., Hall-Arber, M., 2008. The missing layer: Geo-technologies, communities, and implications for marine spatial planning. Mar. Policy 32(5), 779-786.

Stram, D.L., Evans, D.C.K., 2009. Fishery management responses to climate change in the North Pacific. ICES J. Mar. Sci.; 66: 1633–1639.

Stokes, G. G., 1847. On the theory of oscillatory waves. Transactions of the Cambridge Philosophical Society 8, 441–455

SWAN Team, 2009a. SWAN scientific and technical documentation v. 40.72ABCDE. Available from: http://www.swan.tudelft.nl

Task group for the extension of the continental shelf, 2009. Continental shelf submission of Portugal – Executive summary – PT-ES/05-05-2009. Portugal: Ministério da Defesa Nacional, Estrutura de Missão para a Extensão da Plataforma Continental, 88 p

Task group for maritime affairs. Portuguese marine protected areas legislation. In <http://www.emam.com.pt/index.php?option=com_content&task=view&id=319&Itemid=222>, accessed in 17/11/2011 [in Portuguese].

Teles-Machado, A., Peliz, Á., Dubert, J., Sánchez, R.F., 2007. On the onset of the Gulf of Cadiz Coastal Countercurrent. Geophys. Res. Lett. 34, 1–5. doi:10.1029/2007GL030091

Thompson, K. R., Sheng, J., Smith, P. C., Cong, L., 2003. Prediction of surface currents and drifter trajectories on the inner Scotian Shelf, J. Geo- phys. Res., 108(C9), 3287

Toffoli, A., Lefèvre, J.M., Bitner-Gregersen, E., Monbaliu, J., 2005. Towards the identification of warning criteria: Analysis of a ship accident database. Appl. Ocean Res. 27, 281–291. doi:10.1016/j.apor.2006.03.003

Tonani, M., Pinardi, N., Dobricic, S., Pujol, I., Fratianni, C., 2008. A high-resolution free surface model of the Mediterranean Sea. Ocean Science, 4, 1–14

Topuz, E., Talinli, I., Aydin, E., 2011. Integration of environmental and human health risk assessment for industries using hazardous materials: A quantitative multi criteria approach for environmental decision makers. Environ. Int., 37(2), 393-403.

Torres, R., Barton, E.D., Miller, P., Fanjul, E., 2003. Spatial patterns of wind and sea surface temperature in the Galician upwelling region. J. Geophys. Res. 108, 1–14. doi:10.1029/2002JC001361

Trieschmann, O., 2008. Oil spill issue and the capacity of monitoring the problem by remote sensing. The World Ocean in Globalization: Challenges for Marine Regions, Int. Conf. on Marine Affairs and the Law of the Sea. Oslo, 2008. 169-176

Umlauf and H. Burchard, 2005. Second-order turbulence closure models for geophysical boundary layers. A review of recent work. Continental Shelf Research, 25:725–827

Verjovkina, S., Raudsepp, U., Kõuts, T., Vahter, K., 2010. Validation of Seatrack Web using surface drifters in the Gulf of Finland and Baltic Proper, in: 2010 IEEE/OES US/EU Baltic International Symposium. Riga, Latvia, pp. 1–8.

Verhoef, A., Stoffelen, A., 2011. Validation of ASCAT coastal winds, Tech. Report, version 1.3, SAF/OSI/CDOP/KNMI/TEC/RP/176

Vitorino, J., Soares, C., Almeida, S., Rusu, E., Pinot, J., 2003. MOCASSIM- An operational forecast system for the Portuguese coastal waters. Geophysical Research Abstracts 5, 07438.

WAMDI Group, 1988. The WAM model - a third generation ocean wave prediction model. Journal of Physical Oceanography 18: 1775–1810

Zodiatis G., Lardner R., Demirov E., Georgiou G and Pinardi N., 2002. The Cyprus coastal ocean forecasting system. 3rd EuroGOOS Conference, Athens (Greece)

Zodiatis, G., Lardner, L. Demirov, E., Georgiou, G., Manzella, G., Pinardi, N., 2003[a]. An Operational European Global Ocean Observing System for the Eastern Mediterranean Levantine Basin: The Cyprus Coastal Ocean Forecasting and Observing System. Journal of Marine Technology Society 37: 115–123

Zodiatis, G., Lardner, R., Georgiou, G., Demirov, E., Pinardi, N., Manzella, G., 2003b. The Cyprus coastal ocean forecasting and observing system, a key component in the growing network of European ocean observing systems. Sea Technology 44: 10–15

Zodiatis G., Lardner R., Lascaratos A., Georgiou G., Korres G., Syrimis M., 2003c. High resolution nested model for the Cyprus and NE Levantine Basins, Eastern Mediterranean Sea: Implementation and Climatological Runs. Annales Geophysicae, 21: 221-236

Zodiatis, G., Lardner, R., Hayes, D., Georgiou, G., 2005. An operational oceanographic forecasting and observing system for the Eastern Mediterranean Levantine basin: The Cyprus coastal ocean forecasting and observing system, 4th EuroGOOS Conference Proceedings, Brest (France)